

UNIVERSITY OF ALBERTA

STRIATAL DOPAMINE AND SOCIAL PHOBIA:

A SPECT study using ¹²³I-epidepride

by

Daniel Ming-Ern Li



A thesis submitted to the Faculty of Graduate Studies and Research in partial fulfilment
of the requirements for the degree of *Master of Science*.

Department of Psychiatry

Edmonton, Alberta

Fall 2002



National Library
of Canada

Acquisitions and
Bibliographic Services

395 Wellington Street
Ottawa ON K1A 0N4
Canada

Bibliothèque nationale
du Canada

Acquisitions et
services bibliographiques

395, rue Wellington
Ottawa ON K1A 0N4
Canada

Your file Votre référence

Our file Notre référence

The author has granted a non-exclusive licence allowing the National Library of Canada to reproduce, loan, distribute or sell copies of this thesis in microform, paper or electronic formats.

The author retains ownership of the copyright in this thesis. Neither the thesis nor substantial extracts from it may be printed or otherwise reproduced without the author's permission.

L'auteur a accordé une licence non exclusive permettant à la Bibliothèque nationale du Canada de reproduire, prêter, distribuer ou vendre des copies de cette thèse sous la forme de microfiche/film, de reproduction sur papier ou sur format électronique.

L'auteur conserve la propriété du droit d'auteur qui protège cette thèse. Ni la thèse ni des extraits substantiels de celle-ci ne doivent être imprimés ou autrement reproduits sans son autorisation.

0-612-81434-3

UNIVERSITY OF ALBERTA

LIBRARY RELEASE FORM

NAME OF AUTHOR: *Daniel Ming-Ern Li*

TITLE OF THESIS: *Striatal dopamine and social phobia:
A SPECT study using ^{123}I -epidepride.*

DEGREE: *Master of Science*

YEAR THIS DEGREE GRANTED: *2002*

Permission is hereby granted to the UNIVERSITY OF ALBERTA LIBRARY to reproduce single copies of this thesis and to lend or sell such copies for private, scholarly or scientific research purposes only.

The author reserves other publication rights, and neither the thesis nor extensive extracts from it may be printed or otherwise reproduced without the author's written permission.



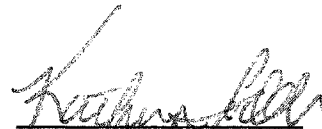

Daniel Ming-Ern Li
1E7.17 Mackenzie Centre
8440-112 Street
Edmonton, AB, T6G 2B7

Date: *OCTOBER 2nd / 2002*

UNIVERSITY OF ALBERTA

FACULTY OF GRADUATE STUDIES AND RESEARCH

The undersigned certify that they have read, and recommend to the Faculty of Graduate Studies and Research for acceptance, a thesis entitled *Striatal dopamine and social phobia: A SPECT study using ^{123}I -epidepride* submitted by *Daniel Ming-Ern Li* in partial fulfilment of the requirements for the degree of *Master of Science*


Dr. K. Todd
Dr. P. Silverstone
Dr. P. Chokka
Dr. A. McEwan
Dr. P. Tibbo

Date: 28/Sept/2002

ABSTRACT

Animal models, genetics, comorbidity research, and treatment studies provide indirect evidence that diminished striatal dopamine plays an important role in the pathophysiology of social phobia. Nevertheless, there remains a paucity of studies specifically addressing the hypothesis of decreased striatal dopamine in social phobia at the neuroreceptor level. Using single photon emission computed tomography (SPECT) and the D2 radioligand ^{123}I -epidepride, striatal D2 binding was measured in 12 social phobia patients and 10 controls, and correlated with measures of anxiety such as the Liebowitz Social Anxiety Scale (LSAS). No significant difference was detected between patient and controls. A significant positive association was found between the LSAS scores of all subjects and the striatal to frontal ratio (e.g. $p=0.049$). Female subjects also had significantly higher striatal to frontal ratios than males (e.g. $p=0.002$), independent of social anxiety scores. Increased striatal D2 binding may reflect post-synaptic compensation for decreased synaptic dopamine transmission in persons with symptoms of social anxiety. Gender differences in striatal D2 binding may be due to the influence of reproductive hormones on striatal D2 receptors. This thesis also discusses the methodologic challenges of using ^{123}I -epidepride, and concludes with a model that provides an integrated understanding of SP in the form of a hypothetical cortical-basal ganglia-thalamic-amygdaloid neural circuit.

ACKNOWLEDGEMENTS

I would like to express my deep gratitude to Dr. Phil Tibbo and Dr. Pratap Chokka for their persistent support and mentorship throughout my graduate studies. Their enthusiasm has made the journey most enjoyable, and their invaluable expertise has been the framework of the entire project. I would also like to thank Dr. Alexander McEwan who, in addition to having visionary research direction, generously provided the SPECT facilities at the Cross Cancer Institute and University of Alberta Hospital. A special thanks goes to Dr. Peter Silverstone, whose timely comments and counsel guided this thesis work to its final completion.

I am extremely grateful for Wayne Logus, whose technical wisdom, extensive labor, and constructive criticism have repeatedly sharpened this thesis; his friendship and partnership on the frontlines have been the cornerstone of this project. I would like to thank Shelly Mantei, with whom I have had many conversations around the hum of a SPECT machine, for her constant encouragement and skills in recruitment and organization. I am very appreciative of John Hanson, who provided repeated statistical consultation throughout the various stages of this project.

Special acknowledgements also go out to Dr. John Scott, Ron Schmidt, Keith Murland, Alummoottil Joshua, Alicia Strelkov, Gail Amyotte, and Kerry Fisher for their technical expertise and consultation.

This research was supported by grants from the University of Alberta Hospital Foundation and the Grey Nuns Hospital Foundation.

DEDICATION

For my Lord Jesus,
a refuge in times of trouble,
and from whom every good and perfect gift comes,
particularly Ilse, Nicholas, and my parents.

TABLE OF CONTENTS

Chapter 1	A Review of the Neurobiology of Social Phobia	1
1.1	Genetic Studies.....	3
1.2	Neuroendocrine Studies.....	5
1.3	Neurotransmitter Systems.....	7
1.3.1	Norepinephrine.....	7
1.3.2	Serotonin.....	10
1.3.3	Gamma-aminobutyric acid (GABA).....	12
1.3.4	Dopamine.....	13
1.4	Conclusion and Future Directions for Investigating the Dopamine Hypothesis of Social Phobia.....	16
Chapter 2	A Review of SPECT Imaging	19
2.1	Radiation Physics.....	21
2.1.1	Radioactive Decay and the Imaging of Photons.....	21
2.1.2	Radioactive Decay Law and Definition of Radiation Units.....	22
2.1.3	Compton Scattering, Attenuation Correction, and Partial Volume Effects.....	23
2.2	SPECT: Scintillation, Photon Detection, Instrumentation, Data Acquisition, and Reconstruction.....	24
2.2.1	Overview of Scintillation, Photon Detection, and Instrumentation..	24
2.2.2	Data Acquisition.....	27
2.2.2.1	Number of Projections per Rotation and Acquisition Time.....	28

Chapter Two (Continued...)

2.2.2.2	Radius of Rotation.....	29
2.2.2.3	Energy Setting and Window.....	30
2.2.2.4	Matrix Size.....	31
2.2.2.5	Collimator Selection.....	32
2.2.2.5.1	Low-Energy Parallel-Hole Collimator.....	33
2.2.2.5.2	Focused or Converging Collimators.....	33
2.2.3	Image Production: Reconstruction and Data Processing.....	34
2.2.3.1	Back Projection.....	34
2.2.3.2	Filtered (Convolved) Backprojection.....	37
2.2.3.3	Two-dimensional Fourier Reconstruction and Iterative Methods of Reconstruction.....	39
2.2.3.4	Frequency Filtering.....	40
2.2.3.5	Attenuation Correction.....	42
2.3	Quality Assurance.....	43
2.3.1	Field Uniformity Assessment and Correction.....	43
2.3.2	Center of Rotation.....	44
2.3.3	Detector Head Alignment with Axis of Rotation.....	45
2.3.4	Pixel Size Calibration.....	45
2.3.5	Collimator Integrity.....	46
2.3.6	System Performance.....	46
2.4	Review of Epidepride.....	46
2.5	Conclusion.....	48

Chapter 3	Rationale and Hypothesis: Social Phobia and Striatal D2 Receptors: A SPECT study using ^{123}I-epidepride	49
Chapter 4	Methods	52
4.1	Synthesis of ^{123}I -epidepride.....	53
4.2	Recruitment and Subject Selection.....	53
4.3	Administration of ^{123}I -epidepride.....	54
4.4	SPECT Imaging Acquisition Times for Patients and Controls.....	56
4.5	SPECT Data Acquisition and Reconstruction Parameters.....	56
4.6	Statistical Analyses.....	59
Chapter 5	Results	61
5.1	Subjects.....	61
5.2	^{123}I -epidepride Synthesis.....	63
5.3	Imaging Time and Striatal to Frontal Ratios.....	63
5.4	Inter-individual Variability in Striatal to Frontal Ratios.....	65
5.5	Analyses of Results: Three Approaches.....	65
5.5.1	Analysis One: 27 Observations.....	69
5.5.1.1	Univariate Analyses 1A and 1B.....	71
5.5.1.2	Multivariate Analyses 1A and 1B.....	71
5.5.2	Analysis Two: Time-Matched Patient and Control Pairs.....	73
5.5.2.1	Univariate Analyses 2A and 2B.....	73
5.5.2.2	Multivariate Analyses 2A and 2B.....	77
5.5.3	Analysis Three: Time-Matched Male and Female Pairs.....	81
5.5.3.1	Univariate Analyses 3A and 3B.....	81

5.5.3.2	Multivariate Analyses 3A and 3B.....	84
5.6	Summary of Results.....	88
Chapter 6	Discussion of Methodology	90
6.1	High Inter-individual Variability of Striatal to Frontal Ratios.....	90
6.2	Improvements in Data Acquisition.....	91
6.3	The Challenge of Epidepride Kinetics.....	94
6.3.1	Rapid Washout of Non-Specific Binding with Resulting High Background Noise.....	94
6.3.2	Inter-individual Variations in the Peak Uptake of Epidepride.....	96
6.3.3	Lipophilic Metabolite Interferes with Imaging of Parent Compound	98
6.3.4	Inter-individual Variability in Plasma Clearance.....	99
6.4	Potential Alternative Techniques to the Measurement of Epidepride D2 Binding.....	100
6.4.1	Three Compartment Modelling.....	100
6.4.2	Equilibrium Analysis (Bolus-infusion paradigm).....	102
6.4.3	Kinetic Analysis (Bolus-injection paradigm).....	104
6.4.4	Graphical Analysis and Simplified Quantification of D2 receptor Binding.....	106
6.5	Future Directions.....	107
Chapter 7	Striatal D2 Receptors, Social Phobia, and Gender	110
7.1	Relationship Between Striatal D2 Receptors and Social Anxiety.....	110
7.1.1	Methodology and Sample Size.....	111

Chapter Seven (Continued...)

7.1.2	Biological Variability in Dopamine D2 Receptors.....	112
7.1.3	Understanding Social Phobia as a Continuum Disorder.....	113
7.1.4	Neurodegenerative Hypothesis.....	114
7.1.5	Role of the Striatum in Social Phobia.....	115
7.2	Toward an Integrative Understanding of Social Phobia.....	118
7.3	Gender and Striatal D2 Receptors.....	124
7.3.1	Animal Models of Estrogen and Striatal Dopamine.....	124
7.3.2	Human Studies of Gender Differences in Striatal D2 Receptors...	125
7.3.3	Relevance of Sex Hormone Modulation of D2 Receptors to Schizophrenia and Parkinson's Disease.....	126
Chapter 8	Conclusion	129
	Bibliography.....	133
	Appendix A.....	146

LIST OF TABLES

Table 4.1	Time of Imaging and Matrices Used for Patients.....	55
Table 4.2	Time of Imaging and Matrices of Controls.....	57
Table 5.1	Patient Demographics.....	62
Table 5.2	Summary of Patient and Control Results for Analysis 1.....	70
Table 5.3	Univariate Correlation Among Variables of Interest: Analysis 1A and 1B.....	68
Table 5.4	Multivariate Analysis of Results 1A and 1B.....	72
Table 5.5	Summary of Patient and Control Results for Analysis 2.....	74
Table 5.6	Univariate Correlation Among Variables of Interest: Analysis 2A and 2B.....	76
Table 5.7	Multivariate Analysis of Results 2A and 2B.....	78
Table 5.8	Summary of Results for Analysis 3.....	82
Table 5.9	Univariate Correlation Among Variables of Interest: Analysis 3A and 3B.....	83
Table 5.10	Multivariate Analysis of Results 3A and 3B.....	85
Table 6.1	Striatal Counts for each Patient-Control Pair (Analysis 2).....	92

LIST OF FIGURES

Figure 2.1	Cross-section of Parallel Hole Collimator and Gamma Camera.....	26
Figure 2.2	Image Reconstruction and the Backprojection Process.....	38
Figure 4.1	Time of Imaging: Comparison of Control and Patient Groups.....	58
Figure 5.1	Time of Imaging and Striatal to Frontal Ratios: Controls.....	64
Figure 5.2	Time of Imaging and Striatal to Frontal Ratios: Patients vs. Controls.....	66
Figure 5.3	Striatal to Frontal Ratios for Social Phobia Patients and Controls: Imaging Times between 4 and 5 hours.....	67
Figure 5.4	Analysis 2A: LSAS scores versus Striatal to Frontal Ratios for Time-Matched, Patient-Control Pairs.....	75
Figure 5.5	Analysis 2B: Imaging Times and Striatal to Frontal Ratios for Time-Matched, Patient-Control Pairs.....	79
Figure 5.6	Analysis 2B: Imaging Time and Striatal to Frontal Ratio: Males versus Females.....	80
Figure 5.7	Analysis 3A: LSAS score and Striatal to Frontal Ratio: Time-Matched, Male-Female Pairs.....	86
Figure 5.8	Analysis 3B: Imaging Time and Striatal to Frontal Ratio: Time Matched, Male-Female Pairs.....	87
Figure 6.1	Three Compartment Model of Epidepride.....	101
Figure 7.1	Social Phobia Neural Circuit.....	123

LIST OF ABBREVIATIONS

5-HT	5-hydroxytryptamine, serotonin
^{99m}Tc -HMPAO	technetium-99m-hexamethyl-propylenamineoxime
^{123}I - β -CIT	^{123}I -labeled 2 β -carboxymethoxy-3 β -4iodophenyl tropane
AOR	axis of rotation
ART	algebraic reconstruction technique
B_{max}	Receptor density, or the concentration of available binding sites in the region of interest
Bq	Becquerel
C1	plasma compartment
C2	non-displaceable brain compartment, or receptor free brain tissue
C3	receptor compartment
CGI	clinical global impression scale
Ci	curie
$C_{\text{Ma}}(t_e)$	radioactivity of the metabolite in plasma at the time of equilibrium
COV	coefficient of variation
COR	center of rotation
$C_{\text{Pa}}(t_e)$	radioactivity of the parent compound in plasma at time of equilibrium
CSF	cerebrospinal fluid
D2	dopamine type-2 receptor
D4	dopamine type-4 receptor
DA	dopamine
DAT	dopamine transporter
DLPFC	dorso-lateral prefrontal cortex
DRD2	dopamine type-2 receptor

List of Abbreviations Continued...

DRD4	dopamine type-4 receptor
f1	free fraction of plasma parent to metabolites (determined by ultracentrifugation)
FWHM	full width at half maximum
GABA	gamma-aminobutyric acid
GSP	generalized social phobia
HPA	hypothalamic-pituitary-adrenal axis
HPLC	high performance liquid chromatography
HPT	hypothalamic-pituitary-thyroid axis
HVA	homovanillic acid
IBZM	iodobenzamide
ILST	iterative least squares technique
k3	first order rate constant between second and third compartments
k4	first order rate constant between second and third compartments
kBq	kilobecquerels
keV	kiloelectronvolts
Km1	delivery kinetic rate constant for metabolite, between the first and second compartments (C1 and C2)
km2	kinetic rate constant for metabolite, between the first and second compartments (C1 and C2)
Kp1	delivery kinetic rate constant for parent compound, between the first and second compartments (C1 and C2)
kp2	kinetic rate constant for parent compound, between the first and second compartments (C1 and C2)
LSAS	Liebowitz social anxiety scale

List of Abbreviations Continued...

MAOI	monomine oxidase inhibitors
MBq	megabecquerel
<i>m</i> -CPP	<i>m</i> -chloro-phenylpiperazine
MHPG	3-methoxy-4-hydroxyphenylglycol
MLRA	multilinear regression analysis
MRI	magnetic resonance imaging
MRS	magnetic resonance spectroscopy
NA	noradrenaline
OR	odds ratio
PBR	peripheral benzodiazepine receptor
PET	positron emission tomography
PMT	photomultiplier tube
R _f	retention factor
ROI	region of interest
ROR	radius of rotation
SAS	statistical application software
SIAS	social interaction anxiety scale
SIRT	simultaneous iterative reconstruction technique
S:F	striatal to frontal ratio
SP	social phobia
SPECT	single photon emission computed tomography
SRTM	simplified reference tissue model
STRP	short tandem repeat polymorphism
t _{max}	time of peak striatal uptake of parent compound
t _{1/2}	half life

List of Abbreviations Continued...

TRH	thyroid releasing hormone
V_2^*	apparent distribution volume
V_3	volume of distribution in the receptor compartment, C3
V_d	volume of distribution, which is equivalent to the binding potential at steady state (B_{max} / K_d)
V_{m2}	volume of distribution of the metabolite in the non-displaceable brain compartment (C2)
V_{p2}	volume of distribution of the parent compound in the non-displaceable brain compartment (C2)
VOI	volume of interest
VTA	ventral tegmental area

Chapter 1

A Review of the Neurobiology of Social Phobia

Social phobia (SP), also termed social anxiety disorder, is a disorder characterized by extreme anxiety in social and performance situations. Individuals fear that, while others are watching, they will do something embarrassing, be negatively evaluated, or have their excessive symptoms of anxiety noticed (eg. shaking, blushing, sweating). As a result of this persistent fear, social interaction or performance situations are either avoided or endured with intense discomfort, significantly interfering with normal routine or life functioning. SP is classified as either generalized, if the anxiety occurs in most social situations, or discrete, if the anxiety occurs only in a few specific situations (Diagnostic and Statistical Manual of Mental Disorders, 1994).

SP has a lifetime prevalence of 13 to 16% and, in spite of being the third most common psychiatric disorder, is an underrecognized and undertreated condition (Kessler et al, 1994; Weiller et al, 1996; Goldberg et al, 1995; Wacker et al, 1992). The mean age of onset occurs during a critical life period (11-15 years), and is followed by a chronicity and high disability that impacts all areas of life (Burke et al 1990). As a result, individuals with SP are more likely to be single, less educated, in lower socioeconomic classes, dependent on welfare, and have unstable employment histories (Schneier et al, 1992). There is also significantly increased comorbidity in SP that includes simple phobia (61% lifetime risk, odds ratio (O.R.)=8.3), agoraphobia (45%, O.R.=8.3), alcohol abuse (17%, O.R.=2.2), major depression (15%, O.R.=6.8), schizophrenia (13%, O.R.=13.3), generalized anxiety (26.9%, O.R.=4.2), panic disorder (11.6%, O.R.=10.6), and attempted suicide (12%, O.R.=12.8; Davidson et al, 1993). As a common psychiatric disorder with serious disability and comorbidity, it is surprising that until recently there has been little research into the neurobiology of SP. There is mounting evidence that SP is a discrete disorder with a genetic basis, but the biological mechanisms underlying the etiology and pathophysiology of SP remain the object of increasing investigation.

Chapter one will review the evidence for a genetic contribution to SP, and will also discuss the primary neurotransmitter systems thought to be involved—norepinephrine, serotonin, GABA, and dopamine—by incorporating results from animal models, naturalistic challenges, chemical probes, immunology, neuroendocrinology, and treatment studies. Support for a dopamine hypothesis of SP will be presented at the end of this chapter, and following a review of single photon emission computed tomography in chapter two, the rationale for a specific thesis to be tested will be summarized and presented in chapter three: namely that there is diminished striatal dopamine (DA) D2 receptors in SP. The background presented in the first three chapters will be the foundation for further discussion in chapters six and seven, in which more animal models and recent functional neuroimaging

research will be integrated with the results of this study. Chapter seven will also conclude with a model that provides a framework for a current and integrated understanding of SP in the form of a hypothetical cortical-basal ganglia-thalamic-amygdaloid neural circuit.

1.1 GENETIC STUDIES

Several studies provide strong evidence for the familial transmission of generalized SP (GSP), and also validate the classification of generalized and discrete subtypes as separate entities. In a blinded family study, relatives of SP probands were at an increased risk of SP (16.6%, relative risk = 3.12, $n=83$) compared to relatives of normal controls (5%, $n=231$), but not for other anxiety disorders; consequently, the specificity of familial transmission supports the distinctiveness of SP from other anxiety disorders (Fyer et al, 1993). Providing further evidence of heritability, a study of the children of 26 social phobics found that 23% fulfilled DSM-III-R criteria for SP, while another 30% could be diagnosed with overanxious disorder of childhood, one criterion of which is related to the concern of social evaluation (Mancini et al, 1996). Specific differences in genetic transmission of generalized and discrete subtypes of SP are suggested by findings that 16% of relatives of probands with the generalized subtype also have SP, compared with 6% of relatives of probands with the discrete subtype, with no differences between the latter subtype and controls (Mannuzza et al, 1995). Replicating the above findings, Stein et al (1998), in a direct interview of relatives of 23 patients ($n=123$) with GSP and relatives of 24 control subjects ($n=74$), determined that the relative risk for GSP and avoidant personality disorder were 10-fold higher in the relatives of GSP probands; in contrast, the relative risk for discrete and non-generalized SP did not differ between the first-degree relatives of the GSP and control groups. Consequently, family studies indicate a clear familial transmission for SP, but also underscore that this is true only for the generalized subtype of SP.

Twin studies allow some delineation of the genetic contribution to familial transmission in SP: a higher concordance rate for a syndrome in monozygotic twins (whose genetic material is identical), as compared to dizygotic twins (whose genetic material is no more homogeneous than non-twin siblings), suggests a biological causation that is independent from environmental factors. Implicating biological factors, results from a large study of female twins demonstrated a 44.4% concordance rate for SP in monozygotic twins, and a 15.3% concordance rate in dizygotic twins, with disease liability variance due to genetic factors estimated to be 30% for SP (Kendler et al, 1992). Kendler et al (1999) expanded these findings and accounted for the unreliability of single lifetime assessments by interviewing 1708 female twins on two occasions, 8 years apart, and, as such, estimates that the corrected total heritability for SP is 51%, thus suggesting a significant genetic component of at least moderate effect. In summary, then, both twin and family studies support suggestions that SP is familial with important genetic influence in the transmission, while family studies also provide evidence for biological differences between generalized and discrete subtypes, as reflected by their differences in transmission. Expansion of these findings, including adoption studies, and further clarification of the extent of genetic versus environmental contribution, with elucidation of risk factors for the development of SP, is warranted for future investigation.

Although genetic studies in SP are in relatively early stages, inquiry into the genetic basis of personality traits may guide future research in the neurobiology of SP. When identified in very young children, the trait of behavioral inhibition is associated with increased risk of developing SP in adolescence, and thus may be a precursor of SP (Kagan, 1997; Rosenbaum et al, 1993; Beidel and Turner, 1998). Furthermore, in a study of 200 pairs of twins assessed at 14 months of age, behavioral inhibition was demonstrated to have significant genetic heritability (Emde et al, 1992). As potential adult correlates of the temperament of behavioral inhibition, avoidant and schizoid personality traits have been

reported to be strongly associated with dopamine D2 receptor (DRD2) polymorphisms, and less tightly associated with dopamine transporter (DAT1) polymorphisms (Blum et al, 1997). The convergence of these findings with recent neuroimaging results that also implicate the importance of the DRD2 receptor and DAT in SP, and suggest that the phenotypes of avoidant / schizoid personality traits and SP symptoms may share common genetic components (Tiihonen et al, 1997; Schneier et al, 2000). Also of potential relevance are the findings that the personality trait of novelty seeking, which may be considered opposite to the trait of social or behavioral inhibition in SP, has been found in four studies to be significantly associated with dopamine D4 receptor (DRD4) long repeat polymorphisms (Benjamin et al, 1996; Ebstein et al, 1996; Ebstein et al, 1997; Strobel et al 1999). In contrast, five other studies have been unable to replicate these findings, and therefore the feasibility of DRD4 exon III polymorphism as a marker for novelty seeking remains uncertain (Malhotra et al, 1996; Jonsson et al, 1997; Vendebergh et al, 1997; Jonsson et al, 1998; Sullivan et al, 1998). In the most recent addition to the debate, however, Strobel et al (1999) argue that demographic and methodologic differences between studies obscure the small effect of the DRD4 polymorphism on novelty seeking, and after taking these variables into account, report (n=136) that the long DRD4 alleles are significantly associated with increased novelty seeking, exploratory excitability and extravagance. Thus, although research is in the early stages, the genetic nature of heritable traits such as behavioral inhibition, avoidant/schizoid personality traits, and possibly novelty seeking, are being elucidated with potential relevance to understanding the familial transmission and genetic mechanisms of SP.

1.2 NEUROENDOCRINE STUDIES

Abnormalities in thyroid and adrenal function have been demonstrated in panic disorder and depression. Similar studies of the hypothalamic-pituitary-adrenal axis (HPA)

and hypothalamic-pituitary-thyroid axis (HPT) have been done in SP to search for neuroendocrine alterations that would differentiate SP patients from healthy controls and from patients with other psychiatric disorders. Two studies of the HPA axis measuring urine free cortisol levels, and another measuring salivary cortisol, revealed no differences between SP patients and control subjects (Potts et al, 1991; Uhde and Tancer, 1994; Martel et al, 1999). Similarly, when using the dexamethasone suppression test, SP subjects had patterns of suppression no different from normal controls (n=64; Uhde and Tancer, 1994). Consequently, there have been no observations of specific HPA dysfunction in SP patients, though the integrity of the HPA could be tested in future studies using corticotrophin releasing factor. With respect to the HPT axis, studies have demonstrated normal T3, T4, free T4 and thyroid stimulating hormone levels in SP subjects (Tancer et al, 1990a). In a study of the effect of thyroid releasing hormone (TRH) on blood pressure and heart rate, however, SP patients had significantly greater increases in blood pressure 1 minute after TRH infusion, than did panic disorder patients or normal controls (Tancer et al, 1990b).

Consequently, although studies of the HPA axis have not revealed any findings specific to SP, one study of the HPT axis using TRH challenge revealed an increased pressor response that differentiated SP from panic disorder and normal controls—suggesting a biological mechanism specific to SP, possibly involving a disturbance of norepinephrine and hyperactivity of the autonomic nervous system. Given that there is only one study that demonstrates potential dysfunction in the HPT axis, no definitive conclusions can be made, and future research directions therefore include: more clearly defining the role of autonomic dysfunction in SP; searching for neuroendocrine markers; investigating the HPA axis using corticotrophin releasing factor stimulation; and examining the HPA and HPT axis with the purpose of distinguishing between generalized and discrete subtypes of SP.

1.3 NEUROTRANSMITTER SYSTEMS

1.3.1 *Norepinephrine*

Research into the neurobiology of SP initially focused on the role of norepinephrine (NE) because SP patients experience blushing, tremor, palpitations, and sweating--symptoms characteristic of adrenergic overactivity. To date, three main methodologies have been employed in an attempt to elucidate the importance of NE in SP: naturalistic challenges, neuroendocrine and chemical challenges, and treatment studies.

Naturalistic challenge studies have used postural change (orthostatic challenge) and public speaking to investigate possible NE dysfunction in SP. Stein et al (1992) found that SP subjects had significantly higher plasma 3-methoxy-4-hydroxyphenylglycol (MHPG), a metabolite of NE, than controls or panic disorder patients following orthostatic challenge. A subsequent study by the same investigators, however, suggested increased parasympathetic tone relative to adrenergic activity as demonstrated by increased blood pressure responsivity to valsalva maneuvers, exaggerated vagal withdrawal in response to isometric exercise, but normal heart rate, blood pressure and plasma MHPG levels following all other naturalistic challenges (Stein et al, 1994). Further complicating the issue, Coupland et al (1995) report a trend in which SP subjects have a smaller decrease in blood pressure immediately following an orthostatic challenge when compared to healthy controls, thus suggesting sympathetic hyperactivity. Consequently, although a somewhat discordant pattern emerges, naturalistic challenges in SP have implicated both sympathetic and parasympathetic hyperactivity and, in one study, increased NE reactivity.

A study using public speaking challenge did not find any differences in heart rate between generalized SP patients and controls (Levin et al, 1993), but reported, in concordance with another study, that there was increased heart rate reactivity in discrete SP in the first minute of public speaking (Heimberg et al, 1990). A later study by Hofmann et al (1995) using a public speaking challenge also revealed differences in heart rate between

generalized and discrete SP, but in addition, found that SP patients without avoidant personality disorder had greater heart rates than either controls or social phobics with APD. Thus, three naturalistic studies have demonstrated physiological differences that distinguish the two subgroups of SP, which reinforces the importance for future research not only to clarify the neurobiological differences of the two subtypes, but to take into account their distinctiveness in the design of studies. In overview, however, although naturalistic challenges have suggested increased autonomic activity, findings specifically differentiating generalized SP and healthy controls have not been consistently reproduced.

Attempts to delineate the nature of autonomic hyperactivity in SP at the level of receptor function have been done using chemical challenge studies. These studies have been based on the hypothesis that excessive anxiety is associated with enhanced firing of the locus ceruleus, causing increased NE release into the synaptic cleft. More specifically, the alpha-2 receptor has been investigated at the level of the hypothalamus, and it would be predicted that if there is increased NE release in the synaptic cleft secondary to pervasive social anxiety, there should be a downregulation of postsynaptic alpha-2 receptors and a blunting of growth hormone secretion—which is dependent on stimulation of hypothalamic alpha-2 receptors (Uhde, 1994). Unfortunately, however, there have been discrepant findings with respect to this hypothesis: although one study showed that SP and panic disorder patients had blunted growth hormone responses compared with controls (Tancer and Uhde, 1989), these findings were not replicated in a later study using a different dose and route of administration of clonidine (Tancer, 1993). Furthermore, a small crossover study of 6 SP patients given infusions of saline or yohimbine (an alpha-2 antagonist) reported a significant increase in anxiety in response to yohimbine, with concomitant elevation of NE levels—thus suggesting adrenergic hyperactivity and heightened alpha-2 sensitivity in SP patients (Potts et al, 1996). Consequently, although two of three chemical challenge studies have reported possible abnormalities of the alpha-2 receptor in SP, there

remains controversy as to whether there is a super-sensitivity or sub-sensitivity of these receptors.

Other approaches have been employed in an attempt to clarify the role of NE in SP, but still have not yielded findings specific to SP. Investigation of lymphocyte beta-adrenergic receptors, which serve as a possible indirect measure of central adrenergic neuroceptors, did not identify differences between SP patients and controls (Stein et al, 1993). Measurement of plasma neuropeptide Y, an indicator of peripheral sympathetic activity and plasma NE, also did not reveal any differences at resting conditions or following hand immersion in ice water among SP, panic disorder and control groups (Lundberg et al, 1990; Wahlestedt and Reis, 1993; Stein et al, 1996).

In summary, initial research into the neurobiology of SP has provided support for autonomic hyperactivity, increased NE reactivity to orthostatic and yohimbine challenges, possible dysfunction of alpha-2 receptors, and differential heart rate reactivity between discrete and generalized SP. There are many inconsistencies among the studies, however, and results have not always been reproducible. Though further research is warranted, the non-specificity of results suggests that NE may not play a primary role in the etiology of SP; in fact, strong evidence against primary NE dysfunction in SP include three placebo-controlled trials of beta-blockers that have failed to demonstrate clinically significant effects in generalized SP (Falloon et al, 1981; Liebowitz et al, 1992; Turner et al, 1994). Nevertheless, the effective use of beta-blockers for performance anxiety symptoms (e.g. tremor, sweating, tachycardia, and dizziness preceding public speaking), particularly in discrete SP, reinforces the possibility that NE dysfunction in SP may be the end pathway in the expression of what may be primary dysfunctions of other neurotransmitter systems (James et al, 1977; James and Savage, 1984). Furthermore, in comparison to panic disorder, SP patients have different responses to lactate, carbon dioxide and epinephrine challenges, which underscores that there are distinct neurobiological mechanisms to each

disorder. Despite these findings, their frequent co-occurrence, overlapping clinical characteristics (e.g. panic attacks and pervasive anxiety) and evidence of autonomic overactivity suggests that both disorders may share a common anxiety circuit with dysfunction in the NE system (Liebowitz et al, 1985; Gorman et al, 1988; Papp et al, 1988; Tancer et al, 1991). Accordingly, Stein (1993) has noted that techniques employed to investigate NE in panic disorder and post traumatic disorder, including fear-potentiated startle, have yet to be employed in SP, and that there still remains a relative paucity of research in NE and its associated neural circuitry. Consequently, although support for NE abnormalities in SP exists, clarification of its particular role awaits disorder-specific, repeatable findings.

1.3.2. Serotonin

The role of serotonin (5-hydroxytryptamine; 5-HT) in the neurobiology of SP has been implicated by animal models, chemical challenge studies, and the treatment efficacy of selective serotonin reuptake inhibitors (SSRIs). The role of 5-HT in modulating exploratory activity and anxiety is suggested in a study finding that 5-HT_{1A} receptor-deficient mice had decreased exploration and increased fear-related behaviors—though no specific measures of social interaction were reported (Ramboz et al, 1998). More specifically, studies employing the rat social interaction test have demonstrated that 5-HT_{1C} antagonists increase the social interaction of rats, while 5HT₂, 5HT_{1A}, 5HT_{1B}, 5HT_{1D}, and 5HT₃ antagonists have no effect on social interaction (File and Johnston, 1989; Kennet, 1992). Interestingly, paroxetine administration in rats also significantly increased the time spent in social interaction, an effect that only occurred after 3 weeks, which therefore suggests increased 5-HT presynaptic function and/or downregulation of 5-HT postsynaptic receptors (Lightowler et al, 1994). In primates, Stein (1998) discusses how 5-HT and cortisol may be important for social dominance, and how primate social submissiveness may be a useful model for SP;

accordingly, the administration of 5-HT enhancers such as fluoxetine or tryptophan promotes social dominance in primates (Raleigh et al, 1991). Consequently, although it is difficult to convincingly argue that current 5-HT animal models can be directly extrapolated to SP, animal models strongly suggest that exploratory activity, social interaction, and submission/dominance—traits with significant correlates in SP—are regulated by 5-HT function. Similar to the animal studies, the importance of 5-HT in the regulation of human social activity was demonstrated in the administration of paroxetine to 25 healthy subjects who were free from depression and any psychopathology: a significant increase in the social affiliation index (a measure of sociability) relative to controls was found after 4 weeks of dosing (Knutson et al, 1998).

The role of 5-HT in SP is supported by placebo-controlled trials showing moderate to marked improvement in patients treated with sertraline (Katzelnick et al, 1995), fluvoxamine (den Boer et al, 1994), and paroxetine (Stein et al, 1998; Baldwin et al, 1999). Furthermore, it has been suggested that the efficacy of monoamine oxidase inhibitors (MAOIs) in SP may be primarily due to their serotonergic component (Blier et al, 1987; Versiani et al, 1992). Attempts to delineate the nature of 5-HT dysfunction in SP have been made using fenfluramine and m-chlorophenylpiperazine (m-CPP) challenges. SP patients challenged with fenfluramine, a 5-HT releasing agent, had increased anxiety and cortisol response over controls, though prolactin responses were normal (Tancer, 1993); similarly, challenge with m-CPP, a 5-HT receptor agonist, resulted in increased cortisol response in SP patients over controls, while prolactin responses were also normal (Hollander et al, 1998). These two studies imply that anxiety in SP may be due to hypersensitive post-synaptic 5-HT₂ receptors, while the 5-HT₁ receptors, responsible for prolactin response, are functioning normally.

The importance of 5-HT in anxiety disorders such as panic disorder and obsessive compulsive disorder has been well documented, and thus it is not surprising that 5-HT also has a role in social anxiety. The challenge remains, therefore, to further define intricacies of

the neural circuitry and 5-HT receptor subtypes involved in SP. On the basis of the obsessional quality of the ruminative negative cognitions in SP, and the high comorbidity of obsessive compulsive disorder in SP (18.6%; O.R.=8.6), hypothetical neural circuits in SP may include 5-HT pathways that parallel those thought to be of importance in obsessive compulsive disorder (e.g. thalamic-basal ganglia-frontal cortex loop; Tibbo and Warneke, 1999). In addition, Stein (1998) discusses that SP may result from a deficiency in integrating social information from mesolimbic reward pathways originating in the ventral tegmental area (VTA; Insel, 1997), such that the “risk” of social interaction exceeds any “reward”. Accordingly, the midbrain raphe nuclei have 5-HT projections to the VTA that modulate dopamine release (Herve et al, 1987), and treatment with fluoxetine enhances DA neurotransmission of this mesolimbic pathway—thus potentially increasing the “reward” of social interaction with theoretical relevance to SP (Maj and Moryl, 1992; Hammer et al, 1993; Prisco and Esposito, 1995).

1.3.3 GABA

Evidence that GABA may play a role in SP originates with the clinical observation that alcohol decreases social anxiety and inhibition, a fact that is reinforced by the high incidence of comorbid alcohol abuse in SP (17.2%; Davidson et al, 1993), and by the demonstrated efficacy of benzodiazepines in the treatment of SP (Munjack et al, 1990; Gelernter et al, 1991; Davidson et al, 1993). In a 14 week, placebo-controlled study of 69 SP patients, gabapentin also produced a significant reduction in SP symptoms, and although the mechanism of action of gabapentin is not well established and includes activity at voltage-sensitive Na⁺ and Ca²⁺ channels, its putative efficacy in SP may be due to increased central GABAergic neurotransmission (Pande et al, 1999).

Although few in number, there are two studies that attempt to directly examine the GABAergic system in SP. Peripheral benzodiazepine receptors (PBRs) are important in the

regulation of stress responses, and are diminished in panic disorder, post traumatic stress disorder, generalized anxiety disorder, but not obsessive compulsive disorder or major depression; in a study of 53 patients with SP, there was a significant decrease in PBRs compared with controls, suggesting that PBRs may be part of a shared mechanism of GABA dysfunction in several anxiety disorders (Johnson et al, 1998). To further explain the specific nature of GABA dysfunction in anxiety disorders, it has been suggested that panic responses to flumazenil, a benzodiazepine receptor antagonist, may be associated with situational fears such as social cues. To test this hypothesis, Coupland et al (2000), using a double blind crossover challenge design, infused flumazenil and placebo infusions in SP patients (n=14) and matched controls, and did not find an increase in panic symptoms in patients versus controls. Thus, although GABAergic agents have been shown to diminish SP symptoms, and while PBRs may represent a site of GABAergic dysfunction shared with other anxiety disorders, future studies delineating the specific role of GABA in SP are required. To this end, recent advances in the imaging of benzodiazepine receptors with ^{123}I -lomazenil single photon emission computed tomography (SPECT) or ^{11}C -Flumazenil positron emission tomography (PET) hold promise for investigating GABA in SP (Morimoto, 1999).

1.3.4. Dopamine

Making it distinct from other anxiety disorders, Liebowitz et al (1987) first suggested that diminished central DA plays a key role in the neurobiology of SP, and this has been subsequently supported by increasing evidence from animal models, clinical studies, and neuroimaging results. In a study of depressed patients, it was found that introversion, a characteristic of social anxiety, was significantly associated with decreased DA in the cerebrospinal fluid (CSF; King et al, 1986). Similarly, in a study of 49 panic disorder patients with SP, significantly lower levels of homovanillic acid (HVA), a metabolite of DA, were found

in the CSF compared to controls; in addition, a trend towards lower levels of HVA was also noted in those with SP compared to panic disorder patients (Johnson et al, 1994). In a treatment study of depressed patients with increased rejection sensitivity, a trait seen in SP, phenelzine had significantly greater efficacy over imipramine, and this may be secondary to DA enhancing effects of phenelzine that are absent with imipramine (Liebowitz et al, 1984).

More specifically, research has implicated dysfunction in the striatal DA system in SP. A timid mouse strain was found to have markedly decreased DA in the caudate nucleus (Mayleben et al, 1992). Clinical observations have noted that in Tourette's syndrome, a disorder with dopaminergic dysfunction in the basal ganglia, some patients develop social anxiety and avoidance following treatment with the DA antagonist haloperidol (Mikkelsen et al, 1981). A magnetic resonance imaging (MRI) study measuring brain volumes in SP patients and healthy controls revealed no significant differences with respect to cerebral, caudate, putamen, and thalamic volumes, but did find a greater age-related reduction in putamen volumes in SP patients compared to controls (Potts et al, 1994). This possible greater age-related atrophy of the putamen in SP may provide some explanation for observations that there is a higher than expected incidence of SP that predates the onset of Parkinson's disease--an illness that involves loss of dopaminergic neurons in the basal ganglia (Lauterbach and Duvoisin, 1987; Stein et al, 1990; Chase et al, 1998).

Although limited in number in SP, neuroimaging studies also promise considerable potential for clarifying and increasing our understanding of the role of striatal DA in SP. As previously discussed, primate social submission/dominance has been associated with 5-HT/cortisol abnormalities and may serve as a useful animal model for SP (Raleigh et al, 1991; Stein, 1998); interestingly, in a PET study of female monkeys, animals with low social dominance also had significantly lower striatal D2 binding (Grant et al, 1998), and these results suggest that both diminished striatal DA and 5-HT/cortisol are significant in modulating social behavior in this potential animal model of SP. In humans, a study using

SPECT and ^{123}I - β -CIT (^{123}I -labeled 2 β -carboxymethoxy-3 β -4iodophenyl tropane), a radioligand for the DA and 5-HT transporters, demonstrated markedly lower striatal presynaptic DA reuptake site densities in persons with SP compared to controls (Tiihonen et al, 1997). Schneier et al (2000) examined striatal postsynaptic DA function using SPECT and the D2 radioligand ^{123}I -IBZM (^{123}I -labeled iodobenzamide), and found diminished striatal D2 binding in 10 patients with SP relative to controls. Consequently, evidence for the importance of striatal DA in SP continues to grow, and both pre- and postsynaptic abnormalities have been documented and correlated with clinical symptoms in SP. Future replicative studies are needed, and it will be necessary to clarify whether D2 binding abnormalities reflect receptor abnormalities and/or differences in synaptic levels of DA that influence the competition of study ligands for binding. In addition, it will be important to examine other basal ganglia neurotransmitters, such as glutamate, and to incorporate pre and post treatment arms to test the response of the striatal DA system to therapy.

Of particular interest, striatal dopamine has not only been correlated with SP symptoms, but several studies suggest associations with other related personality attributes that include avoidant and schizoid traits, and detachment. Studies have shown that the density of striatal D2 receptors vary considerably among healthy subjects, possibly related to differential participation of DRD2 genotypes (Jonsson et al, 1999). As discussed earlier, Blum et al (1997) report a strong association between the dopamine D2 receptor Taq A1 allele and schizoid/avoidant behavior, while a weaker association of the dopamine transporter gene with schizoid/avoidant behavior was also detected. On a similar note, a positron emission tomography (PET) study using ^{11}C raclopride, a D2 radioligand, found that the personality trait of detachment, as measured by the Karolinska Scale of Personality, was significantly associated with decreased D2 receptor binding (Farde et al, 1992). These findings were not only replicated in a later PET study of 18 adults, but were extended to include findings that D2 receptor density was specifically related to the trait of detachment

as defined by the Karolinska Scale of Personality, but not to forms of detachment defined by the Tridimensional Personality Questionnaire (Breier et al, 1998). A recent PET study investigating whether a similar correlation exists between detachment and striatal DAT found that DAT binding in the putamen correlated negatively with detachment scores on the Karolinska Scales of Personality (Laakso et al, 2000). Consequently, the convergence of research from the perspectives of SP, avoidant / schizoid personality traits, and detachment implies that perhaps the common element--avoiding involvement with other people and / or avoiding giving and taking confidences in others (as defined by the Karolinska Scale of Personality)—is the specific attribute that is associated with striatal D2 receptor and DAT abnormalities. Accordingly, it would be helpful for future SP neuroimaging research to incorporate the Karolinska Scale of Personality into the protocol, with further efforts made to understand the specific nature of the trait that is associated with striatal dopamine in SP. Also of relevance to this discussion, novelty seeking, an attribute opposite to social inhibition, has been correlated with striatal uptake of DA precursor and (Cloninger, 1994), as previously discussed, inversely correlated with short alleles of the DA D4 receptor (Benjamin et al, 1996; Ebstein et al, 1996; Strobel, 1999). These initial findings may also argue for a dimensional understanding of SP, in which introversion and extraversion form two poles of a continuum, with the extreme pole of introversion representing those with social anxiety.

1.4 Conclusion and Future Directions for Investigating the Dopamine

Hypothesis of Social Phobia

In recent years, significant progress has been made in understanding the neurobiology of SP. One of the cautions of synthesizing research in SP is that the diagnostic criteria have evolved in the transitions from DSM-III (1980), to DSM-III-R (1987), and to DSM-IV (1994). Affecting epidemiological studies, the transition from DSM-III to DSM-III-R ensured that persons with avoidant personality disorder were not excluded from

the diagnosis of SP, which resulted in increased lifetime prevalence of SP in the National Comorbidity Study to 13.3% (Kessler et al, 1994), compared to the Epidemiologic Catchment Area study lifetime prevalence of 2.4% (Schneier, 1992). In the transition from DSM-III-R to DSM-IV, there has been an improved delineation of the phenomenology of SP in children and adolescents, which has implications on child and adolescent epidemiology; and family studies.

In summary, family and twin studies have established that generalized SP is heritable with a significant genetic influence, and molecular and behavioral genetic studies hold promise in further defining the nature of the trait that is actually transmitted—with possible candidates being behavioral inhibition, schizoid and/or avoidant traits, specific SP symptoms, and novelty seeking. Although efforts at delineating the role of NE have resulted in discrepant findings, there is evidence for autonomic hyperactivity, increased NE response to orthostatic and yohimbine challenges, possible dysfunction of alpha-2 receptors, and a differential heart rate reactivity between discrete and generalized SP. Because of the variability and non-specificity of results, however, NE may not play a primary role in the etiology of SP, but its dysfunction could be related to a common anxiety circuit that is shared with other anxiety disorders. Research into the role of GABA in SP is still in early stages, and although there is no doubt as to the efficacy of GABAergic agents, whether SP is associated with primary dysfunction in GABA systems requires further investigation. 5-HT has also been shown in animal and human studies to be important for regulating exploratory activity, sociability, and social hierarchy (e.g. submission versus dominance); and there is early evidence that hypersensitive 5-HT₂ receptors may contribute to anxiety in SP. Treatment efficacy of the selective serotonin reuptake inhibitors in SP is well documented, and may be secondary to actions at cortical structures in the aforementioned cortical-basal ganglia-thalamic circuit, and/or as a result of input to the VTA/mesolimbic reward system where 5-HT modulates DA.

Making it unique among the anxiety disorders, there is persuasive evidence from animal models, clinical studies, neuroimaging research, and investigations of the genetics of personality traits that striatal dopaminergic dysfunction plays a significant role in the neurobiology of SP, and in possibly determining the severity of social anxiety experienced. Although support exists for the importance of diminished central DA in SP, much of it is based on indirect evidence, and there are few replicated studies. Crucial weaknesses in the DA hypothesis of SP include: a paucity of research that directly investigates the role of DA at a neuroreceptor level; a lack of evidence demonstrating the efficacy of dopaminergic agents in treating SP; and a poor understanding of the functional role of DA in SP—especially given the evidence for intertwined involvement of other neurotransmitters such as NE, 5-HT, and GABA. Tiihonen et al (1997) note that while they found increased dopamine reuptake site densities in patients with social phobia, there is a paucity of research examining the striatal post-synaptic D2 receptor in SP. Thus, while preliminary research into the neurobiology of SP has grown in the recent years—providing a DA hypothesis that distinguishes SP from other anxiety disorders—direct studies that further delineate the nature of dopaminergic dysfunction in SP are much needed.

Chapter 2

A Review of SPECT imaging

Recent advances in neuroimaging present the opportunity of studying dopamine in social phobia. In particular, single photon emission computed tomography (SPECT) uses radioactive compounds to assess regional cerebral blood flow on the surface of the brain, termed regional cerebral blood flow (e.g. xenon-SPECT), or blood flow throughout the whole brain (e.g. technetium-99m-*d,l*-hexamethylpropyleneamine oxime or HMPAO). In addition to these compounds, CNS receptors may also be studied by ^{123}I -labeled ligands that bind to muscarinic, dopaminergic, GABAergic and serotonergic receptors. Single photons emitted by SPECT radioligands from within the brain enter detectors that relay information to a photomultiplier tube that amplifies the signal. This signal is converted from analog to digital data and conveyed to a computer that reconstructs a two-dimensional representation of the isotope's distribution within a slice of the brain.

Imaging techniques such as magnetic resonance imaging (MRI), functional magnetic resonance imaging (fMRI), magnetic resonance spectroscopy (MRS), and positron emission tomography (PET) each have important roles in imaging research. Their current disadvantages, however, provide SPECT imaging with a unique position in neuroimaging research. While MRI offers freedom from X-irradiation and excellent spatial resolution, it has limitations: the exclusion of patients with any ferromagnetic body implant, relatively lengthy motionless requirements in claustrophobic conditions, loud noise from radiofrequency bursts, and the inability to do functional imaging. Although fMRI provides the opportunity to measure blood flow using a $T2^*$ sequence, which can then be used to detect active brain regions to which blood flow is increased, fMRI is unable to measure neuronal metabolism and neuroreceptor activity. MRS has the advantage of detecting biologically significant nuclei that enables the study of metabolic processes; however, it has limitations of spatial resolution, contamination from subcutaneous lipid signal contamination, short-echo time spectra acquisition challenges, full brain coverage, and the need for improved spectral analysis techniques. Lastly, PET can be used to study neuronal metabolism, blood flow, and neuroreceptor occupancy with good spatial resolution. Unfortunately, PET is very expensive, requires a cyclotron for radioisotope synthesis, and needs the injections of radioisotopes (Kaplan and Sadock, 1998; Matson and Weiner, in press).

SPECT presents several advantages over other imaging techniques as it allows the study of neuroreceptors through the use of radioligands, is much less expensive than positron emission tomography (PET), and has radioligands with relatively longer half lives that do not require the presence of an expensive on-site cyclotron for synthesis, as is the case for PET. Disadvantages of SPECT, however, include diminished resolution in comparison to PET, and the general computed tomography challenges of Compton

scattering, attenuation, and partial volume effects. The following chapter will review topics that will provide a foundation for understanding the discussion in chapter six, where the methodology of epidepride SPECT imaging will be examined. To this end, the topics of focus in this chapter will include radiation physics, SPECT photon detection process, instrumentation, data acquisition, reconstruction and quality control. It will conclude with a review of epidepride and the ratio method of imaging.

2.1 RADIATION PHYSICS

2.1.1 *Radioactive Decay and the Imaging of Photons*

Radioactive decay occurs when an unstable configuration of particles (i.e. protons and neutrons) and energy states in the nucleus of an atom undergo transformation into a more stable state. This results in the release of particles and energy, called daughter products, which are comprised of other atoms, α particles, β particles, γ -rays, and x-rays. Both γ -rays and x-rays are photons (electromagnetic radiation), but they are distinguished by their source of origin, with γ -rays coming from within the atomic nucleus, and x-rays from the electron shells.

Alpha decay occurs when an atomic nucleus emits an α particle, which is a helium nucleus consisting of two protons and two neutrons, and results in the transmutation of the original nucleus into an atom with an atomic number 2 units lower than the original. Because of their mass and charge, α particles are of little use to nuclear imaging because they are unable to significantly penetrate solid matter, usually having a range less than 1mm.

Beta decay is the release of a β particle, which is either an electron or positron, and results in the transmutation of an element into the element with the next lower (β -

decay) or higher (β^+ decay) atomic number. Beta particles also do not significantly penetrate solid matter, and therefore cannot be imaged. Should a β particle, however, collide with an electron, the two particles will annihilate each other and produce a pair of photons, each with an energy of 511 keV, travelling in opposite directions. These photons can then be imaged, and their original location deduced, as is the case in PET studies.

In contrast to α and β particles, both γ and x-rays can be used directly for imaging because they have a relatively deeper range of matter penetration. Gamma radiation is released several milliseconds following α or β decay because of the excess energy state of the atom that occurs following the ejection of α or β particles. SPECT capitalizes on this phenomenon as the SPECT Anger camera is γ -ray detector. Other imaging techniques are dependent on the detection of X-rays, which are produced through a process called electron capture: an orbital electron is "captured" by a nucleus (e.g. thallium-201) and used to convert a proton to a neutron, causing other electrons to fill the vacancies with subsequent production of x-rays (Taylor and Datz, 1991).

2.1.2 The Radioactive Decay Law and Definition of Radiation Units

Because of the variable imaging times in nuclear medicine, it is important to correct for radioactive decay. The radioactive decay law can be described in terms of the half life ($t_{1/2}$) of a radioisotope, where the half life is defined as the time it takes for 50 percent of the radioactive atoms to decay:

$$N(t) = N(0)e^{-\ln(2)t/t_{1/2}}$$

Where $N(t)$ is the number of radioactive atoms at time t ; $N(0)$ is the number of initial radioactive atoms, and $t_{1/2}$ is the half life of the radioisotope.

The curie (Ci) is defined as 3.7×10^{10} disintegrations per second, and is the conventional unit for measuring the dose of radioisotope being injected. The becquerel (Bq) is replacing the curie as the preferred unit for the measurement of radiation dose, and is defined as one disintegration per second ($1 \text{ Ci} = 3.7 \times 10^{10} \text{ Bq}$). In general, doses in nuclear medicine are usually expressed in terms millicurie, microcurie, or the megabecquerel ($1 \text{ MBq} = 1 \times 10^6$; Taylor and Datz, 1991).

2.1.3 Compton Scattering, Signal Attenuation, and Partial Volume Effects

Crucial to understanding the interaction of radioactive particles with tissue and matter are the concepts of compton scattering, signal attenuation and partial volume effects, which ultimately affect the imaging resolution of both SPECT and PET. Compton scattering is the deviation of emitted photons from a straight path caused by the tissues through which the photons pass. Attenuation refers to the dissipation of energy of the photons as they pass through bone, air, fluid, and brain tissue—with each medium having a different effect on the degree of attenuation. Partial volume effects are the energy contributions from neighboring areas of interest that affect the signal from the area of interest. Because compton scattering, signal attenuation, and partial volume effects limit the ability to accurately deduce the point of origin of a photon, SPECT instrumentation, data acquisition, and computer modelling must be designed to minimize or correct for these natural processes which adversely affect resolution (Kaplan and Sadock, 1998).

2.2 SPECT SCINTILLATION AND PHOTON DETECTION, INSTRUMENTATION, DATA ACQUISITION, AND RECONSTRUCTION

2.2.1 *Overview of the Scintillation and Photon Detection Process*

Minor artifacts can be neglected in planar imaging such as the chest x-ray, but these inconsistencies are amplified significantly in SPECT because of the reconstruction process, and can cause increased noise, artifact, or background. Consequently, in order to ensure that detected photons are a true representation of a target organ, photons that reach the detector must pass through a three step process before they are able to contribute to the formation of an image. Specifically, the photon must have enough energy to pass through attenuating material of the source and cross the distance to the collimator face, be parallel to the collimator septa, and be energetic enough to remain within the acceptance window of the pulse-height analyser.

To examine this three step process more closely, a ^{123}I molecule undergoes radioactive decay to produce ^{123}I gamma photons with an energy of 148 to 170 keV. To reach the detector, a photon must have enough energy to travel through attenuating material like tissue, bone and air. On this route, however, numerous photons will be absorbed by the attenuating media, and in the process generate new Compton photons, which are lower energy photons (e.g. 120-130 keV), some of which will also be travelling towards the collimator.

A collimator determines the type of photons which will strike the detector, and is made of a lead disk with multiple holes which block photons that are not proceeding parallel to the collimator septa (Figure 2.1). Consequently, not only do the original ^{123}I photons need to avoid absorption and have the energy to cross the distance to the collimator face, but the direction of its path must be parallel to the collimator. ^{123}I photons that are not parallel to the collimator septa will be absorbed by the lead septa,

which in turn may generate lead x-rays that join the remaining ^{123}I photons and Compton photons in the final leg of the journey towards the detector.

At this point, it is important to highlight that the collimator plays a role in determining the image quality by influencing the balance between sensitivity of detection and resolution of the image, which is a function of collimator hole diameter and septal thickness. For example, increasing the hole diameter will allow an increased number of photons to pass through to the detector, thereby increasing sensitivity but decreasing resolution. On the other hand, increasing septal thickness, which diminishes penetration of nonparallel photons and additional Compton scattering, improves resolution at the expense of sensitivity.

Once passing through the collimator, the original ^{123}I photons are accompanied by some "impure" Compton photons, and lead X-ray photons and subsequently impact the gamma camera detector, which is a thallium activated sodium iodide crystal. Gamma photons interacting with the iodide cause the release of electrons, through photoelectric absorption and Compton scattering, and these electrons interact with the crystal lattice to produce light photons. Thus, a large number of light photons are emitted per absorbed gamma ray, in direct proportion to the energy and position of the gamma ray; this burst of light photons is called scintillation.

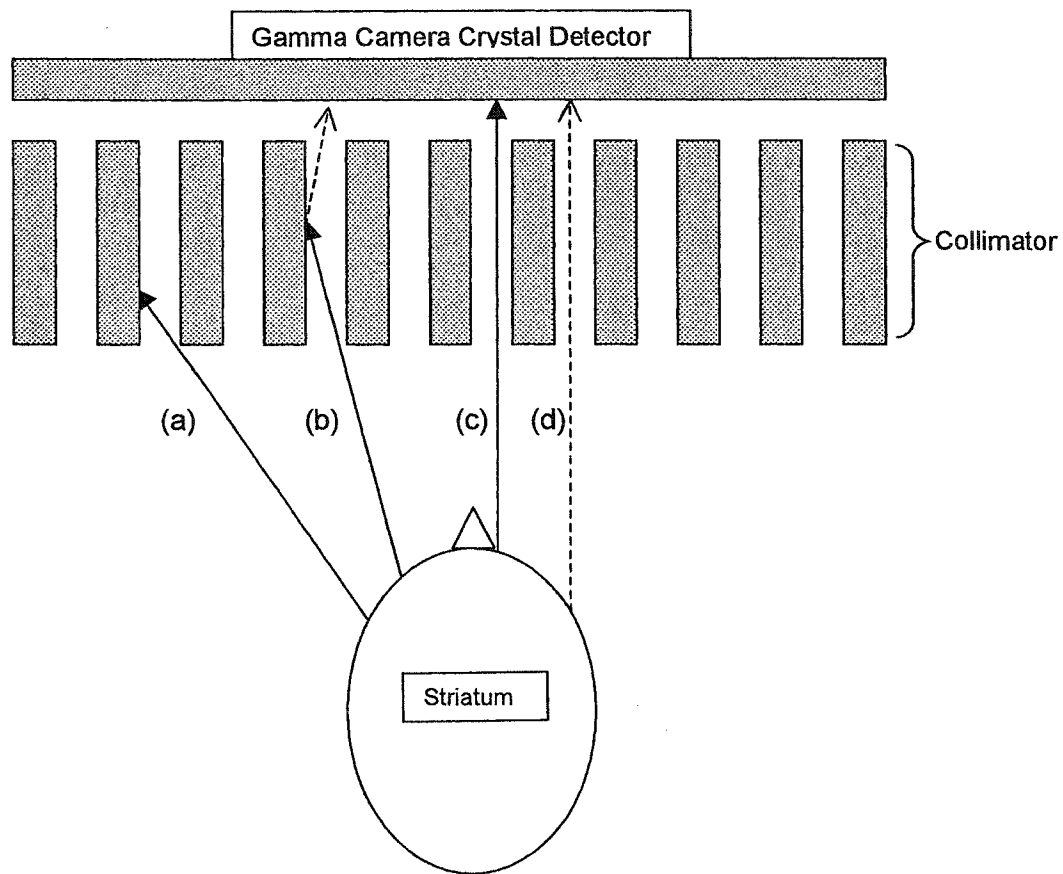


Figure 2.1 Cross-section of a Parallel-Hole Collimator and Gamma Camera. ^{123}I photons, depicted by the solid arrows, proceed from the striatum towards the gamma camera crystal detector. The ^{123}I photons can (a) become absorbed by the collimator septa because they do not enter parallel to the collimator, (b) collide with the collimator and generate lead x-rays that also hit the detector; (c) enter parallel to the collimator septa and register valid information regarding the position of a scintillation event; or (d) generate compton photons.

The light photons are not intense enough to be processed meaningfully, and consequently, light photons traverse through the crystal lattice and are reflected using a white aluminium oxide surface onto the photocathode of a photomultiplier (PMT) tube. The photomultiplier tube absorbs the light photons and converts them into electrons (7 to 10 light photons required to produce one electron), and this signal is then amplified through a series of plates called dynodes, until a small electrical pulse (10^{-9} volts) is detected at the anode of the photomultiplier tube. The voltage (or height) of this pulse, arising from a single scintillation, is proportional to the amount of light photons released by the crystal; and this in turn represents the energy of the gamma-radiation absorbed by the crystal. Subsequently, a pulse height (i.e. voltage) analyser, which has an energy window set to accept all gamma-rays with energies distributed around the photopeak of the radionuclide of interest, ensures that pulses corresponding to "impure" gamma-rays, whose energies are outside the energy window of the radionuclide of interest, are rejected. The electric pulse, once accepted by the pulse height analyser, is conveyed to an electronics system with information regarding the Cartesian (x and y) coordinates of the original gamma-ray impact on the crystal, and is finally converted into a digital signal that activates a pixel on a computer screen (Grune and Stratton, 1981; Croft, 1986; Taylor and Datz, 1991).

2.2.2 Data Acquisition

Having reviewed the basic instrumentation and the processes of scintillation and photodection, the foundation is set for discussing the collection of data. Data acquisition in SPECT is governed by the principle of attaining optimal resolution within the shortest reasonable time. A compromise among parameters for data collection must be established to achieve optimal resolution while taking into account patient tolerance for imaging time, less than desired count statistics related to limited radionuclide dose

administration, and limitations in SPECT technology. Thus, in the process of data acquisition, the following variables require examination: number of projections per rotation, acquisition time, radius of rotation, energy selection, matrix selection, attenuation correction, and collimator selection.

2.2.2.1 Number of Projections per Rotation and Acquisition Time

In SPECT imaging, the camera moves in an arc around the patient, and a series of planar images are obtained through either a continuous acquisition or a step-and-shoot technique. Focussing on the latter, in a step-and-shoot technique, the detector head stops at regular intervals in its orbital arc, with each stop lasting a set period of time, during which a planar image is obtained. As a result, the length of the imaging study is determined by the number of projections multiplied by the time per stop or projection. The length of the study is restricted to approximately 30 to 40 minutes, the upper limit of what the average patient can comfortably tolerate, during which time a balance must be struck between the number of projections obtained (increasing projection number improves reconstructed imaging quality), and imaging time per projection, which must be long enough to enable the acquisition of adequate count statistics for sufficient image reconstruction. For example, to acquire tomographic images of good statistical quality in a count poor study, a situation that often occurs in brain imaging, longer stop time is required for adequate count statistics, and therefore, the total number of projections are diminished accordingly. On the other hand, in a count rich study such as liver perfusion imaging, stop times can be much shorter because adequate count statistics are more quickly obtained, allowing for increased number of projections. In summary, the compromise between the number of stops and time per stop must take into consideration patient comfort and risk of motion, and the count statistics, which are

determined by the type of study (e.g. liver vs brain), dose of radionuclide, and the resolution required (Grune and Stratton, 1981).

With respect to our study parameters, which will be discussed in more detail in chapter four, we employed a step-and-shoot technique that collected 120 images. Given a 360° orbital arc with 120 stops or collected images, each at 30 seconds, a total imaging time of 60 minutes would be required. This is beyond the limit of most patients, and any advantages conferred by the increased count statistics would be quickly negated by patient movement during the last portion of a lengthy exam. Because we used a triple headed camera, however, this allowed 120 images to be collected at 40 steps, with 30 seconds per step, yielding a total acquisition time of 20 minutes. Thus, a triple headed camera is able to acquire increased count statistics, allowing better reconstruction, over a period that would require a single headed camera three times the amount of time to obtain--which increases the risk of patient motion.

2.2.2.2 Radius of Rotation

A drawback of SPECT imaging is that there is relatively poor resolution in comparison to other imaging techniques, and this is primarily compounded by the source-to-detector distance. Because a shorter source-to-detector distance enhances the potential for increased resolution, the orbital radius of rotation (ROR), must be minimized. It can be easily seen, therefore, that a standard circular orbit around a body is not ideal because the organ of interest-to-detector distance varies significantly depending to the orbital detector position. In particular, brain imaging can potentially be difficult because a larger ROR is dictated by the shoulders. Consequently, to minimize the ROR and improve resolution, single and multi-head cameras have the capability of travelling in elliptical orbits and body contour orbits, and this may improve resolution by as much as 2-3 mm, and also enhance lesion contrast by up to three fold (English, 1995).

2.2.2.3 *Energy Setting and Window*

Energy peak settings are important in order to focus the camera to only accept electron pulses from the photomultiplier tubes that correspond to energies of the gamma-radiation produced by the radionuclide of interest. Once an energy peak is selected to center on the photopeak of the gamma radiation of the primary radionuclide, the width of the window setting becomes the next important variable. The window width must allow detection of as much of the primary gamma radiation as possible, while also excluding, as best as possible, Compton scatter radiation and radiation from other non-primary radionuclides. An important consideration, however, is that a narrower window width, while decreasing the amount of scatter radiation in an image, will cause increased count uncertainty because of lower count density. Window width is expressed as a percentage of the peak setting and, for example, a 20% window at a 150keV energy photopeak corresponds to a window width from 135keV to 165 keV.

Conventional Anger camera imaging simply centered the window width symmetrically around the energy peak setting; however, because the scatter radiation is lower in energy than that of the primary radiation, it is not symmetrical around the peak, but forms a subpeak on the low-energy side. Consequently, some camera systems allow the energy window to be chosen independently of the energy peak, such that it may be placed asymmetrically to favor the high energy side, thereby avoiding as much scatter radiation as possible. It is crucial that if asymmetrical photopeaking is chosen, that the uniformity and correction matrix (see below) be stable enough to allow a narrow asymmetrical window (Croft, 1986).

Depending on the photopeak characteristics of a radionuclide, multiple windows can also be used, which subsequently allows increased count statistics for better image reconstruction, and/or may reduce imaging times required. For example, ^{67}Ga has triple

gamma peaks, where as ^{201}Tl and ^{111}In have dual gamma peaks (English, 1995). Another advantage of setting multiple energy windows includes the possibility of using information from two different radionuclides with different energy photopeaks, which occurs when patient-specific transmission maps are used in combination with emission information to correct for attenuation (will be discussed in a later section; Grune and Stratton, 1981).

2.2.2.4 *Matrix Size*

In most situations, image resolution improves proportionally to increases in the matrix size. The matrix sizes used in SPECT are usually either 64 x 64 (corresponding to a pixel size of 3 x 3 mm), or 128 x 128 (corresponding to a pixel size of 6 x 6 mm). Although potentially improving resolution, increased matrix size may not always be advantageous, and several factors to consider include: computer storage space, number of projections, time per projection, patient dose, processing time, required resolution, and the count statistics of the source. With respect to computer storage space and acquisition parameters, increasing the matrix from 64 x 64 to 128 x 128 causes a fourfold increase in disk space requirements, acquisition time, and processing time—which in many clinical scenarios may not be worth the added spatial resolution. Acquisition time, which discussed previously is partly a function of number of projections and time per projection, needs to be multiplied by a factor of four when doubling a matrix in order for the information density, or counts per pixel, to remain the same. If the acquisition time is kept constant while the matrix is doubled, the count density is reduced by a factor of eight, which adversely diminishes image contrast, and may be insufficient to generate a statistically adequate image reconstructions. Should this be the case, either the acquisition time or dose of the radionuclide administered have to be increased accordingly. Lastly, the optimal pixel size for a clinical study is usually considered to be

at least one-half of the full width at half maximum (FWHM is a measure of the spatial resolution of the system and is defined as the minimum distance between two points of a line where the count rate falls to 50% on a focal plane where the count rate is at 100%). As such, SPECT cameras with a FWHM of 12-20 mm will require no better resolution than a 64 x 64 matrix, where the pixel size is 6 x 6 mm. Thus, when increasing the matrix size for the purpose of improving resolution, it is important to justify the need for the added spatial resolution given the possible increase in computer storage space, number of projections, time per projection, patient dose, and processing time. With recent developments, multicamera SPECT systems have superior computer capabilities and increased sensitivity, and as a result, acquisition times are less compromised with increases in matrix size (Grune and Stratton, 1981; Croft, 1986; English 1995).

2.2.2.5 Collimator Selection

The collimator is the first part of the SPECT system that a photon contacts, and any degradation in the image at this point will be subsequently amplified, even with the best detector and processing system. The choice of a collimator is dependent on the radionuclide used and the desired balance between resolution and sensitivity. As discussed earlier, resolution is enhanced by decreasing hole diameter and by having longer holes, which generally occurs at the cost of sensitivity; on the other hand, sensitivity is improved by increasing the hole diameter, and by having shorter holes and thinner septa. In addition, the radionuclide used also influences collimator selection, as radionuclides with higher energy require longer holes and thicker septa to minimize septal penetration of gamma-radiation with subsequent deterioration of resolution. Thus, collimators need to handle the highest energy released by a radionuclide, and are accordingly classified as low (cover energy up to 200 KeV), medium (cover energy up to 300 KeV), or high energy. It becomes evident that higher energy collimators, which

have longer holes and thicker septa, have diminished sensitivity that can be particularly detrimental in photon poor studies. The potential for diminished sensitivity with increased hole length may not always be the case, as increasing hole length also diminishes the scatter photons which contribute to higher inappropriate sensitivity. Because the collimator design must take into account the multiple interactions of sensitivity, resolution, and minimization of scatter or septal penetration for a particular radionuclide, collimation has such an essential role on image quality that the collimator is frequently assessed and purchased separately from the SPECT system. Some of the principles governing the influence of the aforementioned variables on collimator design will be specifically highlighted in the following two examples of the low-energy parallel-hole collimator and the focused collimators (Croft 1986, English 1995).

2.2.2.5.1 Low-Energy Parallel-Hole Collimator

^{123}I has a photopeak of 159 keV and, at first glance, would be appropriate for a low-energy parallel hole-collimator. In the process of synthesis of ^{123}I from the ^{124}Te (p, 2n) ^{123}I reaction, however, a ^{124}I contaminant is generated that requires a medium energy collimator to shield against higher energy photon penetration. Predictably, this causes a decrease in sensitivity with a secondary increase in acquisition time. An alternative to using a medium-energy collimator is the use of low-energy parallel-hole collimator with increased bore length, which has been shown to reduce the septal penetration of high energy photons as well or better than a shallow-bore-length medium-energy collimator (English, 1995).

2.2.2.5.2 Focused or Converging Collimators

The fan-beam collimator and the cone-beam collimator are two types of focused collimators. The fan-beam collimator consists of holes which slant from the crystal

towards the center of the camera that confer a magnifying property. This design diminishes the degree of resolution degradation that occurs as a function of distance, particularly in comparison to the parallel-hole collimator. Interestingly, the sensitivity increases as the source object moves away from the detector face until it passes the focal plane. This characteristic renders fan-beam collimators ideal for brain imaging, as it minimizes the increased radius of rotation that results from the shoulders. Fan-beam collimation does require unique center of rotation, field uniformity, and reconstruction software routinely supplied by the manufacturer (English, 1995).

2.2.3 Image Production: Reconstruction and Data Processing

2.2.3.1. Back projection

Image production requires the reconstruction of two-dimensional planar images into a three-dimensional representation of the target, and this has been accomplished by increasingly elegant mathematical algorithms in SPECT. These algorithms are based on the concept of back projection. Whereas projection is the acquisition of two-dimensional images by the detector from a given angle (oriented perpendicular to the axis of rotation), the back projection process takes the original acquired projection and casts it in reverse onto an image field (e.g. computer matrix). Cast in reverse, the activity from the projection image is evenly distributed across a computer matrix to produce a ray sum, and when the ray sums from each projection angle are added together, the overlap of ray sums produces a cross-sectional representation of the original source.

To further illustrate, consider the following simplified example (Grune and Stratton, 1981; Croft, 1986; English 1995). The object, in the shape of a box for the sake of simplicity, has non-uniform radioactive intensities as represented by the following cross-section.

2	3
3	5

The object shape and its non-uniform intensity is unknown to the computer and must be reconstructed or deduced by acquiring composite images through a detector that orbits around the object.

Consider the projection obtained by the detector at positions (a) and (b), which represent the ray sum along that angle of projection (Croft, 1986):

(a) Horizontal projection

2	3	\Rightarrow	5
4	5	\Rightarrow	9

(b) Vertical projection

2	3
3	5
\Downarrow	\Downarrow
6	8

The back projection process, which casts in reverse on to an imaging area, the original projections, are then depicted as follows:

(a) Back projection of the horizontal acquisition:

2.5 2.5 \Leftarrow 5

4.5 4.5 \Leftarrow 9

(b) Back projection of the vertical acquisition:

3 4

3 4

\Uparrow \Uparrow

6 8

In the reconstruction process, the ray sums from each back projection angle are then added together to give a composite picture that represents a cross-section of the original object.

5.5 6.5 \Leftarrow 5

7.5 8.5 \Leftarrow 9

\Uparrow \Uparrow

2 8

Now, a constant is subtracted (3.5) from this new composite image to adjust for contrast and, the result is the original object!

3 3

4 5

Incidentally, the constant for contrast adjustment is obtained by the following formula:

$$\begin{aligned}\text{Contrast} &= \frac{(\text{number of projections} - 1) \times (\text{Ray Sum Total for the Image} / \text{number of pixels})}{\text{number of pixels}} \\ &= \frac{(2 - 1) \times ((5.5 + 6.5 + 7.5 + 8.5)/2)}{4} \\ &= 3.5\end{aligned}$$

The process of back projection is illustrated in Figure 2.2, and it becomes evident that while it is the foundation of image reconstruction, it also causes significant artifact that results from the criss-crossing of ray sums at locations which do not correspond to the actual object. This interference produces the characteristic “star artifact,” the beginnings of which can be seen in Figure 2.2B.

2.2.3.2 *Filtered Backprojection*

Because image quality is diminished significantly by the presence of interference such as the “star artifact,” which is caused by the simple back projection process, *filtered* back projection was designed to minimize artifact by the application of a digital filter during the back projection process. To accomplish this, small negative values are added to the side of each ray sum such that, when reprojected, the negative values will diminish or cancel out the density of criss-crossing ray sums, such that only the highest-density ray sums, which represent the true target, remain significant. The type of filter most often used to diminish the star artifact, which causes what is termed “low frequency background,” is the ramp filter (English 1995).

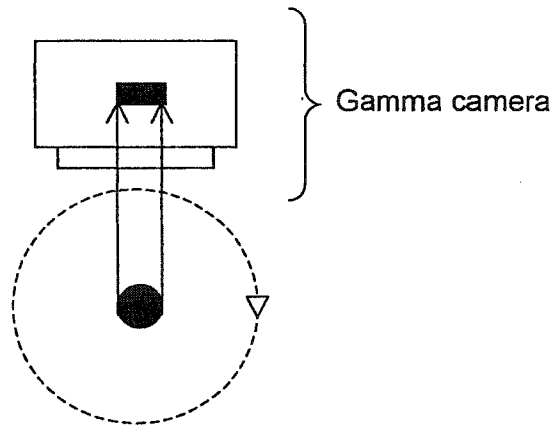


Figure 2.2A The Image Reconstruction and the Backprojection Process. This begins with the acquisition of two-dimensional images consisting of projected ray sums from an object (i.e. solid ball). The gamma camera orbits (represented by the dotted line) and gathers images from various angles.

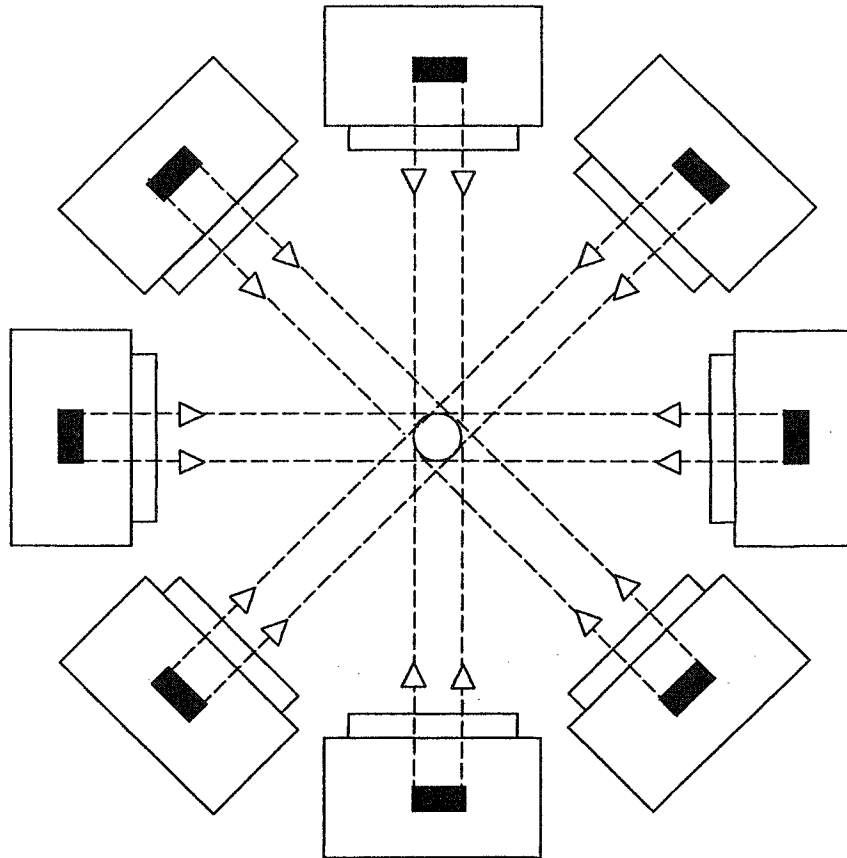


Figure 2.2B. The original acquired projections are cast backwards onto a computer matrix. When the ray sums from each projection angle are added together, the overlap of ray sums produces a cross-sectional representation of the original object. Artifact, however, also occurs from criss-crossing ray sums that do not correspond to the actual object, and the beginnings of a "star artifact" are observable. This artifact is minimized by a digital filter that is discussed in section 2.2.3.2.

2.2.3.3 *Two-dimensional Fourier Reconstruction and Iterative Methods of Reconstruction*

While filtered convoluted backprojection is the mainstay of image reconstruction because of simplicity and speed of reconstruction, it is worthwhile to briefly mention the two other types of reconstructive methods, which include Fourier and iterative reconstruction algorithms. Instead of filtering data in real space (x-y space) such as with convolution filtering, it is possible to transform real space data into frequency space, through a Fourier transform function. In frequency space, the counts in a pixel relate to the amplitude while the pixel is viewed as frequencies with a distinctive separation; thus, the advantage of the Fourier transform is that it can mathematically determine the sine and cosine waves required to synthesize the frequency shape that represents real space. As a result, Fourier transformation is capable of producing mathematically clean and high quality reconstructions, and the application of an inverse Fourier transformation can convert reconstructed data back into real space. Limitations to the Fourier reconstruction method include the fact that the accuracy of Fourier representation is proportional to increased resolution; this increased resolution is not only hampered by limited resolution of imaging devices, but requires—in comparison to filtered convoluted back projection—significantly longer acquisition times, and increased number and time of computer calculations (English, 1995).

Iterative reconstruction techniques aim to produce a transaxial image whose projections are within some statistical significance of the actual measured projections. In general, iterative reconstruction techniques produce potential mathematical solutions, representing a hypothetical transaxial image, that increasingly approximate the actual transaxial image as measured by the ray sums that have been detected. From this hypothetical transaxial image, “guess ray sums” are projected and compared with actual measured ray sums, and a correction factor is derived from these comparisons. (There

are several iterative reconstruction algorithms such as the algebraic reconstruction technique (ART), iterative least-squares technique (ILST), and the simultaneous iterative reconstruction technique (SIRT) which are distinguished by the order and method of applying corrections.) The ray corrections are backprojected and added (or multiplied) to the current solution. This entire process is repeated a number of times until an approximate solution within some acceptable statistical certainty of the true result is reached. As would be expected, increasing the number of views (which increases the number of ray sums), improves the statistical certainty of approaching the true image (English 1995).

2.2.3.4 *Frequency Filtering*

Filters are mathematical functions applied to data to improve image quality by diminishing interference from artifact, background, and noise—while preserving, as much as possible, the desired image data. Prefiltering (or preprocessing) refers to the application of a filter prior to filtered back projection, while postfiltering (or postprocessing) refers to application of a filter after filtered back projection. Filters are described by their effect on spatial frequency, and as noted previously, real space data is converted into frequency data by Fourier transforms. The transformation then enables data to be worked upon by a frequency filter (Grune and Stratton, 1981).

The primary objective of a frequency filter is to suppress as much background and noise as possible without altering the validity of the image data. “Background” in SPECT imaging is created in the back projection process by the build-up of criss-crossing ray sums, exemplified by the “star artifact”, which results in what is termed low-frequency background. On the other hand, the image filtration process also aims to diminish “noise,” which consists of high frequency distortion due to statistical count fluctuations in measurements, or Poisson noise. For example, if an average of 400

radioactive counts are collected in a pixel over one minute, 420 counts in the next minute, and 380 counts in the third minute, the signal to noise ratio is $400 / 20 = 20$. Not only does each pixel have a noise component, but neighboring pixels influence noise such that a noise propagation effect increases as the number of pixels in a given row or column is increased. To increase the signal to noise ratio, and thereby decrease the influence of noise and the noise propagation effect, the number of counts per pixel could be increased, and this is a function of the radiopharmaceutical used, administered dose, and acquisition time. Because adjustments in administered dose and acquisition time have obvious limits, the need for a filter that can adequately suppress high-frequency noise becomes readily apparent (English, 1995).

In overview, each image consists of overlapping components of background, noise, and target data. The ramp filter is the most commonly used frequency filter during the back projection process to reduce low-frequency background like the "star artifact." A ramp filter is called a high-pass filter because it filters out the blurring image effect of low-frequency background while allowing high-frequency noise to pass through; this high-frequency results in sharper, but more "grainy" appearing images (Grune and Stratton, 1981; English, 1995).

Simply using a ramp filter would be appropriate in images with high count statistics because these have an increased signal to noise ratio that renders the high-frequency noise relatively insignificant. More often the case in SPECT imaging, however, when image count statistics are poor, noise interference becomes much more important. In these scenarios, using a ramp filter alone is insufficient, and a window, or additional filter, is added to exclude high-frequency noise while maintaining a balance that maximizes the retention of useful data. Single variable high-frequency filters (e.g. Hamming, Parzen, Hann) have a mathematically derived shape that "rolls off" of the Ramp filter at a predefined frequency or cutoff point. Cutoff values that are low produce

oversmoothed data which may obscure lesions, while high cutoff values cause noisy images with a patchy appearance. Two variable high-frequency filters, however, such as the Butterworth filter, allow the user to define not only the cutoff point, but also the power factor, which enables the determination of the degree of the slope. In comparison to single variable filters, the two variable Butterworth filter has improved control and flexibility with respect to diminishing noise while retaining important target data, and is especially useful in high-information density studies such as brain SPECT. Other filters include the Metz and Wiener filters, which are restoration filters because they augment data using an inverse multiplier to those parts of the image which have the least noise, while attenuating image portions with the most noise. All in all, the choice of a filter must take into account the frequency of the noise and the target frequency of the target being imaged (Grune and Stratton, 1981; English 1995).

2.2.3.5 Attenuation Correction

Photons are attenuated exponentially as they traverse through tissues, and this is complicated by the fact that individual tissue types attenuate photons to different degrees. Thus, attenuation is the most important variable that impairs the use of SPECT to obtain accurate absolute quantification. For example, a strong source attenuated by a long distance can yield the same ray projection as a weaker source at a short distance, resulting in significant ambiguity in measurement (English, 1995).

There are two types of "first order" attenuation corrections that can be applied: the Chang method (post-reconstruction correction), or the Sorenson Technique (pre-reconstruction correction). A disadvantage of the Chang method is that it assumes a uniform attenuation and does not account for variability of attenuation imposed by different tissues and by variations in body thickness. Thus, the Chang method may be

reasonable in brain studies, where there is relatively uniform attenuation, but would not be helpful in thoracic studies where there are non-uniform overlying structures.

This latter problem can be addressed using both transmission and emission acquisition data to properly account for variabilities in attenuation caused by different tissue types. In this method, an external line source of ^{153}Gd or ^{241}Am rotates opposite to the detector and produces a transmission map as the line source transmits photons through the patient. The resulting image can supply data to perform attenuation corrections given the variability of attenuating media overlying the target of interest. Concurrent with acquisition of transmission data, emission data from another radionuclide, which should have a significantly different photopeak, can also be obtained from the target organ of interest, and both emission and transmission images may be recorded by using a dual pulse height window.

2.3 QUALITY ASSURANCE

In SPECT imaging, minor inconsistencies can be amplified throughout the acquisition and reconstruction process to produce artifact and serious deviations. As a result, quality assurance holds a paramount role in SPECT, and several key areas that require regular and strict monitoring include: field uniformity, center of rotation, detector head alignment with axis of rotation, pixel size calibration, collimator evaluation, and system performance. These factors will be briefly outlined in the following discussion.

2.3.1 *Field Uniformity Assessment and Correction*

Field uniformity assessment and correction are probably the most essential quality control procedures to be performed in SPECT. System uniformity, which is defined as the consistency of count distribution measured by a camera system when given a uniform target to image, is determined by the detector uniformity of response (intrinsic

uniformity), collimator integrity (extrinsic uniformity), and the quality of analog-to-digital signal conversion. System uniformity deviation in SPECT must be less than 1% because any larger inconsistencies are amplified in the backprojection process; otherwise, system non-uniformities frequently produce ring visible artifacts, which are stronger in intensity as the distance from the area of non-uniformity to the axis of rotation decreases (Grune and Stratton, 1981).

System non-uniformity is corrected on a weekly basis by the use of a high-count reference flood field image that is acquired under the set conditions and parameters (e.g. matrix size, collimator, radionuclide) that will be used for a specific examination. For a 64 x 64 matrix, a high-count flood field image consists of 30,000,000 counts, while a 128 x 128 matrix requires a flood count of 120,000,000 counts. This flood-field image, which is a uniform target of ^{57}Co plastic sheets or well-mixed $^{99\text{m}}\text{Tc}$ flood tanks, is used as a uniform standard against which any needed adjustments to achieve system uniformity are made and stored in a computer (Grune and Stratton, 1981).

2.3.2 Center of Rotation

Discrepancies in the actual and perceived center of rotation (COR) of the imaging system can be caused by aberrations in the detector or gantry alignment, electronic instability of the detector, and nonlinearities between the camera-computer analog-to-digital converter. As a result, it is important to align the camera COR, which represents the COR of the whole mechanical system (camera and gantry), with the electronic COR, which is what the computer perceives as the center of the matrix. Any significant misalignment of more than 0.5 of a pixel for a 64 x 64 matrix will result in diminished contrast, decreased resolution, and image distortion.

System COR correction, which should be done weekly, can be performed by imaging ^{57}Co or $^{99\text{m}}\text{Tc}$ line source at selected angles, and then at their directly opposing angles. Any small misalignment will result in blurring of the image of the line source,

while large misalignments will cause a doughnut artifact. To correct for any such misalignments, a SPECT system usually has computer software which will calculate and adjust for any offsets between the computer matrix COR and the mechanical COR; furthermore, corrections may also be made by physically shifting the camera rotation axis to overlap with the center of the computer matrix. COR calibration should also be performed separately for each collimator, zoom factor, matrix size, radionuclide, and energy registration circuit (Grune and Stratton, 1981).

2.3.3 *Detector Head Alignment with Axis of Rotation*

Planar images obtained must be perpendicular to the camera axis of rotation (AOR) because a 1% camera tilt with respect to the AOR will cause a shift of one pixel in a 64 x 64 matrix. Camera tilt, which should be assessed every four months, can be evaluated by collecting 36-point source images, aligned perpendicular to the AOR, over 360 degrees. Addition of the images should generate a straight line that is parallel to the x axis.

2.3.4 *Pixel Size Calibration*

The pixel size in the x and y directions must match to provide equivalent dimensions. Faulty x / y gain can result in shifts in the COR, improper attenuation correction, and inaccurate reconstructions of standard and oblique planes. Pixel size calibration, which should be performed every six months, can be done using vendor software. Otherwise, pixel calibration can be done by using three-point sources separated in x / y dimensions by known distances.

2.3.5 Collimator Integrity

Because the collimator is the first piece of equipment that a photon encounters, any degradation of the imaging process at this time will spoil data acquisition, even in the presence of a SPECT system with the finest resolution, sensitivity and detector performance. The collimator should be inspected visually, every four months, with particular attention paid to any damage to the septa. An evaluation of field uniformity, which should be occurring weekly, through the use of high-count flood images, should also be able to alert technicians to problems with collimator integrity by resulting non-uniformities in the field (English, 1995).

2.3.6 System Performance

System parameters such as object contrast, image noise, field uniformity, and accuracy of attenuation correction can be tested using ^{99m}Tc phantoms. This should be done every three months, and each image should contain at least 200,000 counts in a 64 x 64 or 128 x 128 matrix. Consistency in the ROR, filter, and cutoff frequency need to be maintained during these evaluations (Grune and Stratton, 1981).

2.2 REVIEW OF EPIDEPRIDE

Epidepride {(S)-N-[(1-ethyl-2-pyrrolidinyl)methyl]-5-iodo-2,3-dimethoxybenzamide} is a novel benzamide that has received increased attention as a SPECT D2 radioligand because of potential advantages conferred by its high specificity and affinity for the D2 receptor (Kornhuber et al, 1995). For example, in comparison to IBZM, a frequently used SPECT D2 radioligand, epidepride has been proposed to be a superior radioligand for pure D2 imaging because it is less likely to be displaced and influenced by endogenous dopamine (Innis et al, 1992). Furthermore, Kornhuber et al (1994) note that IBZM has low striatal to frontal ratios that are not optimal for imaging, whereas

epidepride has a high target to background ratio that may be particularly advantageous for extra-striatal imaging. Examining other D2 radioligands, Tibbo and Silverstone (1997) review that PET radioligands such as raclopride suffer from an underestimation of endogenous dopamine (Seeman et al, 1990), while spiperone also has high affinity for 5-HT and spirodecane binding sites (Leyson et al, 1987). In overview, then, epidepride has potentially superior characteristics in comparison to other SPECT D2 ligands because of its high affinity and specificity.

With regards to pharmacokinetic considerations, epidepride has a peak striatal uptake of approximately two to four hours and a physical half-life of 6.02 hours (Kessler 1992; Kornhuber 1995; McEwan 1995). Epidepride has three plasma metabolites: a polar metabolite that does not cross the blood-brain-barrier, a lipophilic metabolite that represents 5 to 15% of the original parent compound after the first 3 hours, and the parent compound (41% remains unchanged after 30 minutes; Kuikka et al, 1997). The biological half life of ^{123}I -epidepride is 29 ± 8 hours, and the highest uptake of epidepride occurs in the bladder and intestine, with the critical organ being the lower large bowel. The majority of the radioactivity clears through the urinary tract (Kuikka et al, 1997).

Epidepride has been used to measure striatal D2 binding with the ratio method. Following the injection of a radioligand, the ratio between the radioactive counts in the region of interest (ROI) to the radioactive counts in plasma, at the time of the maximal count rate in the ROI, represents the binding potential at steady state (Pinborg et al, 2000). This "peak equilibrium method" is often simplified by substituting the plasma input function for a receptor-free ROI, such as the cerebellum or frontal cortex, where the binding potential is represented by the ratio of specific binding to non-specific binding at the time of peak uptake (Farde et al, 1989). The ratio method is a semiquantitative technique that offers advantages over quantitative techniques that include: 1) relative ease of use without the need for arterial sampling or lengthy infusion times; 2) and the

ability to control for inter-individual differences in height and weight, dose of radioligand injected, and whole brain uptake (Stephenson et al, 2000). Thus, the ratio method has been, to date, the preferred method of approximating the specific binding of epidepride to striatal D2 receptors (Pilowsky et al, 1994; Tibbo and Silverstone, 1997; Stephenson et al, 2000).

2.3 CONCLUSION

In summary, chapter two reviewed concepts of radiation physics relevant to SPECT, including the phenomena of Compton scattering, partial volume effects and attenuation. The process of SPECT photon detection, instrumentation, data acquisition, and reconstruction were also described; and factors important in quality assurance were discussed. Lastly, the novel radioligand epidepride and the ratio method for determining D2 specific binding were presented. These concepts will provide a foundation for understanding the rationale of the thesis that will be introduced in chapter three, the methodology of the experimental design in chapter four, and finally, the discussion of the data acquisition process and epidepride kinetics in chapter six.

Chapter 3

Rationale and Hypothesis:

Social Phobia and Striatal D2 Receptors:

A SPECT study using ^{123}I -epidepride

There is growing evidence of dopaminergic dysfunction in persons with SP, and in particular, that much of this may reside with abnormalities in the striatum. As reviewed in chapter one, evidence of dopaminergic dysfunction in SP includes: clinical studies showing that depressed patients with introversion have significantly decreased cerebrospinal fluid (CSF) DA levels (King et al, 1986); patients with social phobia have diminished HVA, a DA metabolite, in the CSF compared with controls (Johnson et al, 1994); and depressed patients with increased interpersonal rejection sensitivity respond better to phenelzine as opposed to imipramine, an effect that may be due to the dopaminergic activity of phenelzine (Liebowitz et al, 1984). With regards to striatal

dopaminergic abnormalities, a timid mouse model has significantly decreased DA in the caudate nucleus (Mayleben, 1992); and patients with basal ganglia dysfunction such as Tourette's syndrome have a predisposition to developing social anxiety with haloperidol D2 blockade (Mikkelsen et al, 1981). More recently, neuroimaging studies have been able to demonstrate more specific DA abnormalities in SP, and a SPECT study using and ^{123}I - β -CIT, a radioligand for the DA and 5-HT transporters, shows markedly lower striatal presynaptic DA reuptake site densities in persons with SP compared to controls (Tiihonen, 1997).

Tiihonen et al (1997) raise a further question of whether or not post-synaptic D2 abnormalities also exist in SP, and hypothesize that diminished striatal post-synaptic D2 receptors, in conjunction with pre-synaptic DAT abnormalities identified in their study, may be indicators of neuronal loss in persons with SP. Preliminary indirect evidence for neuronal loss in SP can be found in a MRI study revealing greater age-related reductions in putamen volumes in SP patients compared with controls (Potts et al, 1994). There are also two studies showing that there is a higher than expected incidence of SP that predates the onset of Parkinson's disease, which may coincide with the loss of dopaminergic neurons in the basal ganglia (Lauterbach and Duvoisin, 1987; Stein et al, 1990).

Converging with emerging research on the relationship of striatal dopamine to SP, there has been increasing interest in the role of striatal dopamine and personality traits: primate models of female monkeys with low social status reveal lower striatal D2 binding in the striatum (Grant et al, 1998); polymorphisms of the DA D2 receptor have been associated with schizoid-avoidant traits (Jonsson et al, 1999); and PET studies show a correlation between detachment and diminished striatal D2 receptor density (Farde et al, 1990).

With the exception of the neuroimaging studies by Tiihonen et al (1997) and Potts et al (1994), most of the evidence for diminished central DA in SP is based on indirect evidence, with few replicated studies. Thus, there is a need to directly examine striatal dopaminergic dysfunction at a receptor level. While there is significant research that points to the association of SP with striatal hypodopaminergic function, possible increased neuronal loss, and evidence of striatal D2 abnormalities in schizoid/avoidant traits, there have been no studies done at the time of initiation of this thesis to extend these findings by examining the role of post-synaptic striatal D2 receptors in SP.

Consequently, this study hypothesizes that there is diminished striatal D2 receptor density in SP—a reflection of hypodopaminergic function and possible neuronal loss—and proposes to test this in 10 healthy volunteers and 10 persons with SP using SPECT and ^{123}I -epidepride. ^{123}I -Epidepride is a novel SPECT D2 receptor ligand that has been receiving increasing attention because of its high affinity for D2 receptors. Furthermore, the use of the ratio method, in which the ratio of counts from a region with specific binding to counts from a region with non-specific binding is calculated, has been used for ^{123}I -epidepride with relative ease to measure D2 receptor binding (Tibbo and Silverstone, 1997). Thus, this study will investigate post-synaptic striatal D2 receptor binding in SP using ^{123}I -epidepride and SPECT imaging.

Chapter 4

Methods

In order to study the role of striatal D2 receptors in social phobia, a case-control design was established that incorporated the increasing use of the high affinity D2 receptor ligand, ^{123}I -epidepride, with an objective of obtaining a minimum of 10 social phobia patients and 10 healthy controls. Proposals for research ethics committees were approved at the University of Alberta Hospital, Grey Nuns Hospital, and the Cross Cancer Institute. Subject recruitment, screening, and selection took place at the Departments of Psychiatry in the University of Alberta Hospital and the Grey Nuns Hospital. The synthesis and administration of ^{123}I -epidepride, along with the SPECT data acquisition and reconstruction, was performed at the Cross Cancer Institute. Consultation for statistical analyses was provided by John Hanson at the Cross Cancer Institute. The following sections will expand in detail the particulars of the study design

with respect to ^{123}I -epidepride synthesis; subjection recruitment and selection; ^{123}I -epidepride administration; imaging time acquisition for patient and controls; SPECT data acquisition and reconstruction parameters; and statistical analyses.

4.1 *Synthesis of ^{123}I epidepride*

5 μl of the tributyltin precursor of epidepride (17 nmol, 2 mg/ml in 95% ethanol), 5 μl of 4N HCl, and 5 μl of 3% H_2O_2 were added to 185 mBq of ^{123}I sodium iodide in 30 μl 0.1N NaOH (MDS Nordion Inc.). The reaction proceeded for 30 minutes at room temperature, and was stopped with the addition of 5 μl of 4N ammonium hydroxide. The product was purified by high performance liquid chromatography using a $\mu\text{Bondapak CN}$ column (3.9 x 150 mm), and eluted with a mixture of 20 mM sodium phosphate buffer (70%) and 95% ethanol (30%) at a flow rate of 0.5 ml per minute. Retention time of the ^{123}I -epidepride was 25 minutes. The product was collected in 4 ml of eluate which was sterilized by filtration with a 0.2 μL filter into a sealed sterile vial. Product yield and final purity were determined by thin layer chromatography with Eastman Kodak Silica Gel strips developed with ethyl acetate:98% ethanol 1:1. In this system, ^{123}I -epidepride had a retention factor (R_f) of 0.1-0.3 while iodide had a R_f of 0.7.

4.2 *Recruitment and Subject Selection*

After radiation safety committee and hospital ethics approval, 12 patients (mean age 34.3 ± 7.9 yrs; 8 men, 4 women), and 10 controls (mean age 33.9 ± 6.5 yrs; 7 men, 3 women) were recruited through advertisements and provided written informed consent. All modules of the Scheduled Clinical Interview for DSM-IV (SCID-IV) were administered to each subject to exclude comorbid psychotic, affective, anxiety, substance, dissociative, and somatoform disorders. A thorough clinical interview with physical

examination was performed to exclude organic brain illnesses and major medical conditions. As such, both patients and controls in this study were free of psychiatric medications, and had no comorbid medical or psychiatric diagnoses.

All subjects had symptom severity rated with the Liebowitz Social Anxiety Scale (LSAS, Fresco et al, 2001), the Social Interaction Anxiety Scale (SIAS; Mattick and Clarke, 1998), and the Clinical Global Impression Scale (CGI, American Psychiatric Association, 2000).

Administration of the SCID-IV, clinical interview, rating scales, and physical examinations were done by the author in all patients and controls with the exception of patients K.E. and J.B (Table 3.1). These patients had a complete psychiatric and medical interview with physical examination that was completed by Dr Chokka, while SCID-IV and LSAS, CGI, and SIAS rating scales were administered by Shelly Mantei, an experienced research nurse.

4.3 Administration of ^{123}I -epidepride

^{123}I -epidepride was synthesized as previously described at the Department of Oncologic Imaging, Cross Cancer Institute, by Dr. John Scott, Mr. Ron Schmidt, and Ms. Alummoottil Joshua. Four hours after synthesis, subjects received ^{123}I -epidepride intravenously at an average dose of 152 ± 17 mBq. Intravenous injection was performed as a bolus over a period of two minutes, followed by a saline flush.

4.4 SPECT Imaging Acquisition Times for Patients and Controls

With regards to patient data acquisition, a fixed imaging time was not practical because of clinic constraints, and the 12 patients received a single SPECT scan between 4 and 7 hours after injection for a total of 12 observations (Table 4.1).

Table 4.1: TIME OF IMAGING AND MATRICES USED FOR PATIENTS

OBSERVATION	PATIENTS	IMAGING TIME (hours)	MATRIX
1	D.L.	4.17	64 X 64
2	T.H.	4.20	64 X 64
3	C.D.	4.45	128 X 128
4	B.L.	4.67	64 X 64
5	H.T.	4.85	64 X 64
6*	K.E.	4.90	64 X 64
7	J.Z.	5.42	128 X 128
8	A.E.	5.50	64 X 64
9	J.D.	5.78	128 X 128
10	R.P.	6.20	128 X 128
11*	J.B.	6.32	64 X 64
12	R.R.	6.48	64 X 64

* These patients had their SCID-IV interview and rating scales done by Shelly Mantei. Dr. Chokka subsequently performed a clinical interview and physical examination.

For the purpose of clearly assessing the relationship between striatal frontal ratios and imaging time, controls were selected to undergo repeated SPECT imaging, to a maximum of 3 scans, between 2 and 7 hours post-injection. The process of determining the number of scans each control was to participate in was based on personal availability. Thus, 7 of the 10 controls were scanned between 2 and 3 hours, all controls were scanned between 4 and 5 hours, and 5 of the 10 controls were scanned between 5 and 7 hours (Table 4.2). As will be elaborated upon in the subsequent chapter, only the control data acquired between 4 and 7 hours, for a total of 15 observations, was used for comparison to the patient data in the final analysis (Table 4.2). The additional scans (or observations) for controls provided increased time points that allowed more effective comparison of patient and control groups, given the spread of imaging times over the 4 to 7 hour period. Figure 3.1 provides a scatter plot summary of the imaging times of controls in comparison to patients.

4.5 *SPECT Data Acquisition and Reconstruction Parameters*

Images were acquired with a Picker prism 3000S three headed camera and an ultra high fan beam collimator located at the University of Alberta Hospital, Department of Radiology. Total acquisition time was 20 minutes (40 steps at 30 seconds per step), and a total of 120 images were acquired on a 128 X 128 matrix for all controls and 4 patients, and on a 64 X 64 matrix for 8 patients (Table 4.1). The radius of rotation varied slightly between 12.6 and 13.0 cm. The energy window was set to 20%.

Reconstruction was done using Picker Odyssey software and combined Ramp and 2D Butterworth filters with minimum cut off. In the volume of interest (VOI), which covered the striatum, 8 transverse reconstructed slices, parallel to the canthomeatal line, were added to give a total thickness of 17.0 to 14.7 mm. The slice containing the

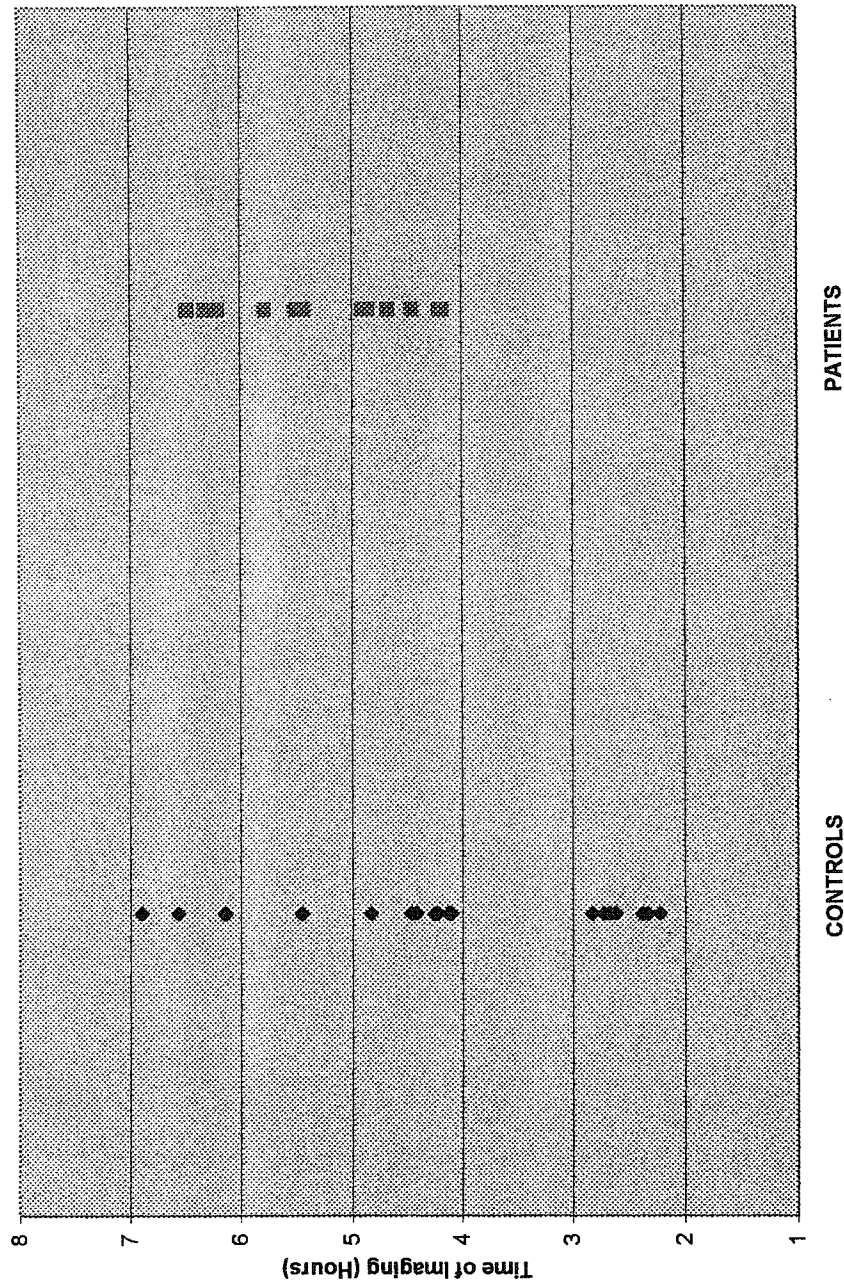
Table 4.2: TIME OF IMAGING AND MATRICES OF CONTROLS

OBSERVATION	CONTROL	IMAGING TIME (hours)	MATRIX
N/A*	F.N.	2.08	128 X 128
N/A	W.L.	2.62	128 X 128
N/A	I.C.	2.72	128 X 128
N/A	M.F.	2.22	128 X 128
N/A	L.D.	2.33	128 X 128
N/A	B.B.	2.38	128 X 128
N/A	G.S.	2.67	128 X 128
1**	M.F.	4.10	128 X 128
2	B.Y.	4.12	128 x 128
3	L.D.	4.13	128 X 128
4	W.L.	4.23	128 x 128
5	M.B.	4.25	128 X 128
6	B.B.	4.42	128 X 128
7	I.C.	4.43	128 X 128
8	R.T.	4.47	128 X 128
9	G.S.	4.83	128 X 128
10	F.N.	5.45	128 X 128
11	W.L.	6.13	128 X 128
12	M.F.	6.15	128X 128
13	L.D.	6.15	128 X 128
14	B.B.	6.57	128 X 128
15	F.N.	6.90	128 X 128

* N/A, or not applicable, refers to the fact that these observations were not included in the final analysis nor in the comparison of patients and controls.

** These are the control observations used in the final analysis and in the comparison of patients and controls.

Figure 4.1 Time of Imaging: Comparison of Control and Patient Groups



Note: Imaging results from controls that were done between 2 and 3 hours were excluded from the final analysis and from statistical comparisons to the patient group.

striatum was selected such that the majority of activity was centered in one frame with equal spill over into adjacent slices.

Striatal D2 binding was measured using striatal to frontal ratios which approximate the sum of specific and non-specific binding divided by non specific binding. Striatal to frontal ratios were measured by taking the total counts per pixel for left and right striatal volumes of interest divided by total counts per pixel for VOIs placed over each frontal cortex. Each VOI was 8 x 8 x 8 pixels for 128 x 128 matrix acquisition, while for the 8 patients imaged on 64 x 64 matrix acquisition, the VOI was 4 x 4 x 4 pixels.

Use of the frontal cortex as a reference region was chosen over the cerebellum because, while both have low concentrations of D2 receptors (Farde et al, 1986, 1988), the body position required to obtain cerebellar images can be uncomfortable for subjects. Furthermore, at the imaging times between 4 and 7 hours, interference from extrastriatal binding in the frontal cortex is minimal (Kornhuber et al, 1995).

All counts were dose-normalized by taking the total counts per pixel divided by the dose of ^{123}I -epidepride that was injected. Decay correction was also performed using the following formula:

$$N(t) = N(0)e^{-\ln(2)t/t_{1/2}}$$

Where $N(t)$ is the number of radioactive atoms at time t ; $N(0)$ is the number of initial radioactive atoms, and $t_{1/2}$ is the half life of the radioisotope (6 hours for epidepride).

4.6 Statistical analyses

Statistical analyses were performed using SAS software and the statistical package of Microsoft Excel 2000. Univariate analysis was employed to identify correlations among the variables of group (i.e. social phobia patient or control), age, gender, time, dose, rating scales (i.e. CGI, SIAS, and LSAS), and outcome measures

(i.e. S:F). After identifying significant correlations, multivariate analysis was performed with primary interest in the independent variables of imaging time, gender, and either group or LSAS score; and the dependent variable as the S:F ratio.

Chapter 5

Results

5.1 Subjects (Table 5.1)

There were 12 patients (8 males, 4 females) and 10 controls (7 males, 3 females). The average age of patients was 34.3 ± 7.9 years, while that of controls was 33.9 ± 6.5 years of age, with no significant differences between the groups. Patient scores for the CGI, SIAS, and LSAS were 4.4 ± 0.3 , 56.9 ± 6.9 , and 90.3 ± 12.2 respectively; and 1.0 ± 0 , 11.3 ± 8.4 , and 23.7 ± 9.1 for controls. Mean length of illness for patients was 26.4 ± 7.4 years, with the average age of onset being 8.5 years.

Of the 12 patients, only was one married, while six were single, four were separated or divorced, and one was living common law. All of the subjects had received college or university level educations with the exception of R.P. and J.B., both of whom had grade 11 education.

TABLE 5.1 PATIENT DEMOGRAPHICS

PATIENT	AGE	SEX	HAND	MARITAL	EDUCATION	EMPLOYMENT	MEDICAL HISTORY AND MEDICATIONS	PSYCHIATRIC HISTORY	FAMILY HISTORY
J.Z.	23	F	R	Single	High School	Unemployed	Nil	Nil	Nil
E.A.	25	M	R	Single	University Student	P/T Fast food	Nil	Nil	Excessive shyness in father
R.R.	26	M	R	Single	College	Lab Technologist	IDDM: humulin R 30U; humulin N 28U	Nil	Depression in mother and maternal grandmother
J.B.	28	F	R	Common Law	High School	Nanny	Nil	1 beer per day to help social situations	Excessive shyness in brother
J.D.	31	M	R	Single	University	P/T Retail Job	Nil	Nil	Alcoholism, depression, excessive shyness
T.H.	31	F	R	Divorced	University	Office Customer Service	Migraines	Nil	Depression, suicide, psychosis, excessive shyness
H.T.	36	M	R	Separated	NAIT student	Restaurant Manager	Nil	Untreated Depression 1997	Nil
C.D.	37	M	R	Single	University	Night Auditor	Nil	Nil	Nil
K.E.	38	F	R	Divorced	University	Accountant	Synthroid 0.15mg qd since 1989	Depression in 1991. Trial of Fluoxetine 1991.	Depression in sister
B.L.	41	M	R	Married	College	Unemployed	Inner ear tumor removed 1987	Nil	Excessive shyness in maternal grandfather
D.L.	41	M	R	Single	College	Service Manager	Nil	Nil	Excessive shyness in 2 siblings
R.P.	49	M	L	Divorced	High School	Pipe Valve Fitter	Migraines; Hypercholesterolemia	Nil	Nil

Two patients had recently dropped out of university secondary to social anxiety symptoms, as E.A. described himself as being too self-conscious to ask the professor or classmates when papers and exams were due, which resulted in numerous incomplete assignments. Similarly, J.Z. dropped out of a health professional program because of intense anxiety around the group work that was being performed. Interestingly, C.D. is a man who took a night job for the purpose of avoiding the increased social contact that occurred during the day, while H.T. was struggling with keeping employment as a night manager secondary to excessive social anxiety.

With respect to current DSM-IV diagnoses, all patients fulfilled the criteria for generalized SP while four patients fulfilled the additional criteria of avoidant personality disorder. E.A. also had agoraphobia without panic disorder, and T.H. suffered from a specific phobia. R.P. noted that he had mild dyslexia. Past psychiatric history included major depression (E.K. in 1991; H.T. in 1997), and alcohol dependence (B.L. over 20 years prior). Evaluation of family history in patients elicited 6 of 12 families with suspected individuals suffering from excessive shyness, and four families with at least one member who had probably suffered from a clinical depression.

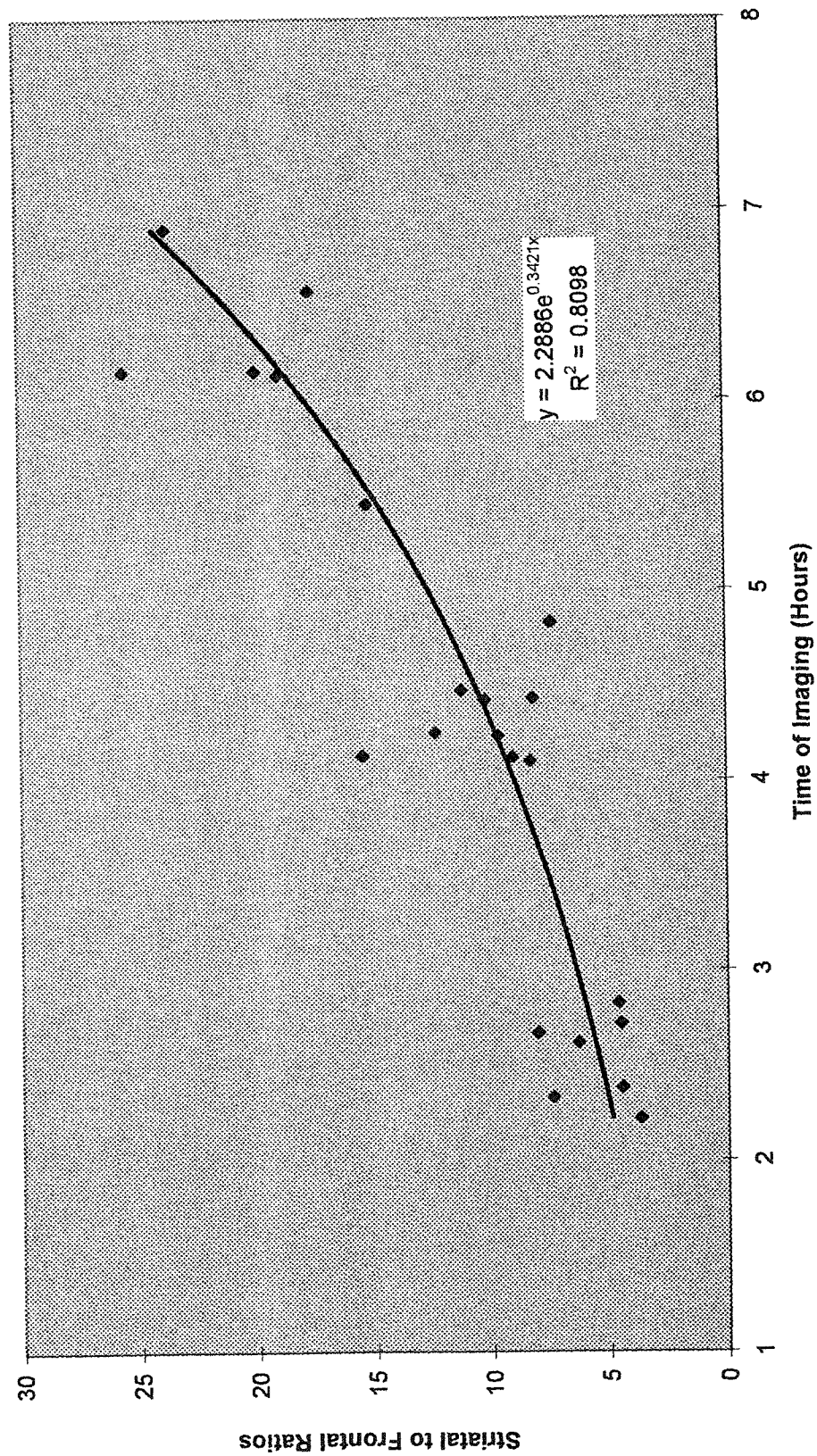
5.2 ^{123}I -Epidepride synthesis

Product yield was $92.0 \pm 1.7\%$. Product purity was $97.8 \pm 2.3\%$ following HPLC purification. The mean injected dose of ^{123}I -epidepride was 149.7 ± 16.6 mBq for patients, and 156.0 ± 17.3 mBq for controls, with no significant differences between the groups.

5.3 Imaging Time and Striatal to Frontal Ratios

There is an exponential increase in the striatal to frontal ratio with increasing imaging time, and figure 5.1 depicts this relationship for the controls. The exponential

Figure 5.1 Time of Imaging and Striatal to Frontal Ratios: Controls



increase is described by the equation $y = 2.886e^{0.3421x}$, with an R^2 value of 0.8098. For the purpose of pictorial comparison, figure 5.2 adds the data points from the patients with regards to imaging time and striatal to frontal ratios, and an increasing relationship between imaging time and the striatal to frontal ratio is also seen for the patients. Univariate statistical analysis reveals that striatal to frontal ratios, from both control and patient groups (as depicted in figure 5.2), are significantly correlated with the imaging time (table 5.3; $p=0.0014$).

5.4 Inter-individual variability in Striatal to Frontal Ratios

Evaluating the inter-individual variability of the striatal to frontal ratios between 4 and 5 hours (figure 5.3), the controls have striatal to frontal ratios that span from 7.39 to 15.49, with a range of 8.1, a mean of 10.21, a standard deviation of 2.53, and a coefficient of variation (COV) of 25%. Patient results from the same time period span from 9.56 to 35.69, with a range of 26.13, a mean of 13.25, a standard deviation of 9.90, and a COV of 75%. For this particular set of results, univariate regression analysis demonstrates that there is a trend for increasing imaging times to be associated with the striatal to frontal ratio ($p=0.07$), and that there is a trend for the patients to have increased striatal to frontal ratios in comparison to the controls ($p=0.07$).

5.5 ANALYSIS OF RESULTS: THREE APPROACHES

There are three approaches to the analysis of the data, and the following paragraphs provide the rationale for each of the methods used. In overview, analysis 1 attempts to control for the variations in imaging time by maximizing the number of observations ($n=27$), at the detriment of repeating observations from the same subjects. In contrast, analysis 2 time-matches each control, as closely as possible, to one of the patients, with the disadvantage of

Figure 5.2 Time of Imaging and Striatal to Frontal Ratios: Patients versus Controls

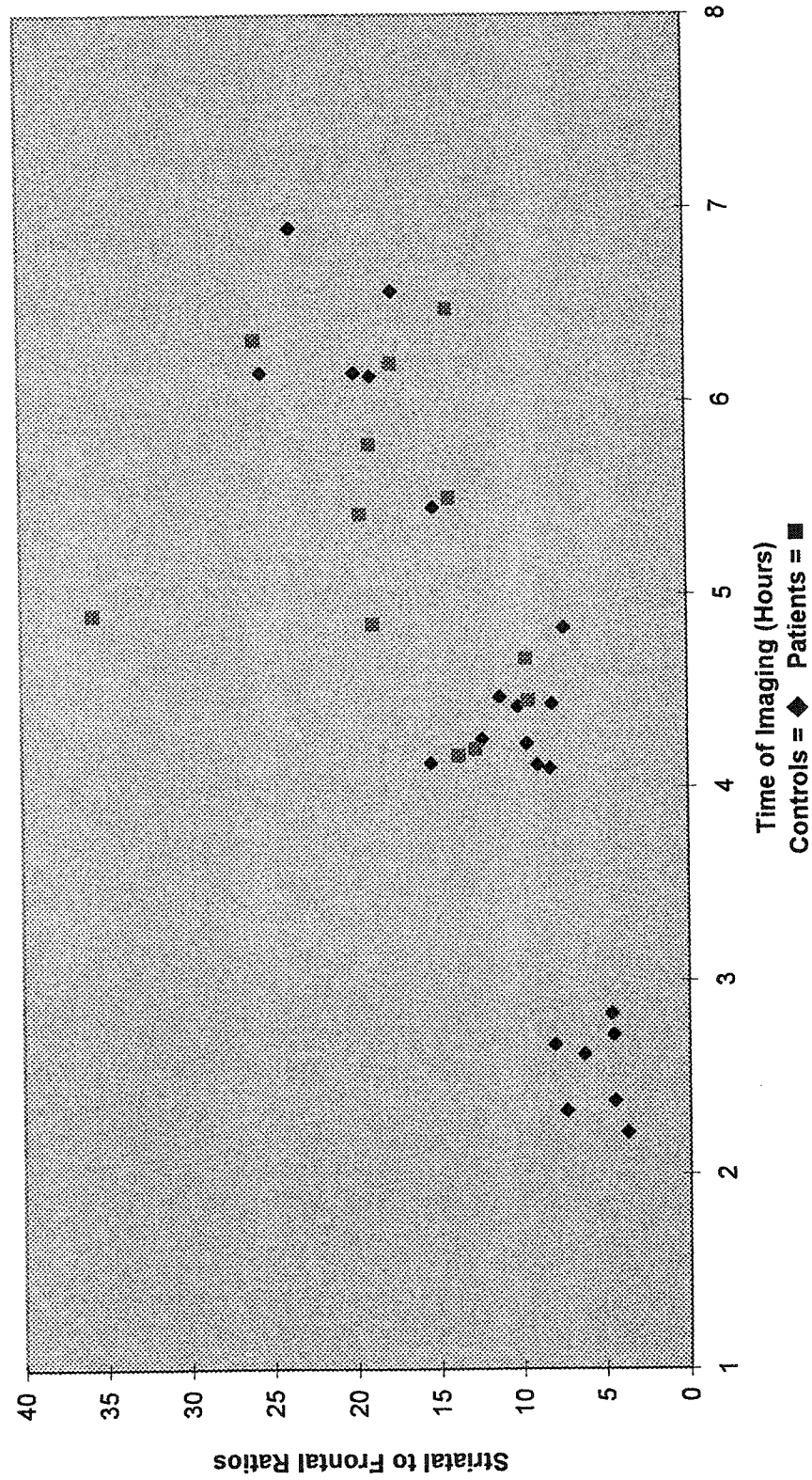


**Figure 5.3 Striatal to Frontal Ratios for
Social Phobia Patients and Controls:
Imaging Times between 4 and 5 hours**

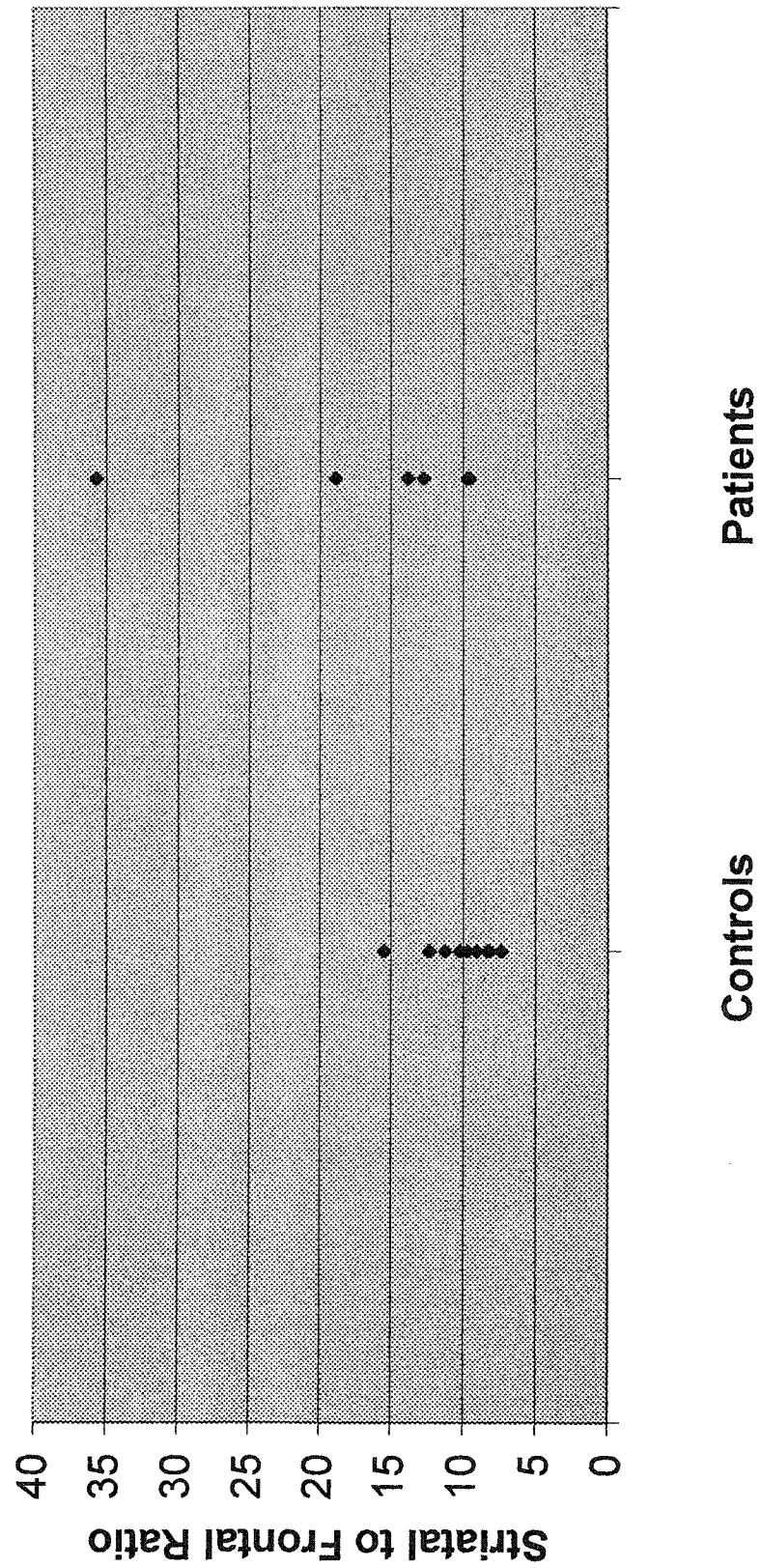


**TABLE 5.3: UNIVARIATE CORRELATION AMONG
VARIABLES OF INTEREST WITH P-VALUES:
ANALYSIS 1A (n=27)**

	Group	Striatal : Frontal
Imaging Time	0.43	0.0014
Dose	0.075	0.15
Matrix	1.9×10^{-5}	0.22
Gender	1	0.0036
Age	0.64	0.51
Group	--	0.19
LSAS	1.1×10^{-16}	0.12
CGI	1.5×10^{-19}	0.20
SIAS	7.4×10^{-14}	0.13

**TABLE 5.3: UNIVARIATE CORRELATION AMONG
VARIABLES OF INTEREST WITH P-VALUES:
ANALYSIS 1B (n=26)**

	Group	Striatal : Frontal
Imaging Time	0.62	3.87×10^{-6}
Dose	0.052	0.18
Matrix	5.06×10^{-5}	0.69
Gender	0.75	0.012
Age	0.55	0.69
Group	--	0.42
LSAS	3.14×10^{-16}	0.40
CGI	4.25×10^{-19}	0.59
SIAS	4.23×10^{-13}	0.30

decreasing the power, or number of observations ($n=22$). Lastly, while analyses 1 and 2 focus on primarily examining the relationship among the variables of striatal to frontal ratio, group, and symptom severity, analysis 3 focuses on the relationship between striatal to frontal ratios and gender. To this end, analysis 3 time-matches female and male pairs, regardless of whether the female is from the social phobia or control group. Also of importance, because the S:F ratio of K.E. is more than 2.5 standard deviations from the mean, each analysis is done with and without the score of K.E., and is respectively labelled analyses 1A and 1B, 2A and 2B, and 3A and 3B.

5.5.1 Analysis One: 27 Observations

Analysis 1 involves the inclusion of 27 observations that are comprised of 10 controls, 5 of whom had repeated scans 6 hours post-injection, and 12 patients (Table 5.2). Including 15 observations from the control group is advantageous because the striatal to frontal ratios are highly correlated to imaging time ($p=0.0014$), and the added number of control observations allow better comparison to the significant spread of imaging times in the patient group (range of patient imaging times is 4.17 to 6.48 hours, with a standard deviation of 0.24). The disadvantage of this first approach of data analysis is the unequal comparison of control and patient observations, as observations from the same subject are made *twice* in the control group for 5 cases, whereas observations are only taken *once* from each patient. As noted in the previous chapter on methods, all control observations made less than 4 hours post-injection were excluded.

Table 5.2 SUMMARY OF PATIENT AND CONTROL RESULTS FOR ANALYSIS 1: Gender, Imaging Time, Symptom Severity^a, Length of Illness^b and Striatal to Frontal Ratio^c

OBS	Patients	Age	Sex	Dose	Matrix	Imaging time	LSAS	SIAS	CGI	LOI	S:F
1	D.L.	41	M	163	64	4.17	69	47	4	36	13.79
2	T.H.	31	F	122	64	4.20	66	64	4	27	12.72
3	C.D.	37	M	140	128	4.45	98	56	5	27	9.56
4	B.L.	41	M	164	64	4.67	92	63	5	23	9.66
5	H.T.	31	M	122	64	4.85	96	63	4	24	18.92
6	K.E.	39	F	166	64	4.90	98	59	5	34	35.69
7	J.Z.	24	F	145	128	5.42	98	51	4	--	19.64
8	A.E.	25	M	132	64	5.50	91	55	5	12	14.26
9	J.D.	31	M	169	128	5.78	91	55	5	24	19.00
10	R.P.	50	M	165	128	6.20	81	56	4	38	17.67
11	J.B.	28	F	139	64	6.32	94	69	4	23	25.86
12	R.R.	26	M	131	64	6.48	77	48	4	22	14.30

OBS	Controls	Age	Sex	Dose	Matrix	Imaging Time	LSAS	SIAS	CGI	LOI	S:F
13	M.F.	35	M	176	128	4.10	16	11	1	0	8.28
14	B.Y.	31	M	137	128	4.12	2	7	1	0	9.04
15	L.D.	40	F	173	128	4.13	8	0	1	0	15.49
16	W.L.	48	M	169	128	4.23	16	8	1	0	9.67
17	M.B.	27	F	139	128	4.25	25	12	1	0	12.38
18	B.B.	33	M	172	128	4.42	16	14	1	0	10.23
19	I.C.	33	M	141	128	4.43	0	3	1	0	8.15
20	R.T.	27	M	135	128	4.47	27	20	1	0	11.26
21	G.S.	28	M	148	128	4.83	19	9	1	0	7.39
22	F.N.	37	F	170	128	5.45	8	29	1	0	15.24
23	W.L.	48	M	169	128	6.13	16	8	1	0	18.98
24	M.F.	35	M	176	128	6.15	16	11	1	0	19.94
25	L.D.	40	F	173	128	6.15	8	0	1	0	25.55
26	B.B.	33	M	172	128	6.57	16	14	1	0	17.61
27	F.N.	37	F	170	128	6.90	8	29	1	0	23.72

^a Observation number

^b Liebowitz Social Anxiety Scale (LSAS); Social Interaction Anxiety Scale (SIAS); and Clinical Global Impression Scale (CGI)

^c Length of Illness (LOI)

^d Striatal to Frontal Ratio (S:F)

5.5.1.1 *Univariate Analysis 1A and 1B*

Table 5.3 shows the results from univariate correlation analysis among variables of interest. To look for possible confounding factors that might bias group differences, correlation analysis of group versus variables of interest shows that, for both analysis 1A and 1B, there are no significant differences between patients and controls with respect to imaging time, administered dose of epidepride, gender, or age. There is, however, a significant difference in matrix, as a 128 x 128 matrix was used for all controls, while a 64 x 64 matrix was used for 8 patients, and a 128 x 128 matrix used for 4 patients. Of importance, in both analysis 1A and 1B, striatal to frontal ratios were not significantly correlated to the matrix used, dosed administered, age, or group.

The striatal to frontal ratio was significantly correlated to imaging time ($p=0.001$) and gender ($p=0.004$) in analysis 1A. With the removal of the outlier F.N., analysis 1B shows a marked increased significance in imaging time ($p<0.001$), and a decreased significance of gender ($p=0.012$), with respect to the striatal to frontal ratio. There is also a trend for the administered epidepride dose to be higher in controls than patients ($p=0.075$ and $p=0.052$, for analysis 1A and 1B respectively).

5.5.1.2 *Multivariate Analysis 1A and 1B*

Because univariate correlation analysis demonstrates that both time and gender are significantly associated with the striatal to frontal ratio, table 5.4 shows multivariate correlation analysis using three independent variables of time, gender, and a variable of interest (i.e. group, age, LSAS, SIAS, and CGI) versus the dependent variable of striatal to frontal ratio. Results show that when the imaging time and gender are taken into account, there are no significant correlations between group, age, SIAS, and the striatal to frontal ratio for analysis 1A or 1B. In analysis 1A, however, there is a correlation in which increasing LSAS scores are significantly associated with higher striatal to frontal

TABLE 5.4 ANALYSIS 1A: MULTIVARIATE ANALYSIS OF RESULTS FOR N=27 OBSERVATIONS

Each table illustrates the correlations, given in *p-values*, between a set of multiple independent variables of interest and the dependent variable (not shown), which is the striatal to frontal ratio.

TIME	0.00072	TIME	0.00062	TIME	0.00060	TIME	0.0010	TIME	0.00059	TIME	0.00065
SEX	0.0017	SEX	0.00093	SEX	0.00086	SEX	0.0018	SEX	0.00089	SEX	0.0016
GROUP	0.18	AGE	0.17	LSAS	0.049	SIAS	0.18	CGI	0.077	---	

TABLE 5.4 ANALYSIS 1B: MULTIVARIATE ANALYSIS RESULTS FOR N = 26 OBSERVATIONS

Each table illustrates the correlations, given in *p-values*, between a set of multiple independent variables of interest and the dependent variable (not shown), which is the striatal to frontal ratio.

TIME	0.0000011	TIME	0.00000075	TIME	0.0000011	TIME	0.0000015	TIME	0.0000011	TIME	0.00000063
SEX	0.0010	SEX	0.00076	SEX	0.00088	SEX	0.0014	SEX	0.0010	SEX	0.0012
GROUP	0.28	AGE	0.22	LSAS	0.23	SIAS	0.43	CGI	0.35	---	

ratios ($p=0.049$), while there is also a trend for increasing CGI scores to be associated with higher striatal to frontal ratios ($p=0.077$). In analysis 1B, when the observation for K.E. is taken out, there is no longer a significant association between the LSAS ($p=0.23$) or CGI ($p=0.35$) scores and the striatal to frontal ratios ($p=0.23$, and $p=0.35$ respectively).

In multivariate analysis 1A, imaging time ($p<0.00065$) demonstrates a significant positive correlation to the striatal to frontal ratio ($p<0.001$), while females have significantly higher striatal to frontal ratios than males ($p=0.002$). With the removal of the outlier in analysis 1B, the significance of the imaging time is markedly increased ($p=0.00000063$), while the significance of gender remains steady ($p=0.0012$).

5.5.2 Analysis Two: Time-Matched, Patient and Control Pairs

The second approach to the analysis of data involves selecting 10 observations from the controls, without having any observation taken from a subject more than once, based on matching the control subject imaging time, as closely as possible, to the imaging time of a corresponding patient. Thus, in contrast to analysis 1, where variations in imaging time are dealt with by increasing the number of control observations, analysis 2 accounts for variations in imaging time by directly matching the imaging time of a control subject to a corresponding patient imaging time. With the approach of analysis 2, there is no significant difference between the imaging times of patients and controls, and the data set used for analysis 2 is presented in Table 5.5, and graphically depicted in Figure 5.4. Analysis 2 is also divided into 2A, which includes the S:F ratio of K.E., and 2B, which excludes the result of K.E.

5.5.2.1 Univariate analysis 2A and 2B

Similar to univariate analysis 1A and 1B, Table 5.6 shows that there are no statistically significant differences between social phobia patients and controls with regards to imaging time, administered dose of epidepride, gender, or age. As explained in the previous section, there is a

**Table 5.5 SUMMARY OF PATIENT AND CONTROL RESULTS FOR ANALYSIS 2:
TIME-MATCHED PATIENTS AND CONTROLS AND THEIR GENDER, IMAGING TIME, SYMPTOM
SEVERITY, AND STRIATAL TO FRONTAL RATIO**

Match ^a	Control	Time	Dose	Matrix	Age	Sex	LSAS	SI	AS	CGI	S:F	Match	Patient	Time	Dose	Matrix	Age	Sex	LSAS	SI	AS	CGI	S:F
1	B.Y.	4.12	137	128	31	M	2	7	1	9.04		1	D.L.	4.17	163	64	41	M	69	47	4	13.79	
2	L.D.	4.13	173	128	40	F	8	0	1	15.49		2	T.H.	4.20	122	64	31	F	66	64	4	12.72	
3	M.B.	4.25	172	128	33	F	25	12	1	12.38		3	C.D.	4.45	140	128	37	M	98	56	5	9.56	
4	I.C.	4.43	141	128	33	M	0	3	1	8.15		4	B.L.	4.67	164	64	41	M	92	63	5	9.66	
5	R.T.	4.47	135	128	27	M	27	20	1	11.26		5	H.T.	4.85	160	64	37	M	96	63	4	18.92	
6	N/A ^a											6	K.E.	4.90	166	64	39	F	98	59	5	35.69	
7	G.S.	4.83	148	128	28	M	19	9	1	7.39		7	J.Z.	5.42	145	128	24	F	98	51	4	19.64	
8	F.N.	5.45	170	128	37	F	8	29	1	15.24		8	A.E.	5.50	132	64	25	M	91	55	5	14.26	
9	N/A ^a											9	J.D.	5.78	169	128	31	M	91	55	5	19.00	
10	W.L.	6.13	169	128	48	M	16	8	1	18.98		10	R.P.	6.20	165	128	50	M	81	56	4	17.67	
11	M.F.	6.15	176	128	35	M	16	11	1	19.94		11	J.B.	6.32	139	64	28	F	94	69	4	25.86	
12	B.B.	6.57	172	128	33	M	16	14	1	17.61		12	R.R.	6.48	131	64	26	M	77	48	4	14.3	
Mean							13.7 ^b					Mean							87.6 ^b				

^a No control was matched to this particular patient. ^b The difference between the LSAS score means is $p < 0.00001$.

Figure 5.4 Analysis 2A. LSAS scores vs Striatal to Frontal Ratios for Time-Matched, Patient-Control Pairs

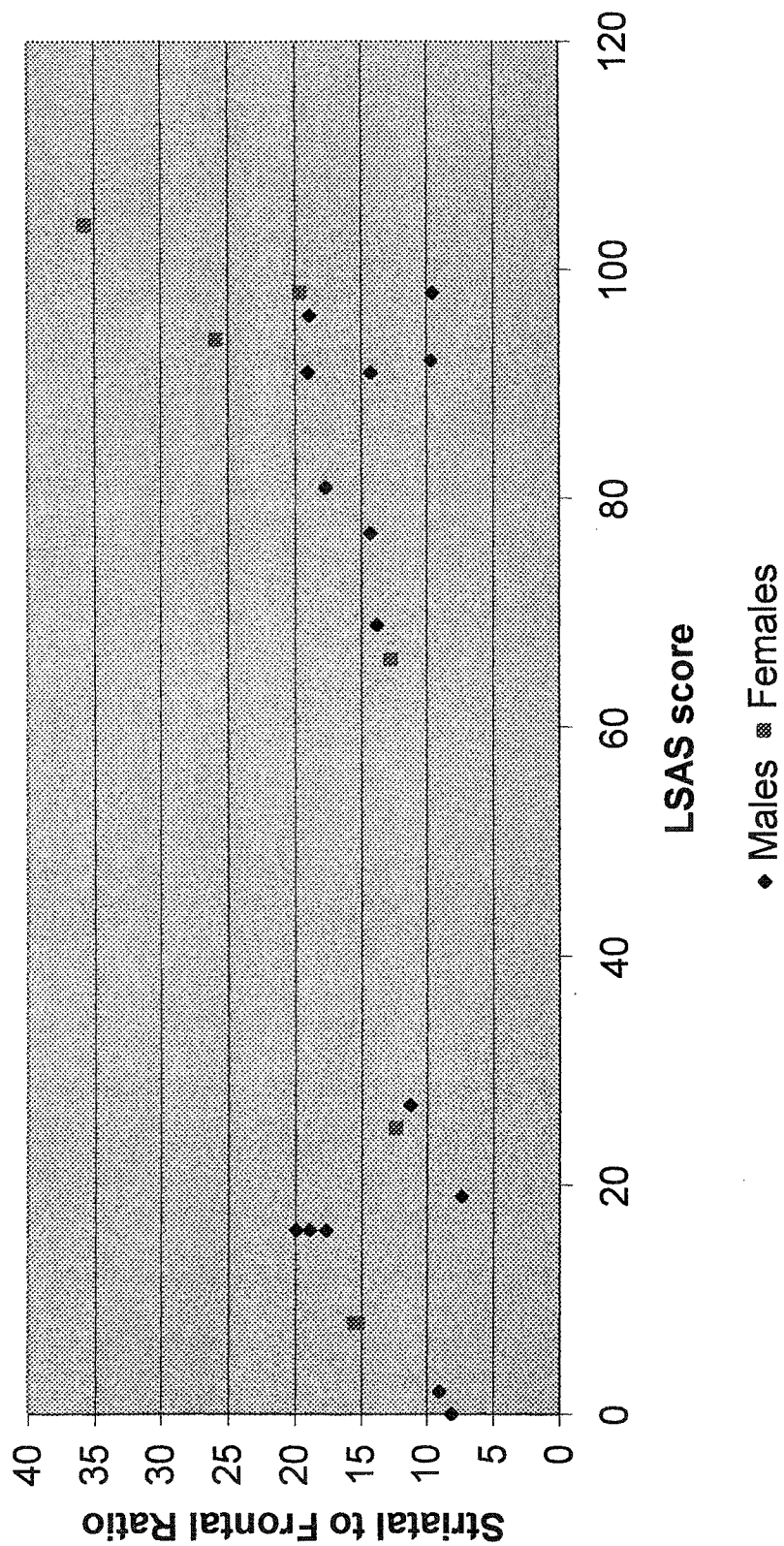


TABLE 5.6 UNIVARIATE REGRESSION BETWEEN VARIABLES OF INTEREST: ANALYSIS 2A (n=22)

	Group	Striatal : Frontal
Imaging Time	0.64	0.038
Dose	0.39	0.078
Matrix	0.00038	0.19
Gender	0.87	0.054
Age	0.93	0.44
Group	--	0.15
LSAS	6.87 x 10-13	0.059
CGI	4.67 x 10-15	0.15
SIAS	5.86 x 10-12	0.098

TABLE 5.6 UNIVARIATE REGRESSION BETWEEN VARIABLES OF INTEREST: ANALYSIS 2B (n=21)

	Group	Striatal : Frontal
Imaging Time	0.58	0.00064
Dose	0.30	0.10
Matrix	0.00080	0.58
Gender	0.90	0.21
Age	0.96	0.69
Group	--	0.26
LSAS	1.75 x 10-12	0.17
CGI	1.27 x 10-14	0.42
SIAS	2.96 x 10-11	0.17

difference in the matrix used between the two groups, but the matrix does not correlate significantly to the striatal to frontal ratio in either analysis 2A or 2B. Also in keeping with the results from the previous section, increasing imaging time is significantly correlated with increasing striatal to frontal ratios ($p=0.038$), and this association is strengthened when the outlier (K.E.) is taken out ($p=0.00064$).

Compared to univariate analysis 1, there is only a trend for female gender to be significantly correlated to increasing striatal to frontal ratios ($p=0.054$), and this trend disappears when the outlier is taken out ($p=0.21$). Also different from analysis 1, there is a trend for the administered dose to be positively correlated to the striatal to frontal ratio, as opposed to the group, which is no longer evident when the outlier is removed in analysis 2B.

5.5.2.2 Multivariate analysis 2A and 2B

Table 5.7 shows multivariate correlation in which the three independent variables of imaging time, gender, and a variable of interest are evaluated for their relationships to the dependent variable of the striatal to frontal ratio. When imaging time and gender are taken into account, there is no significant association between the variables of group (Figure 5.5), age, SIAS, CGI and the striatal to frontal ratio. Similar to analysis 1, but of diminished strength, analysis 2A shows a trend for increasing LSAS scores to be associated with increasing striatal to frontal ratios ($p=0.07$, Figure 5.4); however, this trend is not present when the outlier is removed in analysis 2B.

As in analysis 1, table 5.7 reveals that the imaging time has a significant positive correlation to the striatal to frontal ratio ($p=0.008$), and this correlation is increased when the outlier is removed ($p<0.001$). Female gender is also significantly associated with the striatal to frontal ratio ($p=0.01$), and similar to analysis 1, this association remains steady when the outlier is removed. The relationship between gender and the striatal to frontal ratio is graphically depicted in figure 5.6.

TABLE 5.7 ANALYSIS 2A: MULTIVARIATE ANALYSIS OF RESULTS FOR N=22 OBSERVATIONS.
Each table illustrates the correlations, *given in p-values*, between a set of multiple independent variables of interest and the dependent variable (not shown), which is the striatal to frontal ratio.

TIME	0.0087	TIME	0.0064	TIME	0.010	TIME	0.012	TIME	0.0077	TIME	0.0075
SEX	0.0094	SEX	0.0056	SEX	0.010	SEX	0.015	SEX	0.0082	SEX	0.010
GROUP	0.16	AGE	0.16	LSAS	0.07	SIAS	0.18	CGI	0.11	----	

TABLE 5.7 ANALYSIS 2B: MULTIVARIATE ANALYSIS RESULTS FOR N = 21 OBSERVATIONS
Each table illustrates the correlations, *given in p-values*, between a set of multiple independent variables of interest and the dependent variable (not shown), which is the striatal to frontal ratio.

TIME	0.00012	TIME	0.000093	TIME	0.00014	TIME	0.00016	TIME	0.00012	TIME	0.000080
SEX	0.013	SEX	0.0099	SEX	0.012	SEX	0.018	SEX	0.013	SEX	0.014
GROUP	0.24	AGE	0.30	LSAS	0.18	SIAS	0.27	CGI	0.32	----	

Figure 5.5 ANALYSIS 2B: IMAGING TIMES AND STRIATAL TO FRONTAL RATIOS FOR TIME-MATCHED PATIENT AND CONTROL PAIRS

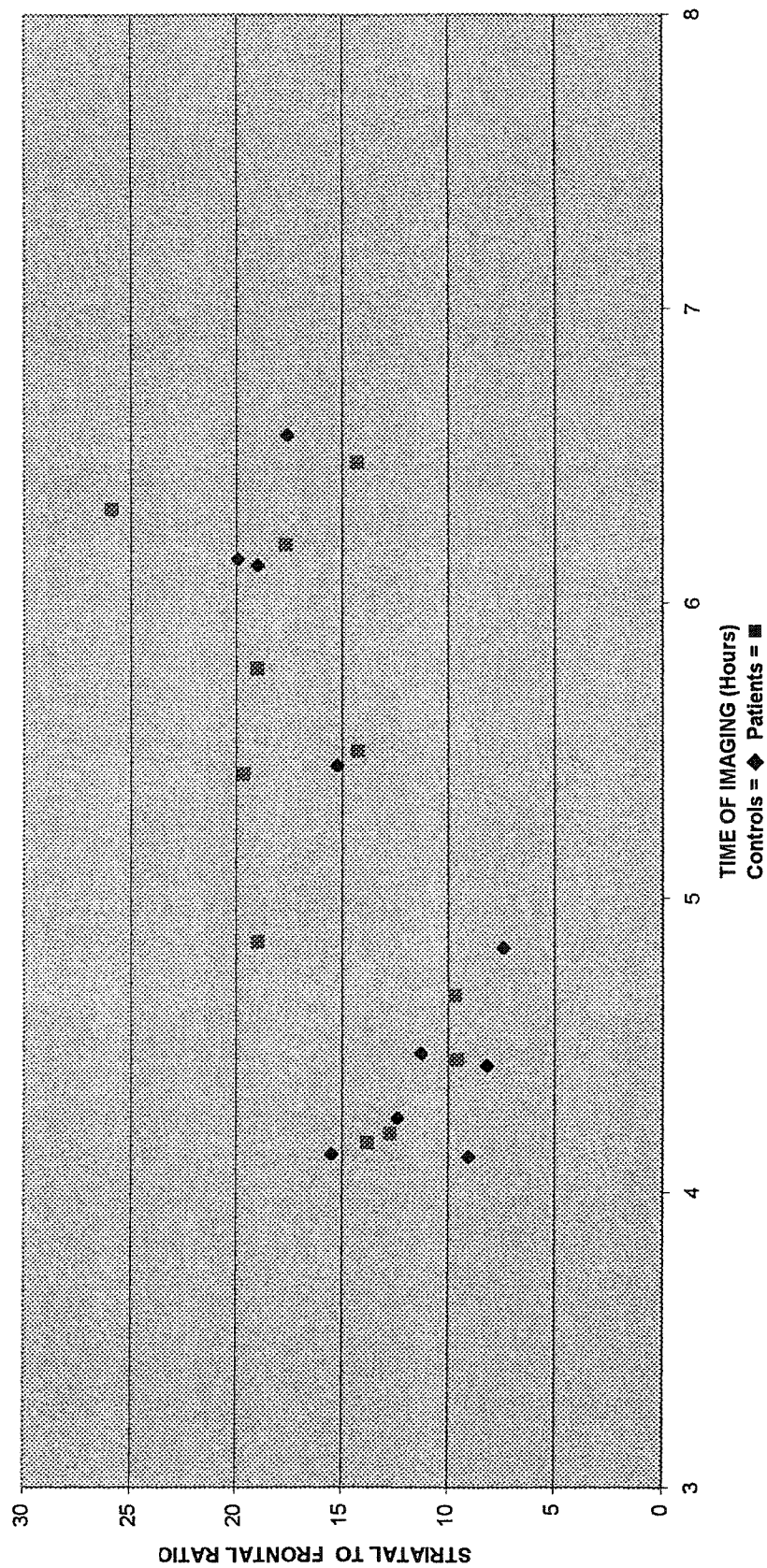
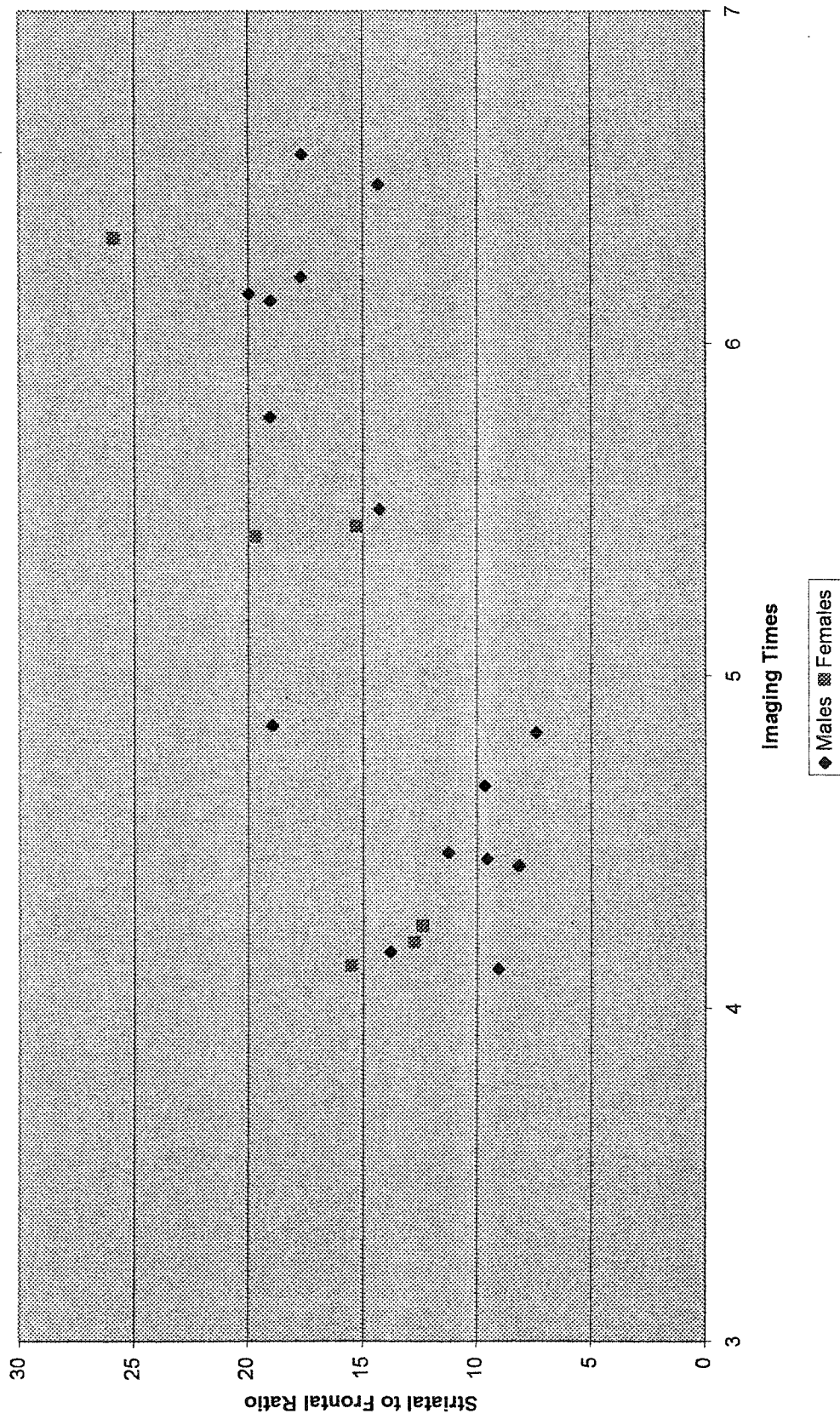


Figure 5.6 Analysis 2B: Imaging Time and Striatal to Frontal Ratio: Males versus Females



5.5.3 Analysis Three: Time-Matched Male and Female Pairs

While both analyses 1 and 2 found significant associations among the variables of imaging time, striatal to frontal ratio, and gender, the number of male observations is greater than the number of female observations. In analysis 2A, for example, there are 7 females versus 15 males. This inequality introduces a bias in the statistical analysis of gender and striatal to frontal ratios. To eliminate this bias, analysis 3 matches the 7 female subjects to the 7 male subjects whose imaging times most closely match each female subject, regardless of group. The data used for analysis 3 is summarized in table 5.8.

5.5.3.1 Univariate analysis 3A and 3B

Table 5.9 summarizes the data for univariate analysis 3A and 3B. Of note, there is no difference between males or females with regards to imaging time, dose, matrix, age, group nor measures of social anxiety. There is a trend for gender to be significantly correlated to the striatal to frontal ratio ($p=0.069$), but this disappears when the outlier pair is removed ($p=0.20$). Interestingly, in analysis 3A, social phobia patients ($p=0.042$) and increasing LSAS ($p=0.008$), CGI ($p=0.024$), and SIAS ($p=0.020$) scores are all significantly associated with the striatal to frontal ratio. When the outlier pair containing K.E. is removed, the LSAS ($p=0.025$) and SIAS ($p=0.032$) scores still remain significantly associated with the striatal to frontal ratio, while there is a weak trend for the group ($p=0.079$) and CGI ($p=0.094$) to be associated with the striatal to frontal ratio. The imaging time is significantly correlated to the striatal to frontal ratio ($p=0.014$) only when the outlier pair is removed in analysis 3B.

**Table 5.8 SUMMARY OF RESULTS FOR ANALYSIS 3: TIME-MATCHED MALES AND FEMALES
TIME-MATCHED PATIENTS AND CONTROLS AND THEIR GENDER, IMAGING TIME, SYMPTOM
SEVERITY, AND STRIATAL TO FRONTAL RATIO**

Match ^a	Males	Time	Dose	Matrix	Age	LSAS	SIAS	CGI	S:F	Match	Females	Time	Dose	Matrix	Age	LSAS	SIAS	CGI	S:F
1	B.Y.	4.12	137	128	31	2	7	1	9.04	1	L.D.	4.13	173	128	40	8	0	1	15.49
2	D.L.	4.17	163	64	41	69	47	4	13.79	2	T.H.	4.2	122	64	31	66	64	4	12.72
3	W.L.	4.23	169	128	48	16	8	1	9.67	3	M.B.	4.25	139	128	27	25	12	1	12.38
4 ^b	G.S.	4.83	148	128	28	19	9	1	7.39	4 ^b	K.E.	4.90	166	64	39	98	59	5	35.69
5	J.D.	5.78	169	128	31	91	55	5	19.00	5	J.Z.	5.42	145	128	24	98	51	4	19.64
6	A.E.	5.50	132	64	25	91	55	5	14.26	6	F.N. ^b	5.45	170	128	37	8	29	1	15.24
7	R.R.	6.48	131	64	26	77	48	4	14.30	7	J.B.	6.32	139	64	28	94	69	4	25.86

^a Match number corresponds to a male-female pair that has been matched as closely as possible with regards to imaging time.

^b Match pair number 4 was taken out of analysis 3B because her striatal to frontal ratio is greater than 2.5 standard deviations away from the mean. Please see text for details.

^c Liebowitz Social Anxiety Scale (LSAS); Social Interaction Anxiety Scale (SIAS); and Clinical Global Impression Scale (CGI)

^d Striatal to Frontal Ratio (S:F)

TABLE 5.9: UNIVARIATE CORRELATION AMONG VARIABLES OF INTEREST WITH P-VALUES: ANALYSIS 3A (n=14)

	Gender	Striatal : Frontal
Imaging Time	0.90	0.17
Dose	0.94	0.45
Matrix	1	0.14
Gender	0	0.069
Age	0.89	0.91
Group	1	0.042
LSAS	0.81	0.0081
CGI	0.89	0.024
SIAS	0.57	0.020

TABLE 5.9: UNIVARIATE CORRELATION AMONG VARIABLES OF INTEREST WITH P-VALUES: ANALYSIS 3B (n=12)

	Gender	Striatal : Frontal
Imaging Time	0.88	0.014
Dose	0.85	0.92
Matrix	0.60	0.52
Gender	0	0.20
Age	0.59	0.22
Group	0.60	0.079
LSAS	0.74	0.025
CGI	0.43	0.094
SIAS	0.95	0.032

5.5.3.2 *Multivariate analysis 3A and 3B*

Knowing that previous analyses suggest that imaging time, gender--and possibly social anxiety symptom severity--have an influence on the striatal to frontal ratio, table 5.10 examines these relationships in a multivariate correlation analysis. In analysis 3A, female gender ($p=0.033$) and increasing LSAS scores (0.022) are significantly associated with the striatal to frontal ratios (Figure 5.7); however, imaging time is not significantly associated with the striatal to frontal ratio. When the outlier pair is taken out in analysis 3B, imaging time reverts to being significantly associated with striatal to frontal ratios ($p=0.005$), whereas there is a trend for females to have higher striatal to frontal ratios ($p=0.052$, Figure 5.8), and LSAS is no longer significant ($p=0.12$).

TABLE 5.10 ANALYSIS 3A: MULTIVARIATE ANALYSIS OF RESULTS FOR N=14 OBSERVATIONS.

Each table illustrates the correlations, given in *p-values*, between a set of multiple independent variables of interest and the dependent variable (not shown), which is the striatal to frontal ratio.

TIME	0.50	TIME	0.045	TIME	0.82	TIME	0.61	TIME	0.59	TIME	0.11
SEX	0.035	SEX	0.036	SEX	0.033	SEX	0.079	SEX	0.019	SEX	0.048
GROUP	0.085	AGE	0.19	LSAS	0.022	SIAS	0.12	CGI	0.029	----	

TABLE 5.10 ANALYSIS 3B: MULTIVARIATE ANALYSIS RESULTS FOR N = 12 OBSERVATIONS

Each table illustrates the correlations, given in *p-values*, between a set of multiple independent variables of interest and the dependent variable (not shown), which is the striatal to frontal ratio.

TIME	0.041	TIME	0.014	TIME	0.080	TIME	0.061	TIME	0.048	TIME	0.0054
SEX	0.034	SEX	0.060	SEX	0.030	SEX	0.059	SEX	0.027	SEX	0.052
GROUP	0.20	AGE	0.65	LSAS	0.12	SIAS	0.29	CGI	0.17	----	

Figure 5.7 Analysis 3A. LSAS scores and Striatal to Frontal Ratios: Time-matched, Male-Female Pairs

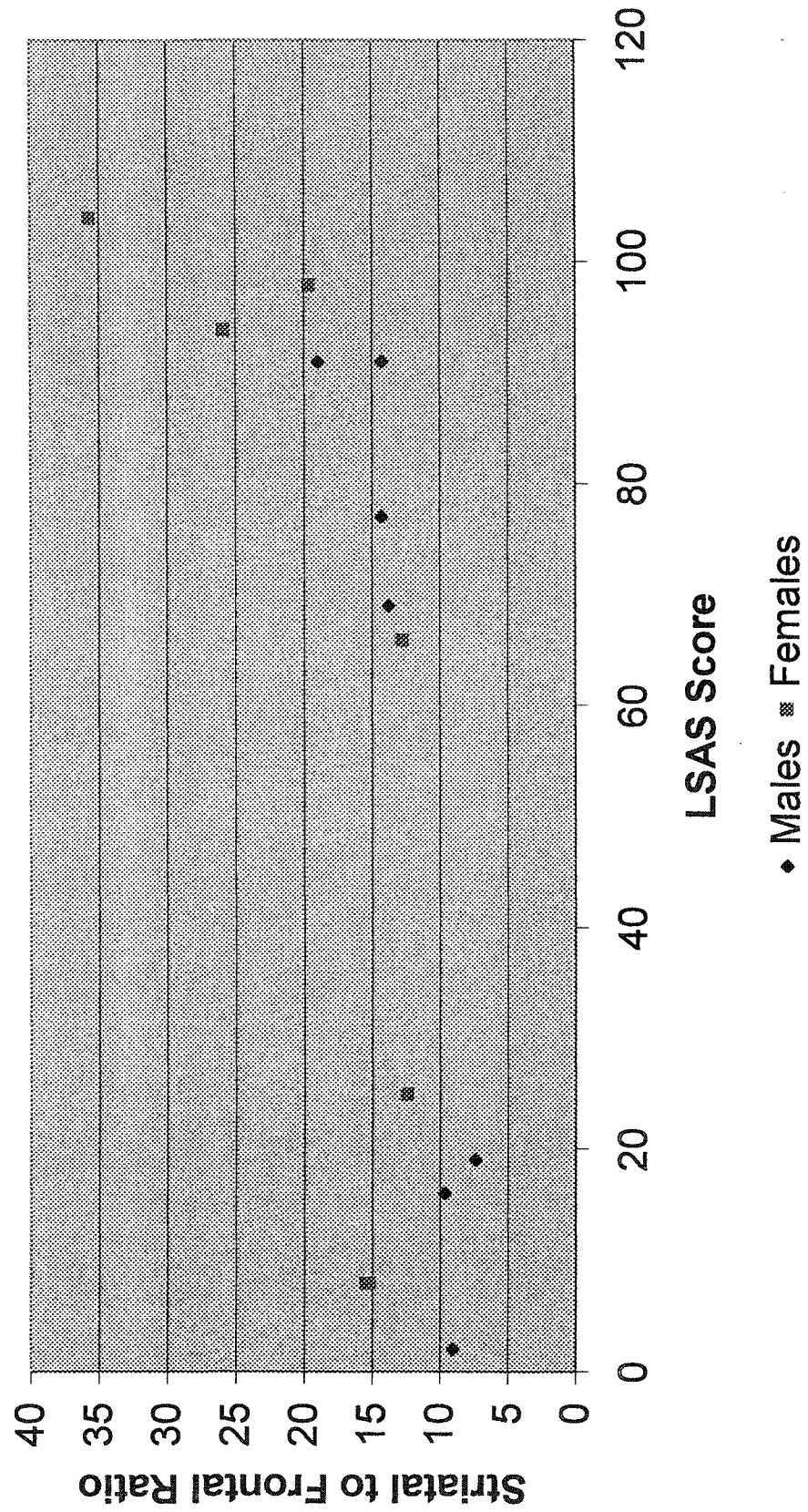
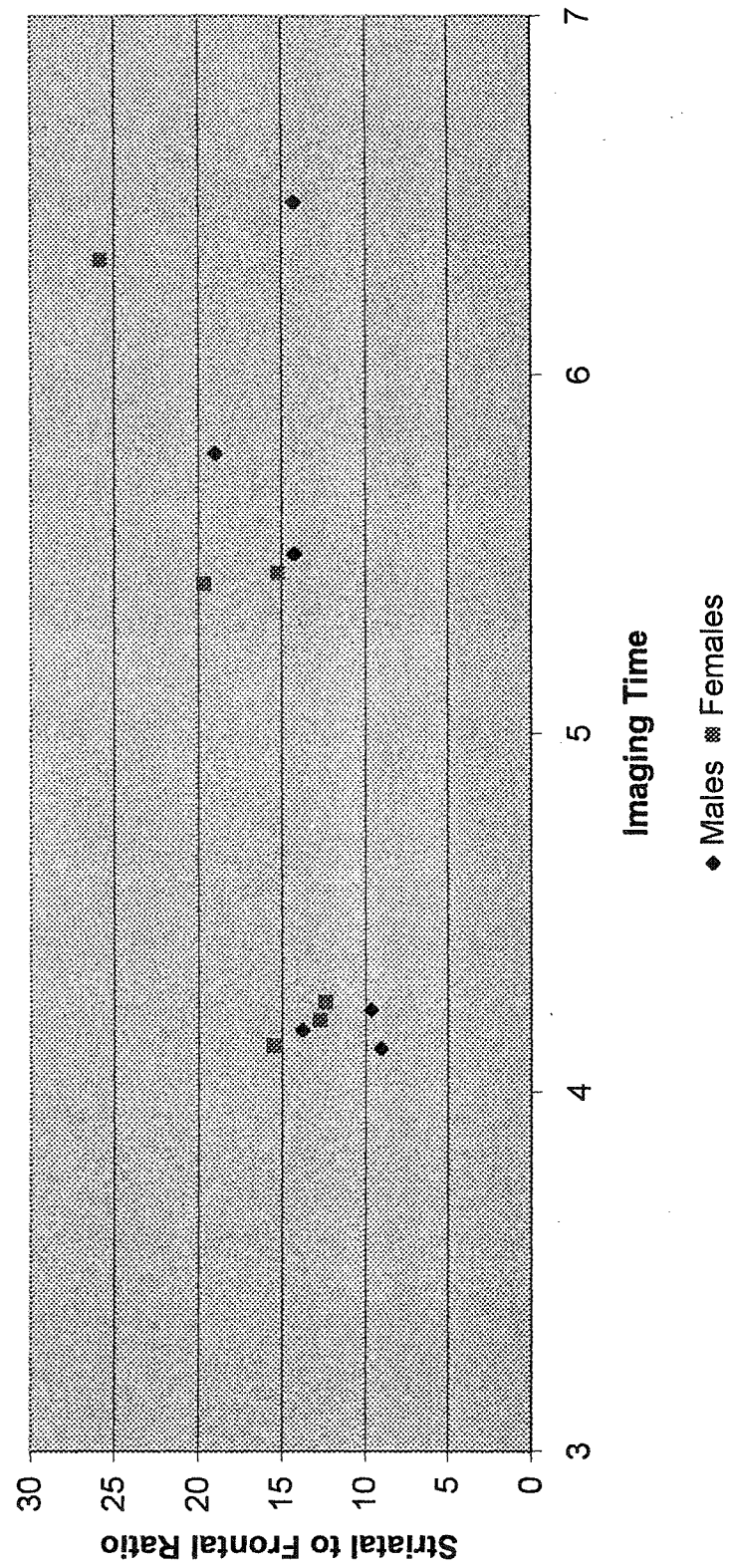


Figure 5.8 Analysis 3B: Imaging Time and Striatal to Frontal Ratio: Time-Matched Males versus Females



Summary of Results

In summary of the key results, the following are noted:

1. Social phobia patients and healthy controls do not differ significantly with respect to age, administered epidepride dose, or overall imaging times. There is a significant difference between patients and controls with regards to matrix, as all controls and 4 patients were done using a 128 x 128 matrix, whereas 8 patients used a 64 x 64 matrix. There is, however, no significant correlation between the matrix used and the resulting striatal to frontal ratio. The striatal to frontal ratio is not significantly correlated to age or administered epidepride dose.
2. There is large inter-individual variability in striatal to frontal ratios, and for imaging times between 4 and 5 hours, there is a COV of 25% for controls and a COV of 75% for patients.
3. In multivariate analyses 1, 2, and 3, there are no statistically significant differences between social phobia patients and healthy controls with respect to striatal to frontal ratios.
4. In multivariate analyses 1A and 2A, increasing imaging time is significantly correlated with increasing striatal to frontal ratios ($p < 0.001$, $p = 0.008$, respectively). There is a marked increase in this significance when the outlier is taken out in analyses 1B and 2B ($p < 0.001$, $p < 0.001$, respectively). In addition, the imaging time, which was not significantly correlated to striatal to frontal ratios in multivariate analysis 3A, becomes significant in 3B ($p = 0.005$) with the removal of the outlier.
5. In multivariate analyses 1A, and 3A, there is a statistically significant positive correlation between LSAS scores and the striatal to frontal ratio ($p = 0.049$, and $p = 0.022$), and a trend towards significance in analysis 2B ($p = 0.07$). When the

outlier is taken out, however, in analyses 1B, 2B, and 3B, there are no significant multivariate correlations among the variables of LSAS scores and striatal to frontal ratios.

6. In multivariate analyses 1A and 2A, female gender is significantly associated with higher striatal to frontal ratios ($p=0.002$, $p=0.010$), and the level of significance remains steady even when the outlier is taken out ($p=0.002$, $p=0.014$). With the removal of the outlier from analysis 3A, the level of significance diminishes slightly ($p=0.048$) to a trend level of significance ($p=0.052$).

Chapter 6

Discussion of Methodology

6.1 HIGH INTER-INDIVIDUAL VARIABILITY OF STRIATAL TO FRONTAL RATIOS

The results of this study show that there is a statistically significant correlation between increasing LSAS and the striatal to frontal ratio in multivariate analyses 1A and 3A ($p=0.049$, $p=0.022$), with a trend level of significance in analysis 2A. In spite of this, no differences were detected between social phobia patients and healthy controls. A possible explanation includes the fact that measuring social anxiety on a spectrum, via the LSAS scores, allows a more sensitive detection of correlations between social anxiety and striatal dopamine; in contrast, separating individuals into the two groups of patients and controls does not account for the reality that even healthy controls, while not meeting the SCID-IV criteria for social phobia, have a spectrum of social anxiety symptoms that can be measured. In this particular study, discovering potential

differences between social phobia patients and controls is further complicated by the study findings of large inter-individual variability in striatal to frontal ratios where, between the imaging times of 4 and 5 hours, the COV for striatal to frontal ratios is 25% for controls and 75% for patients. Such large inter-individual variability renders it problematic to detect differences between social phobia patients and controls without a large study size.

Other studies have also noted significant inherent variability in striatal to reference region ratios, and have commented on how this might interfere with estimations of binding ratios (Stephenson et al, 2000; Pilowsky, 1999, personal communication). While this variability may reflect underlying biology, there is a need to examine how the data acquisition and experimental design may contribute to the high COV in striatal to frontal ratios. The following section discusses improvements in the data acquisition process that could diminish the variability of striatal to frontal ratios, and then formulates an understanding of the usefulness of striatal to frontal ratios from a review of epidepride kinetics. Suggestions for future experimental designs using epidepride will also be provided.

6.2 IMPROVEMENTS IN DATA ACQUISITION

Given that proper quality control is being done as described in chapter 2, this study could decrease the inter-individual variability in striatal to frontal ratios with the use of a consistent matrix size, fiducial markers, co-registration with MRI images, and attenuation correction. In this study, eight patients were examined using 64 x 64 matrices, while four patients and all ten controls had data acquired using 128 x 128 matrices. Increasing the matrix size improves the spatial resolution, but in order to preserve adequate count statistics from the source, there should be relative increases in variables such as the number of projections, time per projection, patient dose, and

processing time. Accordingly, observations from table 6.1 show that there are three subjects with data acquired using 128 x 128 matrices who have very low count statistics, which is likely a function of insufficient processing time. With poor count statistics in both the striatum, and particularly the frontal region, noise interference from adjacent regions becomes problematic and can introduce error into the measurements.

Table 6.1 Striatal Counts for each Patient-Control Pair (Analysis 2)

Match ^a	Control	Time	Dose	Matrix	Striatal Counts (counts/pixel)	Match	Patient	Time	Dose	Matrix	Striatal Counts (counts/pixel)
1	B.Y.	4.12	137	128	4534	1	D.L.	4.17	163	64	4606
2	L.D.	4.13	173	128	6484	2	T.H.	4.2	122	64	4661
3	M.B.	4.25	172	128	879	3	C.D.	4.45	140	128	6056
4	I.C.	4.43	141	128	6021	4	B.L.	4.67	164	64	4036
5	R.T.	4.47	135	128	5921	5	H.T.	4.85	160	64	5534
6	N/A ^a					6	K.E. ^b	4.9	166	64	5371
7	G.S.	4.83	148	128	647	7	J.Z.	5.42	145	128	6208
8	F.N.	5.45	170	128	13790	8	A.E.	5.5	132	64	4684
9	N/A ^a					9	J.D.	5.78	169	128	142.5
10	W.L.	6.13	169	128	15504	10	R.P.	6.2	165	128	6325
11	M.F.	6.15	176	128	15108	11	J.B.	6.32	139	64	5030
12	B.B.	6.57	172	128	6682	12	R.R.	6.48	131	64	5054

Table 6.1 also shows several controls with high count statistics, and this may be due to longer processing times. When count statistics are sufficient, such as in subjects with high count statistics, the use of different matrices is compensated for by the ratio method; however, when count statistics are poor, there is increased inter-individual variability because of error introduced by noise interference. Thus, improved monitoring of the processing time and ensuring that all subjects have data acquired using the same matrix would have diminished the inter-individual variability in the final striatal to frontal ratios.

In order to take advantage of enhanced resolution with increasing matrix size, it is important to properly compare corresponding brain slices among individuals, and this is best done using fiducial markers. Fiducial markers are radioactive sources (e.g. 200kBq of $^{99m}\text{TcNaTcO}_4$) that are placed on the left and right sides of the head to define the canthomeatal plane. They allow proper positioning of the head with respect to the gantry, and also are used to appropriately coregister (i.e. align) multiple images from each subject so that there is consistent analysis of the same regions of interest from multiple brain slices both within and among individuals. Because SPECT provides poor anatomical resolution in comparison to MRI, it is also possible to specifically identify brain regions in SPECT by coregistering SPECT images to MRI acquired images using specialized software (Friston et al, 1995), thereby providing much more accurate definition of regions of interest than could be acquired by SPECT alone. Moreover, striatal imaging can be more accurately divided into imaging of the caudate and putamen, while frontal cortical imaging can be divided into the superior and middle frontal gyri (Fujita et al, 1999). The use of fiducial markers and SPECT/MRI coregistered images also have additional advantages with regards to attenuation correction. Attenuation correction requires that the edges of the skull are properly identified, and this can be done using fiducial markers, but much more elegantly by a coregistered

SPECT/MRI image of an ellipse drawn around the skull. Attenuation correction is then frequently done by assuming uniform attenuation equal to that of water ($\mu = 0.12\text{cm}$) within the outlined ellipse around the skull. In this study, the striatal to frontal ratios are derived from counts that are not attenuation corrected because it was difficult to define the edges of the skull without fiducial markers, and the application of attenuation correction may consequently introduce more error. In summary, improvements in data acquisition that would likely have diminished the inter-individual variability of striatal to frontal ratios involve the use of a single matrix, fiducial markers, SPECT-MRI image coregistration, and attenuation correction.

6.3 THE CHALLENGE OF EPIDEPRIDE KINETICS

Even if data acquisition in this study were improved, one must consider whether or not inter-individual variability might be complicated by challenges conferred by epidepride kinetics. Interest in the use of epidepride is partially due to its property of high D2 receptor affinity relative to other SPECT D2 ligands such as ^{123}I -IBZM. This property of high D2 receptor affinity may actually pose more challenges when the ratio method is employed, with theoretical implications on rapid non-specific binding washout and the time to the establishment of equilibrium. Other kinetic considerations that may introduce error include the influence of the lipophilic metabolite of epidepride, and differences in plasma clearance. These factors and their potential influence on the measurement of striatal to frontal ratios will be discussed in the following sections.

6.3.1 *Rapid Washout of Non-Specific Binding With Resulting High Background Noise*

Potential reasons for the high interindividual variability can be deduced by noting that if striatal D2 counts are relatively stable between two and seven hours (Appendix A),

while S:F ratios increase with time (Figure 5.1), there must be a diminishing of measured counts from the reference frontal region. The decreasing frontal counts over time is primarily due to washout of free ligand and non-specific binding. There is also a small component of specific binding washout from the frontal cortex that may confound the ability to use the frontal cortex as a reference region to measure specific binding in the striatum; however, specific binding in the frontal cortex is minimal after four hours, and for all purposes, approaches that of the cerebellum at that time (Kornhuber, 1995). The rapid washout of non-specific binding, which is a function of the high affinity of epidepride, may introduce methodologic difficulties in terms of using the ratio method. With increasing time, radioactive counts in the reference regions (e.g. frontal cortex and cerebellum) quickly diminish in an exponential fashion to low levels. Because the reference region rapidly becomes count poor, there is significant noise interference which causes variability in reference region counts; this in turn increases the intra-individual variability of the final striatal to frontal ratios. Such an observation has also been confirmed in other groups using epidepride (Stephenson, 2000; personal communication, Pilowsky).

While there is more inter-individual variability in ratios of the striatum to a reference region because noise interferes with the radioactive counts in reference regions at the time of peak striatal uptake, this is potentially less of a problem for extra-striatal imaging. In the temporal cortex, for example, the peak uptake of epidepride occurs much earlier than that of the striatum (mean = 45 minutes) because of decreased receptor density in the temporal cortex relative to the striatum (Kornhuber et al, 1995). At 45 minutes, the radioactive count statistics in reference regions are much better, thus minimizing noise interference and theoretically rendering the ratio method more appropriate for the study of extrastriatal D2 receptors. Thus, when using the ratio method, the high affinity of epidepride for D2 receptors is potentially more advantageous

for extrastriatal D2 receptor imaging, but introduces challenges for striatal imaging because of the decreased signal to noise ratio at the time of peak striatal uptake.

6.3.2 *Inter-individual Variations in the Peak Uptake of Epidepride*

The purpose of the ratio method is to provide information regarding the binding parameters of a ligand to its receptor. Some of the characteristic measurements include K_d , which is a measure of the affinity of a ligand to its receptors; B_{max} , which is the concentration of available binding sites in the ROI; and V_d , which is the volume of distribution in the compartment with specific binding. Due to the kinetics of epidepride, V_d is also denoted as V_3 in the literature, and is equivalent to the binding potential, which is B_{max} / K_d . Following the injection of a radioligand, the ratio between the radioactive counts in the ROI to the radioactive counts in plasma, at the time of the maximal count rate in the ROI (t_{max}), represents the binding potential at steady-state (V_d) (Pinborg et al, 2000). This “peak equilibrium method” is often simplified by substituting the plasma input function for a receptor-free ROI, such as the cerebellum or frontal cortex in epidepride, where the binding potential is represented by the ratio of specific binding to non-specific binding at the time of peak uptake (Farde et al, 1989).

The problem with the peak equilibrium method or its simplified ratio form, however, is that it is essential to determine the time of peak uptake (t_{max}) because it is the only time at which there are steady-state conditions in a bolus paradigm, such as that used in our study with the initial injection of epidepride. Consequently, the determination of t_{max} is crucial for directly measuring binding potential, or steady-state V_d . Compounding the situation further, it has been recently shown that t_{max} varies widely among individuals, ranging from 238 ± 115 minutes (COV of 41%, Fujita et al, 1999), as a function of differences in receptor density and plasma clearance (Pinborg et al, 2000). The importance of receptor density and t_{max} can be understood by recalling that steady-

state occurs more quickly in regions with a lesser number of receptors; thus, steady-state occurs at an earlier time in the temporal cortex versus the striatum. Extending this principle to inter-individual situations, a patient with increased D2 receptor density in comparison to a control will have a t_{\max} that occurs later. It is easily seen, then, that if the specific binding in the ROI, non-specific binding in the reference region, and the plasma radioactivity are collected at t_{\max} , which is most often defined as the mean peak time of uptake for patients and controls—the ratio method will underestimate the difference between patients and controls, such that true differences may be concealed. Conversely, if a patient group has decreased D2 receptor density in comparison to a control group, the patients will achieve steady-state earlier; if a mean t_{\max} between patients and controls is then applied, there will be an overestimation of the V_d for the patients, which will again diminish differences between patients and controls (Pinborg et al, 2000). In summary, without determining the t_{\max} for each patient, any true differences between patients and controls will be more difficult to detect; more importantly, the binding potential is not correctly derived without first finding the time of peak uptake, which has been shown recently to vary from individual to individual.

Using ^{123}I -epidepride, Fujita et al. (1999) examined the validity of employing specific to non-specific binding ratios to determine the binding potential. In their study, because it can be laborious to determine t_{\max} for every subject, they used a bolus and constant infusion of epidepride to create equilibrium conditions. This design allows the establishment of a steady-state over a period of time, during which one SPECT scan and one blood sample can be used to theoretically determine the binding potential, V_3 . They compared V_3 obtained under the equilibrium conditions with the V_3 approximated by specific to non-specific binding ratios at 3, 4, and 5 hours, and found statistically non-significant correlations between the ratio method and the V_d 's of the striatum or temporal cortex (Fujita et al., 1999). As a result, the ratio method does not provide a fully valid

measurement of the binding potential of D2 receptors which, as previously discussed, is caused by the rapid non-specific binding washing out in the reference region, and by the inter-individual variability in t_{\max} .

The varying times at which ratios were collected in this study, in which t_{\max} is not determined for each individual, renders it difficult to get a direct measure of binding potential. In order to properly determine t_{\max} , multiple and frequent short scans with blood sampling must be done in order to, as closely as possible, determine t_{\max} . Thus, the S:F ratios used in our study do not directly reflect binding potential, but at best, provide a degree of approximation of the binding potential. Interestingly, Ichese et al (1999) found that in comparison with the simple ratio method (ratio of specific binding to non-specific binding), the ratio of striatal binding to temporal cortex binding, also called the "limbic selectivity index", provides a better correlation with quantitative measures of D2 binding potential. Stephenson et al. (2000) state that this is not surprising because the variability from non-specific binding in target regions with D2 receptors, like the striatal cortex and temporal cortex, tend to be similar and thus should ostensibly cancel each other out. Applying the same arguments to this current study, the striatal to frontal ratio may offer a more valid correlation to the true binding potential, than striatal to cerebellum ratios, because variability from non-specific binding in target regions may be more uniform, and are controlled for to a greater extent than in reference regions completely free of D2 receptors.

6.3.3 *Lipophilic Metabolite Interferes with Imaging of Parent Compound*

Another potential reason for the large inter-individual variability in S:F ratios arises from possible interference of radio-labelled metabolites other than the parent compound. Various studies employing gradient high-performance liquid chromatography (HPLC) have demonstrated that epidepride is metabolised into lipophilic

and polar metabolites (Bergstrom et al, 2000). Following studies of benzamide analogues such as remoxipride, a benzamide undergoes metabolism to an N-dealkylated compound and to pyrrolidone and hydroxypyrrolidone derivatives (Halldin et al, 1995). As a result, the lipophilic metabolite of epidepride may be assumed to be a lactam, which does not bind specifically to receptors (Swahn et al, 1997). The lipophilic metabolite, however, will cross the blood-brain barrier, and its presence will likely interfere with imaging of the parent compound binding specifically to D2 receptors.

Bergstrom et al (2000) investigated the influence of the lipophilic metabolite of epidepride on D2 receptor SPECT imaging in 16 health subjects. They found a statistically significant linear correlation between the striatum to cerebellar ratio and the amount of lipophilic labelled metabolite that was measured ($p < 0.02$). Furthermore, the percentage of lipophilic metabolite in subjects varied widely from 0% to 26.1%, while the striatum to cerebellar ratio varied between 10.2% and 15.2%. Thus, the specific binding of epidepride to D2 receptors, when measured using striatal to cerebellar ratios, is affected significantly by the amount of lipophilic metabolite produced—which itself varies among individuals. Therefore, variations in the lipophilic metabolite also account for wide inter-individual variations when the ratio method is employed.

6.3.4 *Inter-individual variability in Plasma Clearance*

Another variable that contributes to inter-individual variability in striatal to frontal ratios is the inter-individual differences in plasma clearance. The plasma concentration of epidepride influences the counts in the non-specific binding compartment, and because this varies from individual to individual, Pinborg (2000) et al describe that there is an inter-individual variability in the rate of exponential decrease of non-specific binding washout. This subsequently introduces more variability into the reference region.

6.4 POTENTIAL ALTERNATIVE TECHNIQUES TO THE MEASUREMENT OF EPIDEPRIDE D2 BINDING

Because of difficulties inherent to the ratio method imposed by rapid washout of non-specific binding with relatively large amounts of background noise; inter-individual variations in the time of peak uptake of epidepride due to differences in receptor density and plasma clearance; and the lipophilic metabolite of epidepride; there has been a movement away from semiquantitative techniques towards quantitative methods of measuring D2 binding. These methods are based on a three-compartment analysis of epidepride kinetics, and include techniques of equilibrium, kinetic, multilinear, and graphical analyses. In the following discussion, the three compartment model of epidepride kinetics will be described, and a summary of the aforementioned quantitative techniques will be outlined.

6.4.1 *Three Compartment Modelling*

As depicted in Figure 6.1, the three compartment modelling of epidepride involves a plasma compartment (C1), non-displaceable brain compartment (C2, or receptor free brain tissue), and a receptor compartment (C3). The non-displaceable brain compartment, C2, consists of free and non-specifically bound radioactivity due to both parent and metabolite epidepride compounds. Several assumptions are made in this model, and they include: 1) The parent and lipophilic metabolite in plasma equilibrate quickly with the plasma proteins such that the free fraction remains constant over time; 2) there is a rapid equilibrium reached between free tissue radioactivity and non-specifically bound radioactivity in C2; 3) the rate of parent to metabolite production is negligible ($k_5 = 0$; Figure 6.1); 4) The distribution volume of free tissue and non-specific binding of the parent and metabolite compounds are the same in the receptor

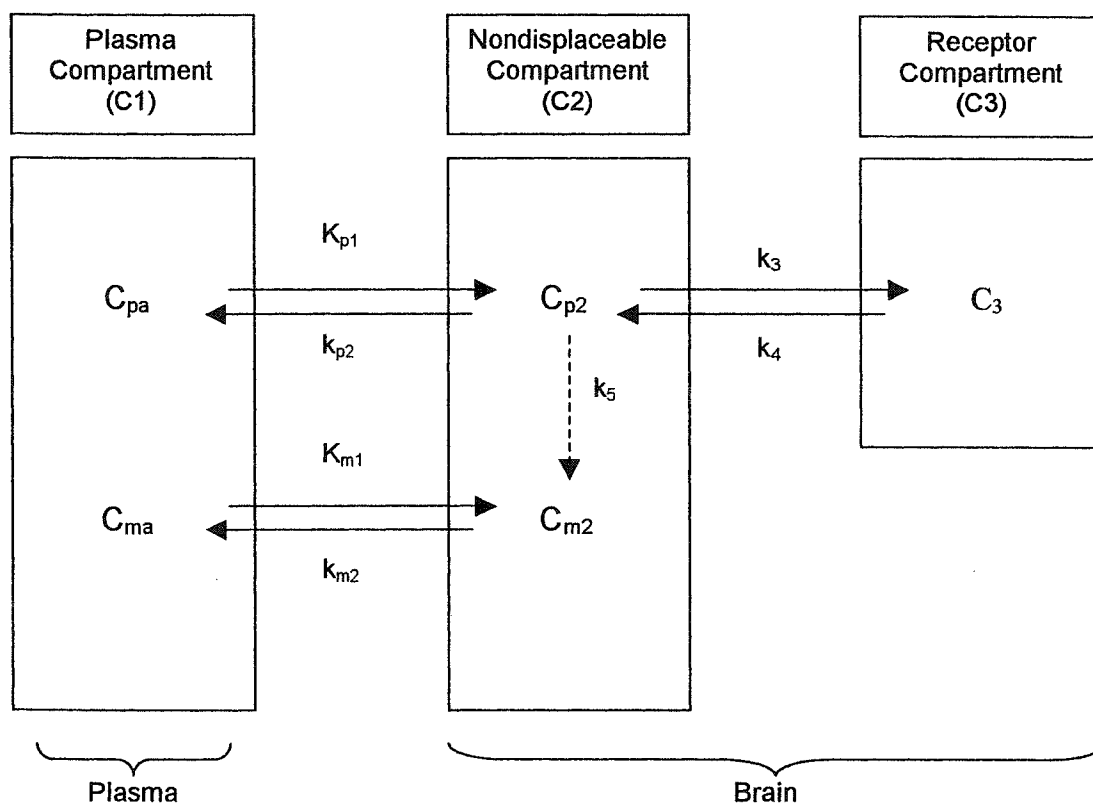


Figure 6.1 Three compartment model of ^{123}I -epidepride kinetics. C_{pa} denotes the radioactivity of the parent compound in plasma, and C_{ma} denotes the radioactivity of the metabolite in the plasma. Six rate constants, K and k , are shown (Adapted from Fujita et al, 1999 and Ichise et al, 1999). Please see text for details.

free tissue (C2) as they are in the receptor compartment (C3); 4) The model follows first-order kinetics for transfer between compartments (Ichise et al, 1999; Fujita et al, 1999).

6.4.2 Equilibrium Analyses (Bolus-Infusion paradigm)

As previously discussed, the binding potential of a receptor can only be determined using the ratio method when the time of equilibrium or peak striatal uptake is obtained. Complicating matters, this time of equilibrium differs from individual to individual due to factors such as plasma clearance and also receptor density. To overcome the difficulty of variations in time of equilibrium, the bolus-infusion paradigm involves a bolus injection of a radioligand that is followed by a constant infusion that establishes a period of steady-state conditions. Under equilibrium conditions when brain and plasma activities are stable, the distribution volume of the parent tracer, or binding potential, can be determined using one image acquisition and one blood measurement. This is given by the following equation:

$$V_3 = \frac{C_i(t_e)}{f_1 C_{pa}(t_e)}$$

where f_1 represents the free fraction of the parent tracer, t_e is the time at which equilibrium is established, $C_i(t)$ is the concentration of the parent tracer in a compartment i (kBq mL^{-1}) at t_e , and C_{pa} is the concentration of the parent tracer in arterial plasma at t_e .

The presence of metabolites can also be accounted for in this equilibrium model provided that certain assumptions are made. Firstly, the metabolite should have negligible affinity for the receptor of interest. Secondly, the distribution volume of the metabolite should be uniform throughout the brain, and therefore equal in the nondisplaceable and receptor compartments (i.e. C2 and C3). Should these assumptions be true, as they are often taken to be in studies of epidepride, the

radioactive counts in the receptor-rich region minus the radioactive counts in the receptor-free region will correct for metabolites and provide an accurate measure of specific or receptor binding. Taking the specific binding and dividing it by the plasma level of the parent tracer provides a measure of the equilibrium distribution volume: This is summarised by the following equation:

$$V_3 = \frac{C_3 - C_2}{f C_1}$$

Of note, determination of f , or the free fraction of radiotracer that is unbound to plasma proteins, may require octanol extraction and HPLC analysis.

There are some potential technical limitations to the equilibrium method or bolus-infusion paradigm with respect to epidepride. Because epidepride has high affinity for D2 receptors, it takes a significant length of time to achieve equilibrium in D2 rich areas such as the striatum. Consequently, Pinborg et al (2000) found that equilibrium conditions in the striatum were not reached even after 11 hours of infusion, with a bolus/infusion ratio of 20 hours. Fujita et al (1999) noted that equilibrium was reached in the striatum between 20 and 30 hours of infusion of epidepride, using a bolus/infusion ratio of 10 hours; furthermore, measurement of radioactivity in extrastriatal D2 regions between 20 and 30 hours results in very low count statistics (Fujita et al, 1999). On the other hand, studies focussing primarily on extrastriatal D2 receptor imaging can be feasibly done because equilibrium is reached much more quickly in regions with lower D2 receptors, and a bolus/infusion ratio of 3 hours with a total study time of 6 hours can be used to study temporal and frontal D2 binding (Pinborg et al., 2000). Other technical considerations in the application of the equilibrium model are that plasma clearance of epidepride may change significantly over a prolonged infusion of epidepride, and is likely further affected by food intake (Fujita et al, 1999).

In summary, the equilibrium model using a bolus/infusion paradigm provides a relatively practical approach to measuring extrastriatal receptors, which can be accomplished with one image acquisition and one blood sample in a period of six hours. Striatal imaging, however, presents more difficult problems because equilibrium is attained between 20 and 30 hours, a lengthy period that is difficult to tolerate and impractical for the average subject, patient, and study design. There are also several theoretical and technical caveats in the use of the equilibrium model that would not take into account any non-uniformities of metabolite distribution in the non-displaceable compartment, and changes in plasma clearance within and between subjects. Interestingly, in comparison to another D2 radioligand frequently used in the study of striatal D2 receptors, ^{123}I -IBZM allows the achievement of equilibrium conditions within one day using a bolus/infusion paradigm because of its larger K_d and resulting faster tissue clearance.

6.4.3 Kinetic Analysis (Bolus-injection paradigm)

In order to account for the lipophilic metabolite in epidepride metabolism, and to circumvent the difficulties of prolonged infusion times in order to obtain equilibrium conditions in the striatum, V_3 can also be determined using kinetic studies. This involves the calculation of V_3 in terms of kinetic rate constants that describe the three compartmental modelling illustrated in Figure 6.1. For example (Fujita et al, 1999),

$$V_3 = \frac{K_{p1}k_3}{k_{p2}k_4f_1} = \frac{B_{\max}}{K_d}$$

Furthermore, the distribution volumes in non-displaceable compartments are given by (Fujita et al, 1999):

$$V_{p2} = \frac{K_{p1}}{k_{p2}f_1}, \quad V_{m2} = \frac{K_{m1}}{k_{m2}f_1}$$

A simplified kinetic model for epidepride has also been tried in which the lipophilic metabolite is ignored. In such a case (Figure 6.1), V_3 can be mathematically derived using the following two equations:

$$V_3 = \frac{K_{p1}k_3}{k_{p2}K_4f}$$

$$V_2^* = \frac{V_{p2} + C_{Ma}(t_e) \cdot V_{M2}}{C_{Pa}(t_e)}$$

where V_2^* is termed the apparent distribution volume.

In a compartmental analysis, the rate constants from the aforementioned equations are solved using non-linear least squares fit modelling and differential equations. The data requires the input values of radioactive counts in multiple arterial plasma samples for parent compounds (and metabolite in two input modelling), and corresponding radioactive counts in the receptor free (C2) and receptor rich compartments (C3) at various times close to the arterial samplings. Fujita et al (1999), for example, studied 11 subjects and measured D2 receptor density in the striatum and temporal cortex, and compared the results obtained from two input compartmental model, the one input compartmental model, and the equilibrium model, the latter being used as the standard. They found that both the one and two input models correlated significantly with results of the equilibrium analyses in the striatum, with a mean COV of 8.3% among the three methods. In contrast, quantification of D2 receptors in lower density areas such as the temporal cortex was found to best correlate with the one input compartmental model. As explained by Fujita et al, this discrepancy is due to the poor identifiability of K_{M1} and k_{M2} , such that the two input model gives a poor estimate of V_{M2} .

Errors and variability in V_{M2} are much more likely to influence estimating $V3$ in brain regions with lower D2 receptor density, such as the temporal cortex, because the relative contribution of V_{M2} is much greater to $V3$ in these areas, than in the striatum.

Although the use of kinetic analyses to account for lipophilic metabolites (two plasma input functions) can closely correlate with D2 receptor density as obtained by the equilibrium method, there are considerable disadvantages to using kinetic analysis and a bolus-injection paradigm. Firstly, multiple arterial blood samples are required in conjunction with multiple SPECT images (greater than 25 per patient in the Fujita et al (2000) study), which limits the patient tolerability of this method; in contrast, the equilibrium method only requires one image acquisition and no arterial blood sampling. Secondly, the non-linear least squares fit and differential equations required to determine D2 receptor binding is a very technically demanding process. Furthermore, and perhaps most importantly, theoretical difficulties with the kinetic paradigm include assumptions which may introduce considerable error: 1) V_{p2} and V_{m2} are assumed to be the same across all brain regions; 2) cerebral blood flow is assumed to be equal across all brain regions. With the above disadvantages in mind, kinetic analyses do offer some benefits over the equilibrium (bolus-infusion paradigm) that include the determination of striatal D2 receptor density within a time period of 12 hours, as opposed to the lengthy 25-30 hours required in equilibrium studies; and the need only for one bolus injection instead of the bolus and constant infusion that is required in equilibrium studies.

6.4.4 Graphical Analysis and Simplified Quantification of D2 Receptor Binding

Ichise et al (1999) have derived complicated differential equations based on the three compartment model of epidepride kinetics to quantify D2 receptor binding using multilinear regression analysis (MLRA), graphical analysis and a "simplified analysis." The reader is referred to their publication (Ichise et al, 1999) to understand their

derivation of these equations. MLRA has an advantage over all other methods of analysis because it does not require the assumption that V_{m2} is identical across all brain regions, especially in light of evidence that V_{m2} is significantly higher in receptor-containing regions compared with the cerebellum (Ichise et al, 1999). MLRA, however, suffers from complicated calculations with some difficulties in identifying parameter estimates. Although necessitating the assumption of equal V_{m2} across all brain regions, Graphical analysis is a relatively simple means of calculating V_3' and allows better identification of parameter estimates than MLRA.

6.5 FUTURE DIRECTIONS

Research on employing epidepride in the recent two years has provided increased understanding of its use in the study of striatal and extrastriatal D2 receptors. During this time, initial excitement regarding the advantages of the high affinity and specificity characteristics of epidepride with regards to striatal imaging have become more tempered. This study illustrates that there is significant inter-individual variability in measures of striatal D2 binding, revealing a COV of 25% for controls and 75% for patients. This variability necessitates an examination of both the process of data acquisition and the theoretical validity of using the ratio method in light of epidepride kinetics. Improvements in the acquisition of data that could diminish the inter-individual variability include using a constant matrix and fiducial markers to allow better consistency of comparison of images both intra- and inter- individually. Fiducial markers would also allow co-registration with MRI images such that there is better anatomic resolution of the striatum, and enable attenuation correction to be performed. While improvements in data acquisition are important, an even more serious question involving the validity of the ratio method must be examined. Difficulties with the use of the ratio method include the fact that identification of the equilibrium time is essential, and this is

complicated by recent studies showing that the equilibrium time varies from individual to individual as a function of the D2 receptor density, which is the parameter of interest! Because of the high D2 specificity of epidepride, there is a relatively longer time to equilibrium in the striatum while non-specific binding washout is rapid from the reference region, resulting in poor signal-to-noise ratio that introduces error into the measurements. Lastly, a recent study demonstrates that the striatal to reference region ratio is significantly associated with the lipophilic metabolite of epidepride, the production of which also varies widely from individual to individual. In summary, this study demonstrates that the ratio method is associated with large inter-individual variability in both patients and controls that is likely explained by various kinetic considerations of epidepride. Given the methodological limitations, the striatal to frontal ratios can be seen, at best, as an approximation of the D2 binding potential.

Because of the aforementioned difficulties, there is a movement away from the semi-quantitative ratio technique towards quantitative techniques, particularly for high-affinity D2 radioligands such as epidepride. While not being widely described in the literature, there are a few studies that have used a bolus-infusion paradigm or a bolus-injection-only design to quantitatively examine D2 receptor densities. Even taking into consideration the usual SPECT challenges of scatter, partial volume and attenuation effects, these quantitative techniques are cumbersome and suffer from lengthy infusion times over 24 hours for striatal imaging (bolus-infusion paradigm), require multiple arterial blood sampling (bolus-injection paradigm), and utilize complicated mathematical derivations with numerous parameters to be fitted—resulting in decreased reliability from assumptions that need to be made.

A promising solution to these obstacles may involve the development of efficient semiquantitative techniques that are validated by the more cumbersome quantitative methods. For example, the simplified reference tissue model (SRTM), devised by

Lammertsma and Hume (1996), uses dynamic data acquired from both the region of interest (ROI) and the reference region (e.g. cerebellum) to produce time activity radioactive curves. The time activity curve of the region of non-specific D2 binding is then used to provide an indirect approximation of the plasma input function, as the dynamic data from the reference region allows the estimation of kinetic parameters of the free ligand (Table 6.1; Gunn et al, 1997). A mathematical equation that involves the binding potential, approximation of the plasma input function, and C3 (radioactivity in the receptor compartment) can be derived, solved in a convolution manner, and then fitted to the time activity curve in a least squares sense (Olsson and Farde, 2001). While this model has not been tested with epidepride, it has been used with high-affinity radioligands such as ^{11}C -FLB 457 (PET) and may have promise for application in SPECT—particularly given that the SRTM does not require arterial sampling and has less cumbersome computations than the quantitative techniques discussed in this chapter. Until more efficient quantitative or semi-quantitative techniques (e.g. SRTM) are developed for high affinity D2 radioligands, ^{11}C -raclopride (PET) and ^{123}I -IBZM may be preferable alternatives for the purpose of striatal D2 imaging.

Chapter 7

Striatal D2 Receptors, Social Phobia and Gender

7.1 Relationship Between Striatal D2 Receptors and Social Anxiety

This study finds that in analysis 1A and 3A, there is a statistically significant positive correlation between LSAS scores and the striatal to frontal ratio ($p=0.049$ and $p=0.022$), with a trend towards significance in analysis 2A ($p=0.07$). When the outlier is taken out, however, there are no significant multivariate correlations among the variables of LSAS scores and striatal to frontal ratios. The implication of these findings will be discussed from three perspectives; that of methodology and sample size, the normal biological variability of striatal D2 receptors, and lastly, a potential neurodegenerative hypothesis accompanied by a discussion of the role of the striatum in social phobia.

7.1.1 Methodology and Sample Size

It is difficult to draw firm conclusions from the finding of a statistically significant positive correlation between the LSAS score and the striatal to frontal ratio for various reasons. Firstly, the striatal to frontal ratio is, at best, an approximation of striatal D2 binding for reasons discussed in chapter four; at worst, the striatal to frontal ratio may have no relationship with striatal D2 receptor binding because this study did not define the time of striatal uptake of epidepride for each individual nor account for the lipophilic metabolite of epidepride. Secondly, the positive correlation between the LSAS score and the striatal to frontal ratio is tenuous because analysis 2, which is the most rigorous treatment of the data, shows only a trend significance that disappears when the one outlier is removed. Thirdly, there is significant inter-individual variability in the striatal to frontal ratios, with a large COV of 25% in controls and 75% in patients, which suggests that any differences between patients and controls may require a larger sample size.

Methodologic difficulties in the use of epidepride, discussed in chapter four, may explain why the findings of this study are in possible conflict with recent trends in research. In a PET study, Grant et al (1998) found that submissive monkeys in a group hierarchy, which may have relevance as an animal model for social phobia, have diminished post-synaptic D2 receptors. With respect to avoidant personality characteristics, a PET study with ^{11}C -raclopride by Farde et al (1997) showed that detachment, or avoidance of social involvement, is associated with decreased D2 receptors in the putamen, a finding replicated in a later PET study of 18 adults (Farde et al). Lastly, in a SPECT study employing ^{123}I -IBZM, Schneier et al (2000) found diminished striatal D2 receptor binding in 10 persons with social phobia relative to controls.

In summary, using the most rigorous treatment of the data in analysis 2, this study is the first to note a trend towards a positive correlation between striatal D2 binding and attributes of social avoidance and social fears, a result that must take into consideration the methodologic challenges of using epidepride, a potential skewing of results from one outlier, a relatively small sample size, and apparent conflict with trends in recent research.

7.1.2 Biological Variability in Dopamine D2 Receptors

Chapter four discusses how inter-individual variability in striatal to frontal ratios in this study that may be caused by challenges with data acquisition or epidepride kinetics. Adding to the complexity of devising appropriate experimental designs, there is a biological variability of striatal D2 receptors inherent in healthy volunteers. Consequently, adequate sample sizes may be needed to detect differences between social phobia patients and healthy controls, and trend results in this study with regards to LSAS score and the striatal to frontal ratio (analysis 2) may be due to the natural variability in dopamine D2 receptors. Farde et al (1995), in a PET study of healthy human volunteers, demonstrated a two to threefold range of inter-individual variability in dopamine D2 receptor density. Potential causes of this natural inter-individual variability are identified by Jonsson et al (1999), who in a ¹¹C-raclopride PET study of 56 healthy subjects, investigated the relationship between dopamine D2 receptor density and D2 receptor gene polymorphisms that exist naturally in the normal population. They found that high D2 receptor density was associated with a particular DRD2 promoter allele (-141C Del), while low dopamine receptor densities were associated with the DRD2 TaqIA1 allele, and the DRD2 TaqIB1 allele. With respect to another DRD2 polymorphism, a common silent intronic DRD2 short tandem repeat polymorphism (STRP) was found to not be associated with striatal D2 receptor density. Thus, the authors conclude that DRD2

genotypes may have differential effects on the regulation of D2 receptor density in healthy human subjects, and may certainly contribute to the inter-individual variability that is seen in healthy volunteers. It would be important to sort out how, even when taking into account alleles that may be associated with social avoidance (e.g. TaqIA1), other DRD2 alleles not associated with social phobia symptoms influence the measurement and comparison of D2 receptor density in studying social phobia and controls. Another important consideration includes the fact that social anxiety occurs along a spectrum even in healthy volunteers, and studies of DRD2 genotypes in “healthy volunteers” should therefore incorporate dimensional measures of extraversion-intraversion, social fears and social avoidance.

7.1.3 Understanding Social Phobia as a Continuum Disorder

Although differences between social phobia and control groups are not detected by this current study design, it is interesting that when both patients and controls are assimilated into one group and organized with regards to LSAS, there is a positive association between striatal to frontal ratios and the LSAS. Analyzing the data in this manner by combining the LSAS scores from both SP and control groups may be more ecologically valid because it reflects the spectrum of social anxiety that occurs in a population. These results may suggest a dimensional or continuum understanding of social anxiety symptoms, with the disorder defined by severity of impairment, as opposed to the current categorical DSM-IV division of discrete social phobia and generalized social phobia. In support of this, Stein et al (2000) examined the relationship among social phobia subtypes, symptoms, and severity in a community study of 2000 respondents, and found that the number of social fears was proportional to the degree of impairment, with no clear diagnostic thresholds or grouping of social phobia sub-types. Similarly, Merikangas et al (Biol Psychiatry, 2002), in a 15 year prospective longitudinal

community study of 4547 participants, provide evidence supporting social phobia as a spectrum disorder, noting a direct association between increasing social anxiety symptoms and severity, family history, autonomic lability, and comorbidity. Of significance, Merikangas et al (2002) observe that understanding social phobia as a spectrum is important because social phobia patients have a course of illness where they shift among having diagnostic, sub-threshold, and symptom levels of social anxiety over time. Furthermore, they noted that 61% of persons seeking treatment for social anxiety symptoms did not meet DSM-III-R criteria for social phobia, but did have sub-threshold and symptom levels of social anxiety. Thus, understanding social phobia as a continuum disorder may provide a more accurate picture of the manifestation and course of the illness, and also have implications for treatment.

7.1.4 Neurodegenerative Hypothesis

While acknowledging the methodologic difficulties in using epidepride, there is a potential explanation for the positive correlation between striatal to frontal ratios and symptoms of social fears and avoidance, as measured by the LSAS, observed in this study. Increased striatal post-synaptic D2 binding may indicate diminished synaptic dopamine in the striatum with secondary post-synaptic D2 upregulation, which would support the hypothesis of diminished dopamine in SP. This conflicts with the recent study by Schneier et al (2000), who report the finding of decreased striatal D2 binding in social phobia in a SPECT study using ^{123}I -IBZM and the ratio method of analysis. When trying to understand the different results between this current study and that of Schneier et al (2000), a possible confounding factor in the study of striatal dopamine in social phobia that requires attention in future studies is MRI evidence for a higher rate of neuronal loss in the putamen with increasing age in social phobia (Potts et al 1994). In addition, there is a high rate of social phobia that predates the onset of Parkinson's

disease (Lauterbach and Duvoisin, 1987; Stein MB et al, 1990). Consequently, decreased dopamine transmission in social anxiety may initially be compensated for by increased D2 receptors, but with increasing age and neuronal loss, subsequently manifest as diminished D2 receptors. As Schneier et al (2000) state, future studies are needed with larger samples and quantitative measures of D2 receptor density.

7.1.5 Role of the Striatum in Social Phobia

As noted in the review of social phobia neurobiology in chapter one, striatal DA has been the only neurotransmitter system identified that can distinguish SP patients from healthy controls and, as in this particular study, is the only neurotransmitter to be correlated with clinical symptoms. This suggests that striatal DA occupies a central role in understanding social phobia. The functional importance of the striatum in social phobia, however, has yet to be elucidated. Recent studies, many coming from translation research, may be integrated into promising hypotheses for the role of the striatum in social phobia, particularly with regards to striatal-amygdala neural circuits. These hypotheses include: 1) participation of the ventral striatum in a dopamine reward system for social affiliation; 2) conditioning of aversive events with striatal-amygdala connections; 3) and hyperactivity of striatal-amygdala circuitry secondary to enhanced sensitivity to facial expressions of disapproval and gaze threat. Lastly, an integrative hypothesis of social phobia will be presented from the perspective of brain circuitry.

L.J. Young et al (2002) elegantly demonstrate that the neuropeptides oxytocin and vasopressin increase social affiliative behavior in prairie voles, and that social contact is also increased in species of voles with high densities of oxytocin and vasopressin receptors in the nucleus accumbens and the ventral pallidum. Dopaminergic input from the ventral tegmental area to the nucleus accumbens and ventral pallidum comprise a dopaminergic reward system that may increase the positive valence of social

interactions. This particular animal model has obvious application to autistic disorders, where there seems to be an impairment in the ability to form social attachments. Social affiliation may also have theoretical and practical importance to social phobia, particularly as there is an increased risk of social phobia in first-degree relatives of autistic children (Smalley et al, 1995). While no direct dopamine-neuropeptide link has been established, Stein (1998) hypothesizes that social phobia may result from an imbalanced appraisal of the risk versus reward of social interactions, possibly caused by dysfunction in the social affiliative-reward circuits. Incorporating the striatum into this circuit, there is evidence that the ventral striatum has a role in the dopaminergic reward-social affiliative circuits. Schultz et al (J Neurophysiol 80,1-27) note that ventral striatal neurons are important in reward prediction, with increased neuronal firing signaling an unexpected reward, whereas decreased neuronal firing indicating the loss of an expected reward. Kampe et al (2001) integrates these findings with an fMRI study of 16 subjects demonstrating that eye gaze and the attractiveness of a face modulate ventral striatal activity, with increasing attractiveness and direct gaze increasing the activity of ventral striatal neurons. Thus, the ventral striatum likely plays a role in evaluating the reward of social interactions, and resulting dysfunction may cause an imbalance in the risk-reward assessment of social affiliation, with social detachment, avoidance or anxiety as possible consequences.

Adverse conditioning events are an important facet in the developmental psychopathology of social phobia, and the biologic basis of this is likely mediated by striatal-amygdala connections. Literature supporting the variable of adverse conditioning in the development of social phobia include findings that 44% to 58% of all persons with social phobia report a humiliating event that accompanied the start of their social anxiety (Ost, 1985; Stemberger et al, 1995). Prospective studies indicate that rejection or neglect by peers is associated with social anxiety, while retrospective studies report that

a history of bullying or harassment is frequently found in shy adolescents. In addition, Beidel and Turner (1998) report that repetitive rejection from peers may sensitize people to be fearful of social contact. Potential biological structures for adverse conditioning include ventral striatal-amygdala circuitry, which de Olmos and Heimer (1999) have demonstrated to be critical for associating complex sensory stimuli with positive and negative rewards. Not only responsible for establishing conditioned fear, the amygdala may also be important for the storage of emotional memories following learned fear (Cahill et al 1999; Faneslow and Le Doux 1999). Thus, ventral striatal-amygdala circuitry may provide a basis for which conditioned fear from social trauma in development may be stored in implicit memory. Because 20% of persons without social phobia also relate having traumatic social experiences (Stemberger et al 1995), there may be a constitutional predisposition of excessive conditionability to social fear and anxiety (Stein 1998), the origins of which could be in the ventral striatal-amygdala circuitry. Although this hypothesis requires future investigation, the role of the amygdala in SP is supported by findings in a functional MRI study of 12 social phobic patients and 12 controls, that the activation of the amygdala and hippocampus differs significantly between social phobics and normal controls in the acquisition of conditioned aversive stimuli (Schneider et al, 1999).

As alluded to earlier, the striatum and the amygdala also have importance for the processing of facial emotion, and this is critical because social phobia patients demonstrate enhanced attention and memory for disapproving faces. In a fMRI study that investigated the neural substrate for processing facial expressions of disgust, Phillips et al (1997) found that mild expressions of disgust activated the anterior insular cortex, while strong expressions of disgust activated a limbic cortico-striatal-thalamic circuit. Interestingly, Calder et al (2000) review neuroimaging evidence that the affect of disgust is processed in the insula and putamen, and then describe a patient with insula

and putamen damage who has difficulties recognizing social signals of disgust. Thus, it can be hypothesized that social phobia patients may have increased processing of disgust through the striatum, which could lead to the initiation of motor avoidance programs such as that observed in primates who undergo social defeat: gaze and head aversion with positioning to flee (Gilbert and Allan, 1998). Along similar lines of reasoning, social phobia patients may also have increased sensitivity to angry faces. Bilateral lesions of the amygdala in mature macaque monkeys results in social disinhibition, with the loss of ability to assess potential threat (Amaral, 2002). Several studies have also demonstrated that the neural substrate for processing expressions of anger reside with the amygdala (Blair and Curran, 1999; Blair et al, 1999). Accordingly, Amaral (2002) suggests that social anxiety may be secondary to hyperactivity in the amygdala such that there is excessive threat assessment, with a particular sensitivity to anger or disapproval, in a social encounter. Further research is required to examine the hypothesis that social phobia patients have an enhanced sensitivity to disapproving affect that may be mediated by hyperactive circuits in the striatum and amygdala.

7.2 TOWARD AN INTEGRATIVE UNDERSTANDING OF SOCIAL PHOBIA

A hypothetical model for integrating much of the current knowledge base of SP into a cortical-basal ganglia-thalamic neural circuit and also a striatal-amygdala circuit may be suggested by comorbidity research, preliminary neuroimaging results, and the previously discussed evidence for the role of striatal-amygdala connections in social phobia (Li et al, 2001). This model can provide a framework for understanding the interwoven involvement of the primary neurotransmitter systems in SP, and also provide a neurobiological understanding for the predisposition, development and maintenance of social phobia symptoms.

The importance of cortical-basal ganglia-thalamic circuits has been described for obsessive compulsive disorder and schizophrenia, and the close proximity of parallel cortical-subcortical pathways may account for the relatively high comorbidity between these two disorders (Tibbo and Warneke, 1999). Interestingly, Cosoff and Hafner (1998) report that the comorbidity of SP and schizophrenia (17%) may be just as high as that of obsessive compulsive disorder in schizophrenia (13%); furthermore, Davidson et al (1998) note that the lifetime prevalence rate of schizophrenia in SP is 13% (O.R.=13.3), which is remarkably high. As a result, perhaps a cortical-basal ganglia-thalamic circuit exists in SP that parallels, in close proximity, certain components of the neural circuitry in schizophrenia.

Neuroimaging data can provide foundational support for a hypothetical cortical-basal ganglia-thalamic neural circuit in SP. Magnetic resonance spectroscopy (MRS) provides access to the biochemistry, physiology, and metabolism of brain regions, and consequently offers significant potential for elucidating the pathophysiology of SP. Two magnetic resonance studies have produced findings in which SP is associated with increased choline and myoinositol (relative to creatine and N-acetylaspartate) in both cortical and subcortical (i.e. caudate, putamen, thalamus) gray matter (Tupler et al, 1997). The significance of these results is unclear, but increased choline may suggest abnormalities in the phospholipase C second messenger pathway activated by dopamine and serotonin (Martinson et al, 1989), while increased myoinositol can result from cytoskeleton breakdown or inositol triphosphate second messenger dysfunction (Ross et al, 1991). The greatest differences were found in cortical gray matter, a region of higher cognitive function and integration, which may ultimately be the source of cognitive distortions in anxiety disorders (Gorman et al, 1989). Of particular interest, SP symptom severity was correlated with decreased choline and myoinositol in subcortical gray matter, which includes the caudate, putamen, and thalamus—providing yet further

evidence, in accordance with previously discussed SPECT studies, for the involvement of basal ganglia circuits in the symptoms of SP (Tupler et al, 1997).

Regional cerebral blood flow in SP has been examined using both SPECT and PET. In a SPECT study measuring brain perfusion with technetium-99m-hexamethylpropylenamineoxime (99m-Tc-HMPAO), no significant differences in regional cerebral blood flow were demonstrated between persons with SP (n=11) and healthy subjects (Stein and Leslie, 1996). This study highlights the necessity for future research to incorporate brain perfusion studies with social anxiety challenges. Accordingly, in a PET study using ^{15}O , cerebral perfusion in a group of SP subjects was imaged during anxiety that was provoked by reading a script of a feared social situation (Bell et al, 1998). Compared with a previous study of conditioned anticipatory anxiety in normal volunteers, both SP and conditioned anxiety groups had increased blood flow in the anterior cingulate gyrus and the insulae. Notably, however, only the SP group had increased blood flow in the right dorsolateral prefrontal cortex (DLPFC) and in the left parietal cortex. As Nutt et al (1998) discuss, these results point to potential neural circuits in SP involving the anterior cingulate gyrus and insulae for regulating anticipatory anxiety and autonomic response, while neural circuits more specific for the negative cognitions and pervasive social anxiety possibly reside in the right DLPFC and the left parietal cortex.

Taking into account the above neuroimaging results, a hypothetical cortical-basal ganglia-thalamic neural circuit can be formulated that also incorporates an interwoven understanding of the primary neurotransmitter systems involved in SP. The centrality of striatal DA dysfunction has been discussed, and both SP and symptom severity have been correlated with striatal abnormalities in this current study and other SPECT and MRS studies (Tiihonen, et al 1997; Tupler et al, 1997; Schneier et al, 2000). Consequently, with DA being a key neurotransmitter system involved, basal ganglia

circuits may determine the degree to which symptoms are experienced, particularly motor programs of avoidance, and possibly provide the biological substrate for the development of SP symptoms. There is evidence that the basal ganglia play an important role in shifting attentional set (i.e. changing conditions that regulate responding), and that basal ganglia dopaminergic dysfunction results in a decreased ability to filter irrelevant sets (Hayes et al, 1998). Furthermore, PET and MR studies in Parkinson's patients show that the basal ganglia function to focus and filter cortical output through the dopaminergic system (Brooks, 2001). Thus, acting as a gate or filter of input from cortical circuits responsible for awareness of body position and social space (e.g. left parietal cortex), basal ganglia-thalamic circuits may modulate output to the (dorsal lateral) prefrontal cortex, where excessive input may result in the recurrent negative cognitions of social evaluation, and where 5-HT and GABAergic systems may be of primary importance (Tupler et al, 1997; Bell et al, 1998; Nutt et al, 1998). The output of pervasive anxiety and adrenergic symptoms may correspond to activation of neural circuits involving the anterior cingulate gyrus and insulae—which could be a possible final common pathway for other anxiety disorders and the site for NE overactivity (Bell et al, 1998; Nutt et al, 1998). This particular model has correlates with cognitive theories of social phobia (Clark and McManus, 2002), as impairment in a basal ganglia-thalamic filter may underlie the difficulty that social phobia patients have in shifting or “filtering” attention away from: autonomic arousal (e.g. tremor, blushing, diaphoresis caused by a common anxiety circuit); increased self-focussed attention relative to the environment (Left parietal cortex and primary association cortex); perceived negative facial cues from people (amygdala, striatum); and negative interpretations of feedback and social events (dorsal lateral prefrontal cortex).

This cortical-basal ganglia-thalamic circuit in SP is influenced significantly by key connections with a striatal-amygdala circuit, which may play an important role in

establishing the biological predisposition for developing social phobia. As discussed earlier, striatal-amygdala pathways are likely central to the reward system of social affiliation, and may be partly responsible for qualities of temperament such as the overall degree of social attachment-detachment. There may also be a constitutional predisposition of excessive conditionability to social fear and anxiety, the origins of which would probably reside in amygdala – ventral striatal circuitry. By mediating the formation of adverse conditioned associative memories, striatal-amygdala circuitry provide a neurobiological explanation for how traumatic social events or humiliating social relationships may serve to increase the risk of developing social phobia when there is already a diathesis present. Lastly, hyperactivity of the amygdala and striatum, possibly resulting from adverse conditioning, may result in enhanced sensitivity to disapproving facial expressions such as fear and disgust, and be partly responsible for the continued maintenance of social phobia symptoms.

In overview, impaired striatal-thalamic filtering and/or excessive conditionability of ventral striatal-amygdala circuitry may form the biological substrate for the constitutional predisposition and development of SP, and interconnections among the described cortical-basal ganglia-thalamic loop and the amygdala would provide the pathways necessary for conditioned fear and reinforcement of negative cognitions—ultimately resulting in the behavioral avoidance seen in SP (Figure 7.1; Li et al, 2001).

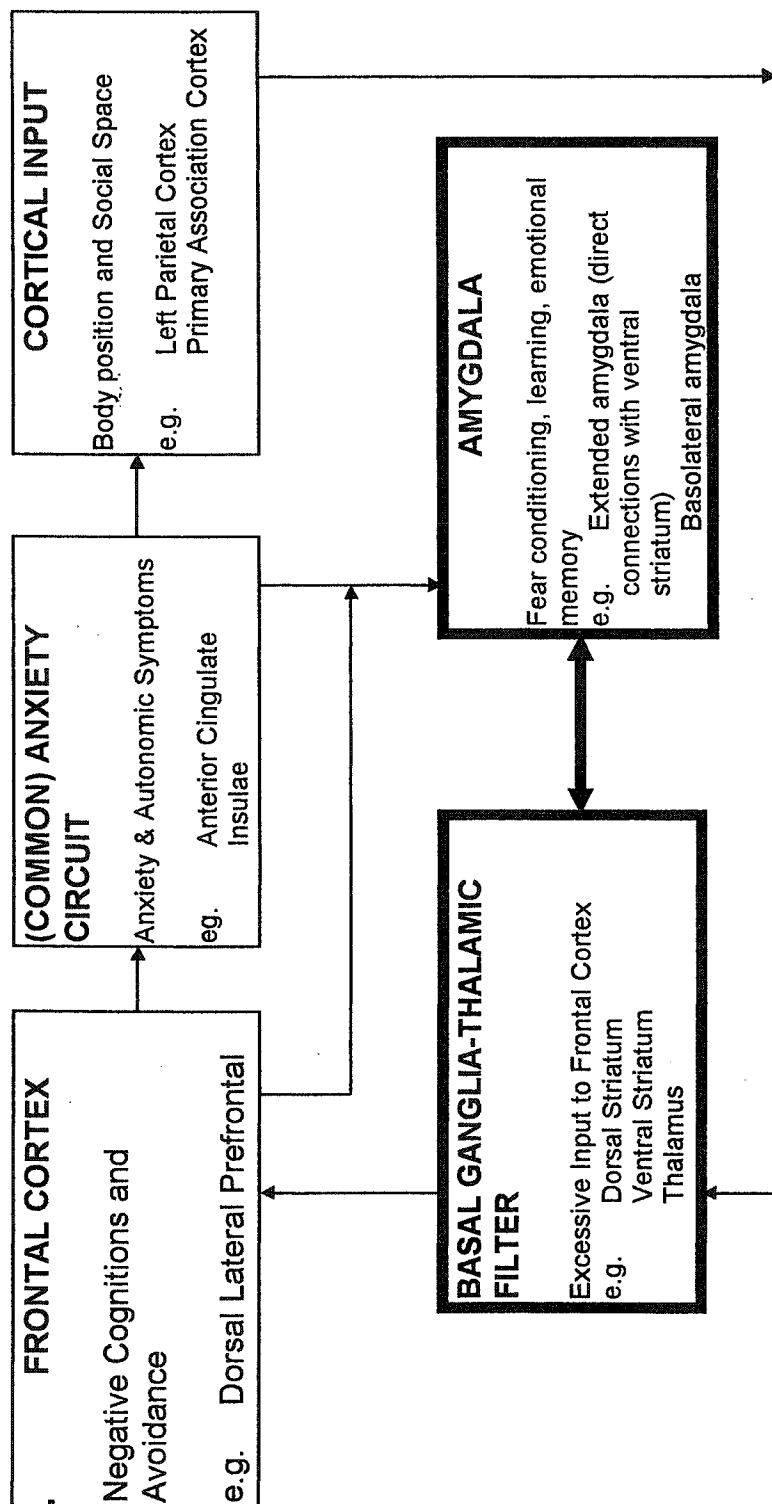


Figure 7.1 (Reprinted from Li et al, 2001, with permission from the authors). Components of a hypothetical neural circuit in social phobia. The chief biological substrate of social phobia in this model is hypothesized to include impaired basal ganglia - thalamic filtering and/or excessive conditionability of ventral striatal - amygdala circuitry. Impaired basal ganglia-thalamic filtering may result in excessive input of information (related to body position and image) to the frontal cortex, where negative cognitions occur and behavioral avoidance is planned. The subsequent output of anxiety in social situations reinforces these pathways, and fear conditioning and learning takes place through amygdala - ventral striatal circuitry.

7.3 GENDER AND STRIATAL D2 RECEPTORS

This study identifies that female gender is significantly associated with higher striatal to frontal ratios, and the level of significance remains steady even when the outlier is taken out in multivariate analyses 1A and 2A ($p=0.0016$, $p=0.014$). In analysis 3A, where the data is analysed after matching each female pair with a male pair, the level of significance diminishes slightly ($p=0.048$) to a trend level when the outlier is removed ($p=0.052$). These gender results are independent of social anxiety symptoms or the diagnosis of social phobia. The following section discusses evidence for the influence of estrogen on striatal D2 receptors and the dopamine system in animal studies, notes the paucity of similar human studies, and then examines the potential relevance of striatal D2 receptors and reproductive hormones to Parkinson's disease and schizophrenia.

7.3.1 *Animal Models of Estrogen and Striatal Dopamine*

While taking into account the methodologic limitations of the ratio method that already have been discussed in detail, the finding that striatal D2 binding is increased in the females of this study may be secondary to interactions between reproductive hormones and the dopamine system. The literature provides strong evidence that striatal D2 receptors and dopamine transmission varies during the estrous cycle of rats and are modulated by estrogen (Cyr et al, 2002). For example, oophorectomy in monkeys causes a loss of 30% of the dopaminergic neurons from nigrostriatal neurons, and Leranth et al (2000) argue that this is because estrogen is essential for maintaining these neurons. More specifically, estrogen has been demonstrated to mediate effects in dopamine release, pre- and post- synaptic DA receptors, and at the dopamine transporter (Di Paolo T, 1994). There have been, however, paradoxical results in which estrogens exert enhancing and inhibitory effects on the dopamine system, and Cyr et al

(2002) explain that this is likely due to varying factors in studies such as dose of estrogen, length of administration, and time after which receptors are measured. With regards to rat studies, acute administration of estrogen in ovariectomized rats causes a downregulation of D2 receptors (Bazzett and Becker, 1994) with a concomitant increase in the breakdown of striatal dopamine (Di Paolo et al, 1985). In contrast, Di Paolo et al (1994) note that high dose estrogen administered over a long-term period resulted in increased dopamine receptor and transporter density. With these studies, it is difficult to extrapolate how estrogen affects dopamine transmission and D2 receptors in true physiologic conditions such as the estrous cycle, where a female rat has repeated exposure to both estrogen and progesterone at varying concentrations. Experiments that have attempted to dissect out these estrogen and progesterone effects have revealed complicated interactions that vary over time, and the reader is referred to other sources for a review (Becker, 1999). With regards to sex differences between male and female rats, there is evidence that the dopaminergic system of the female rat is more sensitive to psychomotor stimulants (Beatty and Holzer, 1978; Beatty et al, 1982), has less striatal D1 receptors (Hruska et al, 1982), a higher density of striatal DA transporter mRNA (Bosse et al, 1997), but no differences in striatal D2 DA receptors compared to males (Hruska et al, 1982).

7.3.2 Human Studies of Gender Differences in Striatal D2 Receptors

Given the large body of evidence demonstrating that estrogen affects dopaminergic transmission and receptors in animal studies, there is a relative paucity of research addressing the effects of reproductive hormones on striatal D2 receptors in humans. There are two conflicting studies that have attempted to address potential gender differences in striatal D2 binding. In a PET study of ^{11}C -raclopride, Norstrom et al (1998) examined five healthy women, four of which had their putamen to cerebellar

ratios measured in two different phases of their menstrual cycle, and they did not find any differences in comparison to men. This study is limited by its study size, so no firm conclusions can be drawn. In a larger study consisting of 33 men and 21 women, Pohjalainen et al (1998) also used a ^{11}C -raclopride PET study to examine sex differences in the loss of D2 receptor density due to aging. They found that women had decreased D2 receptor density in the left striatum compared to men, and that there was a trend for D2 receptor density and binding potential to diminish two times more quickly in men than women. This study, however, did not take into account the menstrual phase at which striatal D2 receptors were imaged, nor personality traits such as degree of social anxiety.

7.3.3 Relevance of Sex Hormone Modulation of D2 Receptors to Parkinson's

Disease and Schizophrenia

The results of this current study, in which striatal D2 receptors appear to be increased in females, and the paucity of studies specifically addressing whether or not striatal D2 receptor parameters vary during the menstrual phase of humans, emphasizes the need for more research and larger studies. This is important because of increasing interest in the role of hormones and reproductive brain circuits in the development of disorders such as Parkinson's disease and schizophrenia. In humans, whether or not estrogens are stimulatory, inhibitory, or both, upon dopaminergic systems remains the subject of debate. In Parkinson's patients, for example, estrogen generally shows an anti-dopaminergic effect on symptoms (Session et al, 1994); however, estrogen also seems to be helpful to women with early Parkinson's disease (Saunders-Pullman et al, 1999), and in post-menopausal women with Parkinson's and fluctuating motor disabilities (Tsang et al, 2000). Furthermore, as previously noted, estrogen is thought to be important in maintaining nigrostriatal neurons in primate animal models (Leranth et al,

2000). Thus, the effect of estrogen on the dopaminergic system in humans still requires clarification, and studies to date have offered contradictory results.

Animals studies of striatal D2 receptors may provide potential models for understanding the pathophysiology and development of schizophrenia. Rat studies, for example, show that during the onset of puberty, male striatal D2 receptor density increases 144%, while female D2 receptor density increases 31%; this is followed by a process of pruning in which male striatal D2 receptor density is eliminated by 55% by adulthood, whereas females have a significantly smaller amount of pruning (Andersen and Teicher, 2000). Although the authors discuss the relevance of their results to attention deficit hyperactivity disorder, such observed developmental changes in striatal D2 receptor density have relevance to emerging theories of the role of reproductive hormones in the onset of schizophrenia. Stevens (2002) posits that schizophrenia results from an imbalance of inhibitory neurotransmitter systems (e.g. dopamine) attempting to compensate excessively for the surge in excitatory effects of estrogen and other reproductive hormones during the adolescent period. Subsequent pruning of receptors in the dopaminergic system may alter the balance between inhibitory and excitatory factors upon subcortical structures, and failure to establish a proper equilibrium is hypothesized to precipitate schizophrenia. Although there is general evidence that estrogen may play an important protective and/or anti-psychotic role in humans (Reicher-Rossler et al, 1994), specific data as to how estrogen or striatal D2 receptors may play a role in mediating the gender differences in the response of dopaminergic systems to reproductive hormones in adolescence, resulting in increased vulnerability to an earlier onset of schizophrenia in males, requires testing and further research. In overview, Cyr et al (2002) comment that clinical studies on estrogenic modulation of the brain are few and often contradictory, and they point to the need for studies that begin utilizing selective estrogen modulators, which have more specific

central estrogenic activity. In addition, the results of this study suggest that there is a need for more detailed investigation of the role of gender and estrogen on D2 imaging, such that sex and hormonal differences may be taken into account when studying D2 receptors in the context of social phobia, personality traits (e.g. detachment), and schizophrenia.

Chapter 8

Conclusion

Social phobia is unique among the anxiety disorders because of increasing evidence that symptom severity may be related to hypodopaminergic function, particularly in the striatum. As reviewed in chapters one and three, this hypothesis has been based on indirect evidence from animal models (Mayleben, 1992; Grant et al, 1998), measures of homovanillic acid in the CSF of social phobia patients (Johnson et al, 1994), treatment studies (Liebowitz et al, 1994), the study of D2 receptors and detachment (Farde et al, 1990), and genetic research regarding D2 polymorphisms and schizoid-avoidant traits (Johnsson et al, 1999). Recent neuroimaging research has attempted to directly investigate the nature of the dopaminergic dysfunction in SP, and diminished striatal DATs have been identified in SP patients (Tiihonen et al, 1997). In spite of the emerging research on SP, there is a paucity of studies that investigate

striatal post-synaptic D2 receptors in SP. Consequently, this thesis tested the hypothesis of diminished striatal D2 receptor density in SP by imaging D2 receptors in 12 persons with SP and 10 controls using SPECT and ^{123}I -epidepride.

This study found that there is large inter-individual variability in striatal to frontal ratios, and for imaging times between 4 and 5 hours, there is a COV of 25% for controls and a COV of 75% for patients. Improvements in data acquisition that could potentially reduce this inter-individual variability include the use of a single imaging time, constant matrix, fiducial markers for intra- and inter- individual comparison of images, and attenuation correction. Perhaps more importantly, the large inter-individual variability in striatal to frontal ratios reflects difficulties in the ratio method imposed by epidepride kinetics. These challenges include: 1) inter-individual variability in the time for epidepride to reach equilibrium in the striatum, which is influenced by individual D2 receptor density and plasma clearance; 2) poor signal-to-noise ratio secondary to the high D2 specificity of epidepride, with resulting rapid non-specific binding washout in the reference region; 3) and interference from the lipophilic metabolite of epidepride. With these challenges in mind, epidepride still has a unique niche as a SPECT radioligand because of its high D2 affinity and specificity, and consequently, there is a need for the development of efficient semiquantitative techniques that are validated by the more cumbersome quantitative methods (e.g. bolus-infusion or bolus-injection) or PET imaging. In the current study, the S:F ratio should be seen as, at best, an approximation of striatal D2 binding.

While this study did not find significant differences between SP patients and controls with regards to S:F measures of striatal D2 binding, statistically significant positive correlations were found between LSAS scores and the S:F ratio in analysis 1A and 3A, with a trend level of association in analysis 2A. Conclusions from these results must be tempered by the aforementioned difficulties with the ratio method, the high COV

in S:F ratios in both patients and controls, the relatively small sample size, and the normal biological variability of D2 receptors. Taking these cautions into account, the finding that S:F ratios are positively correlated with LSAS scores—when patients and controls are analysed as one group—suggests that SP may be best understood as a continuum disorder, which coincides with evidence that SP patients have a course of illness that shifts among diagnostic, sub-threshold, and symptom levels over time (Merikangas et al, 2002). Furthermore, the positive association between striatal D2 binding and increasing social anxiety may reflect diminished synaptic dopamine neurotransmission with compensatory post-synaptic D2 upregulation. It is also possible, however, that a higher rate of neuronal loss in the striatum of SP patients with increasing age (Potts et al, 1994; Lauterbach and Duvoisin, 1987; Stein et al, 1990), may later manifest as diminished D2 receptors in a subgroup of SP persons. Thus, future studies of D2 receptors in SP need to be designed using SPECT quantitative measures and larger samples, and should also take into account the possible effect of neurodegeneration on measurements of striatal D2 binding in SP.

This thesis also develops a hypothetical cortical-basal ganglia-thalamic-amygdaloid circuit of SP that provides an integrated understanding of SP from a current knowledge of SP neurobiology, neuroimaging studies, cognitive theory, and development. Striatal-amygdala pathways are central to the reward system of social affiliation, and may play a role in determining qualities of temperament such as the degree of social attachment-detachment. There may be a constitutional predisposition to SP conferred by excessive conditionability to social fear and anxiety, the origins of which would probably reside in ventral striatal-amygdala circuitry. By mediating the formation of adverse conditioned associative memories, striatal-amygdala circuitry provide a neurobiological explanation for how traumatic social events or humiliating social relationships may serve to increase the risk of developing social phobia when

there is already a diathesis present. Furthermore, hyperactivity of the amygdala and striatum, possibly resulting from adverse conditioning, may result in enhanced sensitivity to disapproving facial expressions such as fear and disgust, and be partly responsible for the continued maintenance of SP symptoms.

Lastly, this study also found that female gender is significantly associated with higher S:F ratios, and these results are independent of social anxiety symptoms and the diagnosis of SP. While a larger sample size is needed, a potential explanation for these findings are suggested by animal model research demonstrating that estrogen modulates striatal dopamine in a complicated manner. There is a paucity of human studies, however, that examine gender differences in striatal D2 binding, and the two relevant studies done to date suffer from limitations that include small sample size (Norstrom et al, 1998), and neglecting the potential influence of the menstrual phase at which striatal D2 receptors are imaged (Pohjalainen et al, 2002). Therefore, the results of this thesis suggest that future striatal D2 imaging—which is important in the research of SP, schizophrenia, basal ganglia disorders, and addiction psychiatry—strongly consider the potential effects of gender differences (e.g. menstrual phase) and social anxiety on striatal D2 binding.

BIBLIOGRAPHY

- Andersen SL, Teicher MH. Sex differences in dopamine receptors and their relevance to ADHD. *Neurosci Biobehav Rev* 2000;24:137-41.
- Amaral DG. The primate amygdala and the neurobiology of social behavior: implications for understanding social anxiety. *Biol Psychiatry* 2002;51:11-17.
- American Psychiatric Association (APA). *Diagnostic and Statistical Manual of Mental Disorders*. 4th ed. Washington, DC: APA Press, 1994.
- American Psychiatric Association (APA). *Handbook of Psychiatric Measures*. 1st ed. Washing, DC: APA Press, 2000, pp. 100-102.
- Baldwin D, Bobes J, Stein DJ, Scharwachter I, Faure M. Paroxetine in social phobia/social anxiety disorder: randomised, double-blind placebo-controlled study. *Br J Psychiatry* 1999;175:120-126.
- Bazzett TJ, Becker JB. Sex differences in the rapid and acute effects of estrogen on striatal D2 dopamine receptor binding. *Brain Res* 1994;637:163-172.
- Beatty WW and Holzer GA. Sex differences in stereotyped behavior in the rat. *J Pharmacol Biochem Behav* 1978;9:777-785.
- Beatty WW, Dodge AM, Traylor KL. Stereotyped behavior elicited by amphetamine in the rat. Organizational and activational effects of the testes. *Pharmacol Biochem Behav* 1982;16:565-568.
- Beidel DC, Turner SM. *Shy Children, Phobia Adults: The Nature and Treatment of Social Phobia*. Washington, DC: American Psychological Association; 1998.
- Becker JB. Gender differences in dopaminergic function in striatum and nucleus accumbens. *Pharmacol Biochem Behav* 1999;64:803-812.
- Bell CJ, Malizia AL, Nutt DJ. The neurobiology of social phobia. *Eur Arch Psychiatry Clin Neurosci* 1998;249 Suppl 1:S11-8.
- Benjamin J, Li L, Patterson C, Greenberg BD, Murphy DL, Hamer DH. Population and familial association between the D4 dopamine receptor gene and measures of novelty seeking. *Nature Genet* 1996;12:81-84.
- Bergstrom KA, Yu M, Kuikka JT, Akerman KK, Hiltunen J, Lehtonen J, Halldin C, Tiihonen J. Metabolism of ¹²³I-epidepride may affect brain dopamine D2 receptor imaging with single-photon emission tomography. *Eur J Nucl Med* 2000;27:206-208.
- Blair RJ, Curran HV. Selective impairment in the recognition of anger induced by diazepam. *Psychopharmacology (Berl)* 1999;147:335-8.
- Blair RJ, Morris SJ, Frith CD, Perrett DI, Dolan RJ. Dissociable neural responses to facial expressions of sadness and anger. *Brain* 1999; 122(Pt 5):883-93.

Blier P, de Montigny C, Chaput Y. Modifications of the serotonin system by antidepressant treatments: implications for the therapeutic response in major depression. *J Clin Psychopharmacol* 1987;7 (suppl 6):24S-35S.

Blum K, Braverman ER, Wu S, Cull JG, Chen TJ, Gill J, Wood R, Eisenberg A, Sherman M, Davis KR, Matthews D, Fischer L, Schnautz N, Walsh W, Pontius AA, Zedar M, Kaats G, Comings DE. Association of polymorphisms of dopamine D2 receptor (DRD2), and dopamine transporter (DAT1) genes with schizoid/avoidant behaviors (SAB). *Mol Psychiatry* 1997;2(3):239-46.

Bosse R, Rivest R, Di Paolo T. Ovariectomy and estradiol treatment affect the dopamine transporter and its gene expression in the rat brain. *Mol Brain Res* 1997;46:343-346.

Breier A; Kestler L; Adler C; Elman I; Wisenfeld N; Malhotra A; Pickar D. Dopamine D2 receptor density and personal detachment in healthy subjects. *Am J Psychiatry* 1998;155(10):1440-2.

Brooks DJ. Functional imaging studies on dopamine and motor control. *J Neural Transm* 2001;108(11):1283-98.

Burke, K.C., Burke, J.D., Regier, D.A., Rae D.S. Age at onset of selected mental disorders in five community populations. *Arch Gen Psychiatry* 1990;47:511-518.

Cahill L, Weinberger NM, Roozendaal B, McGaugh JL. Is the amygdala a locus of "conditioned fear"? Some questions and caveats. *Neuron* 23:227-228.

Calder AJ, Keane J, Manes F, Antoun N, and Young AW. Impaired recognition and experience of disgust following brain injury. *Nat Neurosci* 2000;3(11):1077-8.

Chase TN, Oh JD, Blanchet PJ. Neostriatal mechanisms in Parkinson's disease. *Neurology* 1998;51(2 Suppl 2), S30-5.

Clark DM and McManus F. Information processing in social phobia. *Biol Psychiatry* 2002;51:92-100.

Cloninger CR (ed): *The Temperament and Character Inventory (TCI): A Guide to its Development and Use*. St Louis, Center for Psychobiology of Personality, 1994.

Cosoff SJ and Hafner RJ. The prevalence of comorbid anxiety in schizophrenia, schizoaffective disorder and bipolar disorder. *Aust N Z J Psychiatry* 1998;32:67-72.

Coupland NJ, Bailey JE, Potokar JP. Abnormal cardiovascular responses to standing in panic disorder and social phobia [abstract]. *J Psychopharmacol*. 1995;9(suppl 3), A73.

Coupland NJ, Bell C, Potokar JP, Dorkins E, Nutt DJ. Flumazenil challenge in social phobia. *Depress Anxiety* 2000;11(1):27-30.

Croft BY. *Single photon emission computed tomography*. Chicago, IL.: Year Book Medical Publishers, Inc.; 1986, pp.18-127.

Cyr M, Calon F., Morissette M, Di Paolo T. Estrogenic modulation of brain activity: implications for schizophrenia and Parkinson's disease. *J Psychiatry Neurosci* 2002;27(1):12-27.

Davidson JR; Hughes DL; George LK; Blazer DG. The epidemiology of social phobia: findings from the Duke Epidemiological Catchment Area Study. *Psychol med* 1993;23(3):709-18.

Davidson JR; Hughes DL; George LK; Blazer DG. The epidemiology of social phobia: findings from the Duke Epidemiological Catchment Area Study. *Psychol med* 1993;23(3):709-18.

Davidson JR; Potts N; Richichi E; Krishnan R; Ford SM; Smith R; Wilson WH. Treatment of social phobia with clonazepam and placebo. *J Clin Psychopharmacol* 1993;13:423-8

Davidson, Krishnan KR, Charles HC, et al. Magnetic resonance spectroscopy in social phobia: Preliminary findings. *J Clin Psychiatry* 54(suppl):19-25.

de Olmos JS, Heimer. The concepts of the ventral striatopallidal system and extended amygdala. *Ann N Y Acad Sci*. 1999;29(877):1-32.

den Boer JA, van Vliet IM, Westenberg HG. Recent advances in the psychopharmacology of social phobia. *Prog Neuro-Psychopharmacol and Biol Psychiatry* 1994;18:625-645.

Di Paolo T, Rouillard C, Bedard P. 17 beta-estradiol at a physiological dose acutely increases dopamine turnover in rat brain. *Eur J Pharmacol* 1985;117:197-203.

Di Paolo T. Modulation of brain dopamine transmission by sex steroids. *Rev Neurosci* 1994;5:27-41.

Ebstein RP, Novick O, Umansky R, Priel B, Osher Y, Blin D, Bennett ER, Nemanov L, Katz M, Belmaker RH. Dopamine D4 receptor exon III polymorphism associated with the human personality trait of novelty seeking. *Nature Genet* 1996;12:78-80.

Ebstein RP; Nemanov L; Klotz I; Gritsenko I; Belmaker RH. Additional evidence for an association between the dopamine D4 receptor (D4DR) exon III repeat polymorphism and the human personality trait of novelty seeking. *Mol Psychiatry* 1997;2, 472-7

Emde RN; Plomin R; Robinson JA; Corley R; DeFries J; Fulker DW; Reznick JS; Campos J; Kagan J; Zahn-Waxler C. Temperament, emotion, and cognition at fourteen months: the MacArthur longitudinal twin study. *Child Dev* 1992;63(6):1437-55.

English RJ. SPECT: single photon emission computed tomography: a primer. 3rd ed, New York, NY: Society of Nuclear Medicine, 1995, pp. 24-68.

Falloon IR, Lloyd GG, and Harpin R. The treatment of social phobia: real-life rehearsal with non-professional therapists. *J Nerv Ment Dis* 1981;169, 180-184.

Faneslow MS, LeDoux JE. Why we think plasticity underlying Pavlovian fear conditioning occurs in the basolateral amygdala. *Neuron* 1999;23:229-232.

Farde L, Eriksson L, Blomquist G, Halldin C. Kinetic analysis of central ^{11}C -raclopride binding to D2 dopamine receptors studied with PET: a comparison to the equilibrium analysis. *J Cereb Blood Flow Metab* 1989;9:696-708.

Farde L, Gustavsson JP, Jonsson E. D2 dopamine receptors and personality traits. *Nature* 1990;385:590.

Farde L, Hall H, Pauli S, Halldin C. Variability in D2-dopamine receptor occupancy in relation to extrapyramidal syndromes in patients being treated with neuroleptic drugs. *Psychopharmacol Ser* 1993;10:94-100.

File SE and Johnston AL. Lack of effects of 5HT3 receptor antagonists in the social interaction and elevated plus-maze tests of anxiety in the rat. *Psychopharmacology (Berl)* 1989;99:248-51.

Fresco DM, Coles ME, Heimberg RG, Liebowitz MR, Hami S, Stein MB, Goetz D. The Liebowitz Social Anxiety Scale: a comparison of the psychometric properties of self-report and clinician-administered formats. *Psychol Med* 2001;31:1025-35.

Friston KJ, Ashburner J, Poline JB, Frith CD, Heather JD, Frackowiak RSJ. *Human Brain Map* 1995;2:165-189.

Fujita M, Seibyl JP, Verhoveff NP, Ichise M, Baldwin RM, Zoghbi SS, Burger C, Staley JK, Rajeevan N, Charney DS, Innis RB. Kinetic and equilibrium analyses of ^{123}I -epidepride binding to striatal and extrastriatal dopamine D2 receptors. *Synapse* 1999;34:290-304.

Fyer AJ; Mannuzza S; Chapman TF; Liebowitz MR; Klein DF. A direct interview family study of social phobia. *Arch Gen Psychiatry* 1993;50:286-293.

Gelernter CS; Uhde TW; Cimboic P; Arnkoff DB; Vittone BJ; Tancer ME; Bartko JJ. Cognitive-behavioral and pharmacological treatments of social phobia: a controlled study. *Arch Gen Psychiatry* 1991;38, 938-945.

Gilbert and Allan. The role of defeat and entrapment (arrested flight) in depression: an exploration of an evolutionary view. *Psycho Med* 1998;28:585-98.

Goldberg DP, Lecrubier Y. Form and frequency of mental disorders across centres. In: Ustun TB, Sartorius N, eds. *Mental Illness in General Health Care: An International Study*. New York, NY: John Wiley & Sons; 1995; 323-334.

Gorman JM, Liebowitz MR, Fyer AJ, Stein J. A neuroanatomical hypothesis for panic disorder. *Am J Psychiatry* 1989;146, 148-161.

Gorman JM; Fyer MR; Goetz R; Askanazi J; Liebowitz MR; Fyer AJ; Kinney J; Klein DF. Ventilatory physiology of patients with panic disorder. *Arch Gen Psychiatry* 1988;45, 31-39.

Grant KA, Shively CA, Nader MA, Ehrenkaufer RL, Line SW, Morton TE, Gage HD, Mach RH. Effect of social status on striatal DA D2 receptor binding characteristics in cynomolgus monkeys assessed with positron emission tomography. *Synapse* 1998;29:80-83.

Gray TS. Functional and anatomical relationships among the amygdala, basal forebrain, ventral striatum, and cortex: an integrative discussion. *Ann N Y Acad Sci* 1999, 29(877):439-444.

Gunn RN, Lammertsma AA, Hume SP, Cunningham VJ. Parametric imaging of ligand-receptor binding in PET using a simplified reference region model. *Neuroimage* 1997;6, 279-287.

Halldin C, Swahn C-G, Farde L. Determination of labeled metabolites of the dopamine D-2 receptor antagonist 11^{11} C-FLB 457 in monkey and human plasma by gradient HPLC. *J Labelled Compd Rad* 1995;37:709-711,

Hammer RP, Margulies JE, Lynn AB, et al. Chronic fluoxetine treatment up-regulates dopamine receptors in the mesolimbic forebrain of the rat. *Depression* 1993;1:82-7.

Hayes AE, Davidson MC, Keele SW, Rafal RD. Toward a functional analysis of the basal ganglia. *J Cogn Neurosci* 1998;10(2):178-98.

Heimberg RG, Hope DA, Dodge CS, Becker RE. DSM-III-R subtypes of social phobia: comparison of generalized phobias and public speaking phobias. *J Nerv Ment Dis* 1990;178:172-179.

Herve D, Pickel VM, Joh TH, Beaudet A. Serotonin axon terminals in the ventral tegmental area of the rat: fine structure and synaptic input to dopaminergic neurons. *Brain Res* 1987;435:71-83.

Hofmann SG, Newman MG, Ehlers A, Roth WT. Psychophysiological differences between subgroups of social phobia. *J Abnorm Psychol* 1995;104(1):224-31.

Hollander E; Kwon J; Weiller F; Cohen L; Stein DJ; DeCaria C; Liebowitz M; Simeon D. Serotonergic function in social phobia: comparison to normal control and obsessive-compulsive disorder subjects. *Psychiatry Res* 1998;79(3):213-7.

Hruska RE, Ludmer LM, Pitman KT, De Ryck M, Silbergeld EK. Effects of estrogen on striatal dopamine receptor function in male and female rats. *Pharmacol Biochem Behav* 16:285-291;1982.

Ichese M, Fujita M, Seibyl JP, Verhoeff NP, Baldwin RM, Zoghbi SS, Rajeevan N, Charney DS, Innis RB. Graphical analysis and simplified quantification of striatal and extrastriatal dopamine D2 receptor binding with 123 I-epidepride SPECT. *J Nucl Medicine* 1999;40:1902-1911.

Innis RB, Malison RT, Al-Tikriti M, Hoffer PB, Sybirska EH, Seibyl JP, Zoghbi SS, Baldwin RM, Laruelle M, Smith EO, and others. Amphetamine-stimulated dopamine release competes in vivo for ¹²³I-IBZM binding to the D2 receptor in nonhuman primates. *Synapse* 1992;10:177-84.

Insel TR. A neurobiological basis of social attachment. *Am J Psychiatry* 1997;154:726-735.

James I and Savage I. Beneficial effect of nadolol on anxiety-induced disturbances of performance in musicians: a comparison with diazepam and placebo. *Am Heart J* 1984 Oct;108(4 Pt 2):1150-5.

James IM; Griffith DN; Pearson RM; Newbury P. Effect of oxprenolol on stage-fright in musicians. *Lancet* 1977 Nov 5;2(8045):952-4.

Johnson MR, Marazziti D, Brawman-Mintzer O, Emmanuel NP, Ware MR, Morton WA, Rossi A, Cassano GB, Lydiard RB. Abnormal peripheral benzodiazepine receptor density associated with generalized social phobia. *Biol Psychiatry* 1998; 43:306-9.

Johnson MR; Lydiard RB; Zealberg JJ; Fossey MD; Ballenger JC. Plasma and CSF HVA levels in panic patients with comorbid social phobia. *Biol Psychiatry* 1994;36, 425-427.

Jonsson EG, Nothen MM, Grunhage F, Farde L, Nakashima Y, Propping P, Sedvall GC. Polymorphisms in the dopamine D2 receptor gene and their relationships to striatal dopamine receptor density of healthy volunteers. *Mol Psychiatry* 1999;4(3):290-6.

Jonsson EG; Nothen MM; Gustavsson JP; Neidt H; Brene S; Tylec A; Propping P; Sedvall GC. Lack of evidence for allelic association between personality traits and the dopamine D4 receptor gene polymorphisms. *Am J Psychiatry* 1997;154, 697-9.

Jonsson EG; Nothen MM; Gustavsson JP; Neidt H; Forslund K; Mattila-Evenden M; Rylander G; Propping P; Asberg M. Lack of association between dopamine D4 receptor gene and personality traits. *Psychol Med* 1998;28, 985-9.

Kagan J. Temperament and the reactions to unfamiliarity. *Child Dev* 1997;68,139-143.

Kampe KK, Frith CD, Dolan RJ, Frith U. Rewards value of attractiveness and gaze. *Nature* 2001;413:589.

Kaplan and Sadock. Kaplan and Sadock's synopsis of psychiatry: behavioral sciences, clinical psychiatry. 8th ed, Baltimore: Williams & Wilkins, 1998, p. 131.

Katzelnick DJ; Kobak KA, Greist JH, et al. Sertraline for social phobia: a double-blind, placebo-controlled crossover study. *Am J Psychiatry* 1995;152:1368-1371.

Kendler KS, Karkowski LM, Prescott. Fears and phobias: reliability and heritability. *Psychol Med* 1999;29:539-553.

Kendler KS, Neale MC, Kessler RC. The genetic epidemiology of phobias in women: the interrelationship of agoraphobia, social phobia, situation phobia, and simple phobia. *Arch Gen Psychiatry* 1992;49, 273-281.

Kennet GA. 5-HT_{1C} receptor antagonists have anxiolytic-like actions in the rat social interaction model. *Psychopharmacology (Berl)* 1992;107:379-84.

Kessler RC; McGonagle KA; Zhao S; Nelson CB; Hughes M; Eshleman S; et al. Lifetime and 12 month prevalence of DSM-III-R psychiatric disorders in the United States. *Arch Gen Psychiatry* 1994;51,8-19.

King RJ; Mefford IN; Wang C; Murchison A; Caligari EJ; Berger PA. CSF dopamine levels correlate with extraversion in depressed patients. *Psychiatry Res* 1986;19:305.

Knutson B, Wolkowitz OM, Cole SW, Chan T, Moore EA, Johnson RC, Terpstra J, Turner RA, Reus VI. Selective alteration of personality and social behavior by serotonergic intervention. *Am J Psychiatry* 1998;155:373-9.

Kornhuber J, Brucke T, Angelberger P, Asenbaum S, Pdreka I. SPECT imaging of dopaminergic receptors with ¹²³I-epidepride: characterization of uptake in the human brain. *J Neural Transm* 1995;101:95-103.

Kuikka JT, Akerman KR, Hiltunen J, Bergstrom KA, Rasanen P, Vanninen E, Halldin C, Tiihonen J. Striatal and extrastriatal imaging of dopamine D₂ receptors in the living human brain with ¹²³I-epidepride single-photon emission tomography. *Eur J Nucl Med* 1997;24:483-487.

Laakso A, Vilkkumäki H, Kajander J, Bergman J, Paranta M, Solin O, Hietala J. Prediction of detached personality in healthy subjects by low dopamine transporter binding. *Am J Psychiatry* 2000; 157(2):290-2.

Lauterbach EC, Duvoisin RC. Anxiety disorders in familial Parkinsonism [letter]. *Am J Psychiatry* 1987;148:1274.

Le Douarin DME. Emotion: Clues from the brain. *Annu Rev Psychol* 1995;46:209-235.

Leranth C, Roth RH, Elsworth JD, Naftolin F, Horvath TL, Redmond DE. Estrogen is essential for maintaining nigrostriatal dopamine neurons in primates: implications for Parkinson's disease and memory. *J Neurosci* 2000;20:8604-9.

Levin AP, Saoud JB, Strauman T, et al. Responses of "generalized" and "discrete" social phobics during public speaking. *Journal of Anxiety Disorders* 1993;7, 207-221.

Leyson JE, Niemegeers CJE, Tollenaere JP, Leduron PM. Serotonergic component of neuroleptic receptors. *Nature* 1987;272:168-71.

Li DM, Chokka P, Tibbo P. Toward an integrative understanding of social phobia. *J Psychiatry Neurosci* 2001;26:190-202.

Liebowitz MR, Campeas R, Hollander E MAOIs: impact on social behavior. *Psychiatry Res* 1987;22(1):89-90.

Liebowitz MR; Fyer AJ; Gorman JM; Dillon D; Davies S; Stein JM; Cohen BS; Klein DF. Specificity of lactate infusions in social phobia versus panic disorder. *Am J Psychiatry* 1985;142:947-950.

Liebowitz MR; Quitkin FM; Stewart JW; McGrath PJ; Harrison W; Rabkin J; Tricamo E; Markowitz JS; Klein DF. Phenelzine versus imipramine in atypical depression: a preliminary report. *Arch Gen Psychiatry* 1984;44, 669-677.

Lammertsma AA, Hume SP. Simplified reference tissue model for PET receptor studies. *Neuroimage* 1996;4:153-158.

Liebowitz MR; Schneier F; Campeas R; Hollander E; Hatterer J; Fyer A; Gorman J; Papp L; Davies S; Gully R; et al. Phenelzine versus atenolol in Social Phobia. A placebo controlled comparison. *Arch Gen Psychiatry* 1992;49, 290-300.

Lightowler S; Kennet GA; Williamson IJ, Blackburn TP, Tulloch IF. Anxiolytic-like effect of paroxetine in a rat social interaction test. *Pharmacol Biochem Behav* 1994;49:281-5.

Lundberg JM; Franco-Cereceda A; Lacroix JS; Pernow J. Neuropeptide Y and sympathetic neurotransmission. *Ann N Y Acad Sci* 1990;611:166-74.

Maj J, Moryl E. Effects of sertraline and citalopram given repeatedly on the responsiveness of 5-HT receptor subpopulations. *J Neural Transm Gen Sect* 1992;88:143-56

Malhotra AK; Virkkunen M; Rooney W; Eggert M; Linnoila M; Goldman D. The association between the dopamine D4 receptor (D4DR) 16 amino acid repeat polymorphism and novelty seeking. *Mol Psychiatry* 1996;1, 388-91.

Malizia AL. PET studies in experimental and pathological anxiety [abstract]. *J Psychopharmacol* 1997;11, A88

Mancini C; van Ameringen M; Szatmari P; Fugere C; Boyle M. A high-risk pilot study of the children of adults with social phobia. *J Am Acad Child Adolesc Psychiatry* 1996;35,1511-1517.

Mannuzza S; Schneier FR; Chapman TF; Liebowitz MR; Klein DF; Fyer AJ. Generalized social phobia: reliability and validity. *Arch Gen Psychiatry* 1995;52,230-237.

Martel FL; Hayward C; Lyons DM; Sanborn K; Varady S; Schatzberg AF. Salivary cortisol levels in socially phobic adolescent girls. *Depress Anxiety* 1999;10(1):25-7.

Martinson EA, Goldstein D, Brown JH. Muscarinic receptor activation of phosphatidylcholine hydrolysis: Relationship to phosphoinositide hydrolysis and diacylglycerol metabolism. *J Biol Chemistry* 1989;64:14748-14754.

Matson, G.B. and Weiner, M.W.: Spectroscopy. Chapter in *Magnetic Resonance Imaging*. Third Edition. Editors: D.D. Stark and W.G. Bradley, Jr., Mosby-Year Book, St. Louis, MO. (In press).

Mattick RP and Clarke JC. Development and validation of measures of social phobia

- scrutiny fear and social interaction anxiety. *Behav Res Ther* 1998;36:455-70.
- Mayleben M, Gariepy J, Tancer M. Genetic differences in social behavior: Neurobiological mechanisms in a mouse model. *Biol Psychiatry* 1992;31(Suppl):216A
- Merikangas KR, Avenevoli S, Archarya S, Zhang H, and Angst J. The spectrum of social phobia in the Zurich cohort study of young adults. *Biol Psychiatry* 2002;51:81-91.
- Mikkelsen EJ, Deltor J, Cohen DJ. School avoidance and social phobia triggered by haloperidol in patients with Tourette's syndrome. *Am J Psychiatry* 1981;138:1572-1576.
- Morimoto K. Benzodiazepine receptor imaging in the brain: recent developments and clinical validity. *Kaku Igaku* 1999;36:307-13.
- Munjack DJ; Baltazar PL; Bohn PB; Cabe DD; Appleton AA. Clonazepam in the treatment of social phobia: a pilot study. *J Clin Psychiatry*, 1990;51(Suppl. 5), 35-40.
- Ninan PT. . The functional anatomy, neurochemistry, and pharmacology of anxiety. *J Clin Psychiatry* 1999;60(suppl22):12-17.
- Nordstrom AL, Olsson H, Halldin C. A PET study of D2 dopamine receptor density at difference phases of the menstrual cycle. *Psychiatry Res* 1998, 83:1-6.
- Nutt DJ, Bell CJ, Malizia AL. Brain Mechanisms of Social Anxiety Disorder. *J Clin Psychiatry* 1998;59 (suppl 17), 4-9.
- Olsson and Farde. Potentials and pitfalls using high affinity radioligands in PET and SPET determinations on regional drug induced D2 receptor occupancy—a simulation study based on experimental data. *Neuroimage* 2001;14:936-945.
- Ost L. Ways of acquiring phobias and outcome of behavioral treatments. *Behav Res Ther* 1985;23:683-689.
- Pande AC, Davidson JRT, Jefferson JW, Janney CA, Katzelnick DJ, Weisler RH, Greist JH, Sutherland SM. Treatment of social phobia with gabapentin: a placebo-controlled study. *J Clin Psychopharmacol* 1999;19:341-348.
- Pande AC, Davidson JRT, Jefferson JW, Janney CA, Katzelnick DJ, Weisler RH, Greist JH, Sutherland SM. Treatment of social phobia with gabapentin: a placebo-controlled study. *J Clin Psychopharmacol* 1999;19:341-348.
- Papp LA; Gorman JM; Liebowitz MR; Fyer AJ; Cohen B; Klein DF. Epinephrine infusions in patients with social phobia. *Am J Psychiatry* 1988;145, 733-6.
- Phillips ML, Young AW, Senior C, Brammer M, Andrew C, Calder AJ, Bullmore ET, Perrett DI, Rowland D, Williams SC, Gray JA, David AS. A specific neural substrate for perceiving facial expressions of disgust. *Nature* 1997;389(6650):495-8.
- Pilowsky LS, Costa DC, Ell PJ, Verhoeff NP, Mrray RM, Kerwin RW. D2 dopamine receptor binding in the basal ganglia of antipsychotic-free schizophrenic patients. *Br J Psychiatry* 1994;164:16-26

Pinborg LH, Videbaek C, Knudsen GM, Swahn CG, Halldin C, Friberg L, Paulson OB, Lassen NA. Dopamine D2 receptor quantification in extrastriatal brain regions using ¹²³I-epidepride with bolus/infusion. *Synapse* 2000;36:322-329.

Pohjalainen T, Rinne JO, Nagren K, Syvalahti E, Heitala J. Sex differences in the striatal dopamine D2 receptor binding characteristics in vivo. *Am J Psychiatry* 1998;155:768-73.

Potts NL, Davidson JR, Krishnan KR, Doraiswamy PM, Ritchie JC. Levels of urinary free cortisol in social phobia. *J Clin Psychiatry* 1991;52 (suppl):41-42.

Potts NLS, Book S, and Davidson JRT. The neurobiology of social phobia. *Int Clin Psychopharmacol* 1996;11 (suppl 3), 43-48.

Potts NLS, Davidson JRT, Krishnan KRR, Doraiswamy PM. Magnetic resonance imaging in social phobia. *Psychiatry Res* 1994;52:35-42.

Prisco S, Esposito E. Differential effects of acute and chronic fluoxetine administration on the spontaneous activity of dopaminergic neurones in the ventral tegmental area. *Br J Pharmacol* 1995;116:1923-31.

Raleigh MJ, McGuire MT, Brammer GL, Pollack DB, Yuwiler A. Serotonergic mechanisms promote dominance acquisition in adult male vervet monkeys. *Brain Res* 1991;559:181-190.

Ramboz S, Oosting R, Amara DA, Kung HF, Blier P, Mendelsohn M, Mann JJ, Brunner D, Hen R. Serotonin receptor 1A knockout: an animal model of anxiety-related disorder. *Proc Natl Acad Sci U S A* 1998;95:14472-81.

Reicher-Rossler A, Hafner H, Stumbaum M, Maurer K, Schmidt R. Can estradiol modulate schizophrenic symptomatology. *Schizophr Bull* 1994;20:203-14.

Rosenbaum JF; Biederman J; Bolduc-Murphy EA; Faraone SV; Chaloff J; Hirshfeld DR, et al. Behavioral inhibition in childhood: a risk factor for anxiety disorders. *Harvard Rev Psychiatry* 1993;1,2-16.

Ross BD. Biochemical considerations in 1H Spectroscopy. Glutamate and glutamine; myo-inositol and related metabolites. *NMR Biomed* 1991;4:59-63.

Saunders-Pullman R, Gordon-Elliott J, Parides M, Fahn S, Saunders HR, Bressman S. The effect of estrogen replacement on early Parkinson's disease. *Neurology* 1999;52:1417-21.

Schneider F, Weiss U, Kessler C, Hans-Wilhelm M, Posse S, Salloum JB, Grodd W, Himmelmann F, Gaebel W, Birbaumer N. Subcortical correlates of differential classical conditioning of aversive emotional reactions in social phobia. *Biol Psychiatry* 1999;45:863-871.

Schneier FR, Liebowitz MR, Abi-Dargham A, Zea-Ponce Y, Lin SH, Laruelle M. Low dopamine D2 receptor binding potential in social phobia. *Am J Psychiatry* 2000;157:457-459.

- Schneier, F.R., Johnson, J., Hornig, C.D., Liebowitz, M.R., Weissman, M.M. Social phobia: Comorbidity and morbidity in an epidemiologic sample. *Arch Gen Psychiatry* 1992;45:282-288.
- Schultz W. Predictive reward signal of dopamine neurons. *J Neurophysiol* 1998;80:1-27.
- Seeman P, Niznik HB, Guan HC. Elevation of dopamine D2 receptors in schizophrenia is underestimated by radioactive raclopride. *Arch Gen Psychiatry* 1990;47:1170-2.
- Session DR, Pearlstone MM, Jewelewicz R, Kelly AC, Estrogens and Parkinson's disease. *Med Hypotheses* 1994;42:280-2.
- Smalley SL, McCracken J, Tanguay P. Autism, affective disorders, and social phobia. *Am J Med Genet* 1995;60:19-26.
- Stein MB, Asmundson GH, and Chartier M. Autonomic responsivity in generalized social phobia. *J Affect Disord* 1994;31:211-21.
- Stein MB, Heuser IJ, Juncos JL, Uhde TW. Anxiety disorders in patients with Parkinson's disease. *Am J Psychiatry* 1990;147:217-220.
- Stein MB, Huzel LL, Delaney SM. Lymphocyte beta-adrenoceptors in social phobia. *Biol Psychiatry* 1993;34:45-50.
- Stein MB, Leslie WD. A brain single photon-emission computed tomography (SPECT) study of generalized social phobia. *Biol Psychiatry* 1996;39, 825-828.
- Stein MB, Liebowitz MR, Lydiard RB, et al. Paroxetine treatment of generalized social phobia (social anxiety disorder): a randomized controlled trial. *JAMA* 1998;280:708-713.
- Stein MB, Tancer ME, and Uhde TW. Heart rate and plasma norepinephrine responsivity to orthostatic challenge in anxiety disorders. *Arch Gen Psychiatry*. 1992;49:311-7.
- Stein MB. Neurobiological perspectives on social phobia: from affiliation to zoology. *Biol Psychiatry* 1998;44:1277-1285.
- Stein MB; Chartier MJ; Hazel AL; Kozak MV; Tancer ME; Lander S; Furer P; Chubaty D; Walker JR. A direct-interview family study of generalized social phobia. *Am J Psychiatry* 1998;155(1):90-7.
- Stein MB; Hauger RL; Dhalla KS; Chartier MJ; Asmundson GJ. Plasma neuropeptide Y in anxiety disorders: findings in panic disorder and social phobia. *Psychiatry Res* 1996;59:183-8.
- Stein MB, Torgrud LJ, Walker JR. Social phobia symptoms, subtypes, and severity. *Arch Gen Psychiatry* 57:1046-1051.

Stemberger R, Turner S, Beidel D, Calhoun K. Social phobia: an analysis of possible developmental factors. *J Abnorm Psychol* 1995;104:526-531.

Stevens JR. Schizophrenia: reproductive hormones and the brain. 2002;159:713-719.

Stephenson CME, Bigliani V, Jones HM, Mulligan RS, Acton Pd, Visvikis D, Ell PJ, Kerwin RW, Pilowsky LS. Striatal and extra-striatal D2/D3 dopamine receptor occupancy by quetiapine in vivo. 2000;177:408-415.

Strobel A; Wehr A; Michel A; Brocke B. Association between the dopamine D4 receptor (DRD4) exon III polymorphism and measures of novelty seeking in a German population. *Mol Psychiatry* 1999;4(4):378-84.

Sullivan GM, Coplan JD, Kent JM, Gorman JM. The noradrenergic system in pathological anxiety: a focus on panic with relevance to generalized anxiety and phobias. *Biol Psychiatry* 1999;46:1205-1218.

Sullivan PF; Fifield WJ; Kennedy MA; Mulder RT; Sellman JD; Joyce PR. No association between novelty seeking and the type 4 dopamine receptor gene (DRD4) in two New Zealand samples. *Am J Psychiatry* 1998;155, 98-101.

Swahn C-G, Halldin C, Lundkvist C, Olsson H, Karlsson P, Farde L. Labelling of a lipophilic metabolite of ¹¹C-raclopride and investigation of its brain uptake in a cynomolgus monkey with PET. *J Labelled Compd Rad* 1997;40:179-181.

Tancer ME, Stein MB, Gelernter CS, Uhde TW. The hypothalamic-pituitary-thyroid axis in social phobia. *Am J Psychiatry* 1990a;147:929-933.

Tancer ME, Stein MB, Uhde TW. Effects of thyrotropin releasing hormone on blood pressure and heart rate in social phobia patients, panic disorder patients, and normal controls: results of a pilot study. *Biol Psychiatry* 1990b;27:781-783.

Tancer ME, Stein MB, Uhde TW. Lactate response to caffeine in panic disorder: a replication using an "anxious" control group [abstract]. *Biol Psychiatry* 1991;29:57A.

Tancer ME, Uhde TW. Neuroendocrine, physiologic, and behavioral responses to clonidine in patients with social phobia [abstract]. *Biol Psychiatry* 1989;25, 189A0.

Tancer ME. Neurobiology of social phobia. *J Clin Psychiatry* 1993;54 (suppl 12):26-30.

Taylor A, Datz FL. Clinical practice of nuclear medicine. New York: Churchill Livingstone, 1991, pp 1-3.

Tibbo P, Silverstone PH. A single photon emission computed tomography scan study of striatal dopamine D2 receptor binding with ¹²³I-epidepride in patients with schizophrenia and controls. *J Psychiatry Neurosci* 1997;22:39-45).

Tibbo P, Warneke L. Obsessive-compulsive disorder in schizophrenia: epidemiologic and biologic overlap. *J Psychiatry Neurosci* 1999;24:15-24.

Tiihonen J, Kuikka Jyrki, Bergstrom K, Lepla Ulla, Koponen H, Leinonen E. Dopamine reuptake site densities in patients with social phobia. *Am J Psychiatry* 1997;154:239-242.

Tsang KL, Ho SL, Lo SK. Estrogen improves motor disability in parkinsonian postmenopausal women with motor fluctuations. *Neurology* 2000;54:2292-8.

Tupler LA, Davidson JRT, Smith RD, Lazeyras F, Charles HC, Krishnan KRR. A Repeat Proton Magnetic Resonance Spectroscopy Study in Social Phobia. *Biol Psychiatry* 1997;42:419-424.

Turner SM, Biedel D, and Jacob RG (1994) Social phobia: a comparison of behavior therapy and atenolol. *Journal of Consulting and Clinical Psychology* 1994;62, 350-358.

Uhde T. Anxiety and growth disturbance: Is there a connection? A review of biological studies in social phobia. *J Clin Psychiatry* 1994;55(suppl 6):17-27.

Uhde TW, Tancer ME. Normal urinary free cortisol and post dexamethasone cortisol in social phobia. *Journal of Affective Disorders* 1994;30:155-161.

Vandenbergh DJ, Zonderman AB, Wang J, et al. No association between novelty seeking and dopamine D4 receptor (D4DR) exon III seven repeat alleles in Baltimore Longitudinal Study of Aging participants. *Mol Psychiatry*. 1997;2:417-9.

Versiani M, Nardi AE, Mundim FD, Alves AB, Liebowitz MR, Amrein R. Pharmacotherapy of social phobia: a controlled study with moclobemide and phenelzine. *Br J Psychiatry* 1992; 161:353-360.

Wacker HR, Mulleijans R, Klein R. Identification of cases of anxiety disorders and affective disorders in the community according to ICD-10 and DSM-III-R by using the Composite International Diagnostic Interview (CID). *International Journal of Methods in Psychiatry Research* 1992;2,91-100.

Wahlestedt C and Reis DJ. Neuropeptide Y-related peptides and their receptors--are the receptors potential therapeutic drug targets? *Annu Rev Pharmacol Toxicol* 1993;33:309-52.

Weiller E, Bisslerbe JC, Boyer P, et al. Social phobia in general health care: an unrecognised undertreated disabling disorder. *Br J Psychiatry* 1996;168:169-174.

Young, LJ. The neurobiology of social recognition, approach, and avoidance. *Biol Psychiatry* 2002;51:18-26.

APPENDIX A

